GEORG-AUGUST-UNIVERSITÄT
GÖTTINGEN

Molecular Mechanism of Inhibition of the CREB-coactivator TORC by the mitogen-activated kinase DLK in pancreatic beta-cells

PhD Thesis

for the degree “Doctor of Philosophy” in the GAUSS Program
at the Georg August University Göttingen, Faculty of Biology

submitted by
Do Thanh Phu

born in
Hoa Binh, Viet Nam

June 2010

Molecular Mechanism of Inhibition of the CREB-coactivator TORC by the mitogen-activated kinase DLK in pancreatic beta-cells

PhD Thesis

for the degree “Doctor of Philosophy” in the GAUSS Program
at the Georg August University Göttingen, Faculty of Biology

submitted by
Do Thanh Phu

born in
Hoa Binh, Viet Nam

June 2010

Though a tree grow ever so high,
the falling leaves return to the root

Unknown author

Declaration

I hereby declare that this submission is completely my own work. All references have been clearly cited.

Do Thanh Phu

Göttingen, June 09, 2010

Direct supervisor:	PD Dr. Elke Oetjen
Referent:	Prof. Dr. Ralf Heinrich
Co-referent:	Prof. Dr. Frauke Melchior
Date of exam:	21.07.2010

Table of Contents

TABLE OF CONTENTS **1**
LIST OF FIGURES **5**
LIST OF TABLES **6**
ABBREVIATIONS **7**

1. INTRODUCTION **10**
1.1 General principles of the signal transduction ***10***
1.2 The transcription factor CREB ***11***
1.2.a. Structure of CREB *12*
1.2.b. Characteristics and functions of CREB *12*
1.3 Transducer of regulated CREB (TORC), a CREB coactivator ***14***
1.3.a. Structure of TORC *15*
1.3.b. Regulations and functions of TORC *16*
1.4 Dual leucine zipper bearing kinase ***19***
1.4.a Structure of DLK *20*
1.4.b Characteristics and function of DLK *21*
1.5. Objectives of the study ***25***

MATERIAL AND METHODS **26**
2. MATERIAL **26**
2.1. Equipments & Consumables ***26***
2.1.a. Equipment *26*
2.1.b. Consumables *28*
2.2. Chemicals ***29***
2.2.a. Substances *29*
2.2.b. Stock solutions and buffers *30*
2.2.b.I. Stock solutions 30
2.2.b.II. Buffers 31
2.3. Biological Material ***32***
2.3.a. Kits *32*
2.3.b. Procaryotic and eukaryotic cell lines *32*
2.3.c. Media and material for cell cultures *32*
2.3.d. Plasmids *33*
2.3.d.I. Expression vectors 33

2.3.d.II. Luciferase reporter gene constructs 37
2.3.e. Oligonucleotides 37
2.3.e.I. Oligonucleotides used for PCR cloning 37
2.3.e.II. Oligonucleotides used for quantitative real-time PCR 39
2.3.f. Enzymes and buffers *39*
2.3.g. DNA and protein markers 40
2.3.h. Antibodies *40*

3. METHODS ***42***
3.1. Generation of plasmid DNA ***42***
3.1.a. PCR cloning and site-directed mutagenesis *42*
3.1.a.II. Polymerase chain reaction (PCR) 42
3.1.a.II. Site-directed mutagenesis primerless PCR 43
3.1.b. DNA gel electrophoresis *44*
3.1.c. DNA purification from agarose gels *45*
3.1.d. Restriction digest of DNA *46*
3.1.e. Ligation of DNA *46*
3.2. Amplification of plasmid DNA ***47***
3.2.a. Preparation of competent E.coli *47*
3.2.b. Transformation of competent E.coli *48*
3.2.c. Small scale DNA preparation (Mini-prep) *48*
3.2.d. Large scale DNA preparation (Maxi-prep) *50*
3.2.e. Sequencing *51*
3.2.f. Quantification of DNA concentration *52*
3.3. Analysis of proteins ***53***
3.3.a. Quantification of proteins *53*
3.3.a.I. Bradford assay 53
3.3.a.II. Semi-quantitative SDS-PAGE 53
3.3.b. SDS-PAGE *53*
3.3.c. Detection of proteins with Coomassie stain *55*
3.3.d. Western blot *56*
3.3.e. Analysis of radioactively labeled proteins *57*
3.4. Purification of GST-fusion and His-tagged proteins ***57***
3.4.a. Screening for inducible clones expressing GST- and His-fusion proteins *57*
3.4.b. Purification of GST- and His-fusion proteins *58*
3.5. Labelling of proteins with [^{35}S]-Methionine ***60***

3.6. GST- and His- pull-down assay 61

3.7. Culture of HIT-T15 cells 61

3.8. Transient transfection of HIT-T15 cells 62

3.8.a.Transfection using DEAE Dextran 62

3.8.b.Transfection using Metafectene 63

3.9. Treatment of HIT-T15 cells 63

3.10. Preparation of cell lysates for Western blot 64

3.11. Immunocytochemistry 65

3.12. Co-immunoprecipitation assay 66

3.13. In vitro kinase assay 67

3.14. Chromatin-immunoprecipitation (ChIP) 68

3.15. Luciferase reporter-gene assay 71

3.16. Statistics 73

4. RESULTS 74

4.1. Effect of DLK on the transcriptional activity conferred by the three TORC isoforms 74

4.2. Comparison of the inhibitory effect of DLK on the transcriptional activity of three TORC isoforms 79

4.3. Mapping of TORC1 domains inhibited by DLK 80

4.4. Effect of DLK on the transcriptional activity of TORC1 S167A and of TORC2 S171A 81

4.5. Effect of a dimerization-deficient DLK mutant on the transcriptional activity of the TORC isoforms 82

4.6. Overexpression of DLK wild-type and its mutants in HIT cells 83

4.7. Interaction between DLK and TORC as revealed by an in vitro assay 84

4.7.a. Purification of bacterially expressed proteins 85

4.7.b. In vitro interaction of tested proteins 87

4.7.b.I. Interaction between TORC1 full length and DLK wild-type or DLK mutants 87

4.7.b.II. Interaction between $TORC1_{1-44}$ and DLK wild-type or DLK mutants 89

4.7.b.III. Interaction between $TORC1_{\Delta 44}$ and DLK wild-type or DLK mutants 91

4.7.b.IV. Interaction between DLK wild-type and different domains of TORC 91

4.8. Interaction between DLK and TORC in HIT cells 92

4.9. Effect of DLK on the nuclear localization of TORC 94

4.10. Effect of DLK on the phosphorylation of TORC in an in vitro assay 96

4.11. Effect of DLK on the phosphorylation of TORC in HIT cells 97

4.12. Effect of DLK on the recruitment of TORC to a CRE-containing promoter 101

5. DISCUSSION 104

5.1. DLK inhibits the transcriptional activity of TORC proteins 104

5.2. DLK enhances the phosphorylation of TORC on the regulatory sites 105

5.3. DLK may inhibit TORC through direct interaction 108

5.4. DLK inhibits the nuclear translocation of TORC and recruitment of TORC to CRE-containing promoter 110

6. SUMARY AND CONCLUSION (in English and German) 113

7. REFERENCES 117

ACKNOWLEDGEMENT 131

POSTERS 132

LIST OF FIGURES

Figure 1: CREB structure 12
Figure 2: CREB-directed gene transcription 13
Figure 3: Structure of TORC 15
Figure 4: The nucleo-cytoplasmic shuttling of TORC 18
Figure 5: The structure of DLK protein 20
Figure 6: The role of DLK in MAPK signaling pathway 24
Figure 7: Site-directed mutagenesis by primerless PCR 44
Figure 8: The sketch of plasmid 5xGal4E1BLuc and expression vector of GAL4-TORC 74
Figure 9A-C: Effect of DLK on unstimulated transcriptional activity of TORC isoforms 75
Figure 10A-D: Effect of DLK on the stimulated transcriptional activity of TORC isoforms 78
Figure 11: Increasing amount of overexpression vector for DLK enhances the inhibitory effect on TORCs 79
Figure 12: Effect of DLK on the transcriptional activity of TORC1 domains 80
Figure 13A, B: Effect of DLK on transcriptional activity of TORC1S167A and TORC2 S171A 82
Figure 14: The dimerization-deficient DLK has no inhibitory effect on TORC 83
Figure 15: Expression levels of DLK wild-type and its mutants in HIT cells 84
Figure 16: Purification of His tagged TORC1 full length and His-tagged TORC1$_{\Delta 44}$ proteins 85
Figure 17: Purification of GST protein and GST-TORC1$_{1-44}$ fusion protein 86
Figure 18: Semi-quantification of purified proteins 86
Figure 19A, B: *In vitro* interaction between DLK/CREB and TORC1 full length 88
Figure 20A, B: *In vitro* interaction between DLK/CREB and TORC1$_{1-44}$ 90
Figure 21: Interaction between the N-terminal deleted TORC1 and DLK wild-type, DLKK185A or DLKP-P 91
Figure 22: Interaction between TORC1 full length, TORC1Δ44, TORC1$_{1-44}$ and DLK wild-type 92
Figure 23: Overexpression of DLK wild-type, DLK K185A, DLK P-P and TORC1 in HIT cells 93
Figure 24: Interaction of TORC1 with DLK wild-type, DLK K185A and DLK P-P in HIT cells 94
Figure 25: Typical pictures showing subcellular localization of TORC in the presence of overexpressed DLK wild-type (**A**) or overexpressed DLK K185A (**B**) 95
Figure 26: Effect of DLK on the nuclear localization of TORC 95

Figure 27A-B: TORC proteins were expressed and purified from E.coli 96

Figure 28: *In vitro* kinase assay 97

Figure 29: Western blot: Check the antibody specifically against Ser-151 phospho-mTORC1 (equivalent to Ser-167 hTORC1) 98

Figure 30: Typical Western blot: The effect of DLK on the phosphorylation of TORC on Ser-167 98

Figure 31: DLK wild-type induced the phosphorylation of TORC 99

Figure 32: Typical Western blot: The shift of TORC1 protein phosphorylated on unidentified residue 100

Figure 33: Typical Western blot: Putative involvement of JNK in DLK-induced phosphorylation of TORC1 101

Figure 34: Effect of DLK on TORC dependent CRE-directed gene transcription under combined treatment of KCl and forskolin 102

Figure 35: Effect of DLK on recruitment of TORC to the CRE-promoter 103

Figure 36: DLK inhibits transcriptional activity of TORC at distinct levels 112

LIST OF TABLES

Table 1: Mammalian and bacterial expression constructs 36

Table 2: The primer pairs (forward and reverse) used to generate the constructs in the present work 38

Table 3: Oligonucleotides and TaqMan™ probes for quantitative real-time PCR 39

Table 4: Primary and secondary antibodies 40

ABBREVIATIONS

aa – amino acids
Amp – ampicillin
AMP – adenosine monophosphate
AMPK – AMP-activated protein kinase
ANOVA – analysis of variance
AP1 – activator protein 1
APS – ammonium persulphate
ATF-1 - Cyclic AMP-dependent transcription factor 1
ATP – adenosine triphosphate
BSA – bovine serum albumin
bZip – basic leucine zipper
°C – degree celcius
CaMK – calcium/calmodulin-dependent kinase
cAMP – cyclic adenosine monophosphate
CBP – CREB binding protein
cDNA – complementary DNA
ChIP – chromatin immunoprecipitation
CMV – cytomegalovirus
CRE – cAMP response element
CREB – cAMP responsive element binding protein
CREM - cAMP-responsive element modulator
CRIB (Cdc42/Rac interactive binding
CREB – cAMP response element binding protein
CREM – cAMP response element modulator
CsA – cyclosporin A
CsCl – cesium chloride
DAPI – 4',6-diamidino-2-phenylindol
dATP – deoxyadenosine triphosphate
dCTP – deoxycytidine triphosphate
dGTP – deoxyguanosine triphosphate
DLK - Dual leucine zipper bearing kinase
DMSO – dimethyl sulfoxide
DNA – deoxyribonucleic acid
dNTPs – deoxynucleoside triphosphates
DTT – dithiothreitol
dTTP – deoxythymidine triphosphate
ERK – extracellular signal-regulated kinase
FSK – forskolin
GDP – guanidine diphosphate
GFP – green fluorescent protein
GFPtpz – green fluorescent protein variant topaz
GST – glutathione S-transferase
GTP – guanidine triphosphate

h – hour
HCl – hydrochloric acid
HIT-T15 (cells) – hamster insulin tumour T15 (cells)
Hsp70 – heat shock protein
IPTG – isopropyl-β-D-thiogalactoside
IB/JIP-1 - islet brain/JNK interacting protein-1
JIP – JNK-interacting protein
K_2HPO_4 – di-potassium hydrogen phosphate
KCl – potassium chloride
kDa – kilo Dalton
KH_2PO_4 – potassium di-hydrogen phosphate
KID – kinase inducible domain
LiCl – lithium chloride
LZK - leucine zipper bearing kinase
MAML2 – Mastermind-like 2
MAPK – Mitogen activated protein kinase
MAPKK – Mitogen activated protein kinase kinase
MAPKKK – mitogen-activated protein kinase kinase kinase
MARK - MAP/microtubule affinity-regulating kinase
MBIP - MAPK upstream kinase (MUK)-binding inhibitory protein
MEK – mitogen activated protein kinase
MKP - mitogen-activated protein kinase kinase phosphatase
MLK – mixed lineage Kinase
$MgCl_2$ – magnesium chloride
$MgSO_4$ – magnesium sulphate
min – minute
$MnCl_2$ – maganese chloride
MUK - MAPK upstream kinase
N_2 - nitrogen
Na_2CO_3 – sodium carbonate
Na_2HPO_4 – di-sodium hydrogen phosphate
NaAc – sodium acetate trihydrate
NaCl – sodium chloride
NaH_2PO_4 – sodium di-hydrogen phosphate
NaOH – sodium hydroxide
NES – nuclear export sequence
NLS – nuclear localisation sequence
OD – optical density
PBS – phosphate-buffered saline
PCNA - Proliferating cellular nuclear antigen
PCR – Polymerase chain reaction
PDGF - Platelet-derived growth factor

PEPCK - Phosphoenolpyruvate carboxylkinase
PEG 6000 – polyethylene glycol
PGC1α - peroxisome proliferators-activated receptor γ coactivator 1α
PKA – protein kinase A
PIP_2 – phosphatidylinositol 4,5-bisphospate
PKA – protein kinase A
PMSF – phenylmethylsulfonylfluoride
Pol II – RNA polymerase II
PP1 and PP2A – protein phosphatase 1/2A
RHA - RNA-Helicase A
RNA – ribonucleic acid
RPMI – Roswell Park Memorial Institute
rpm – rounds per minute
SAPK – stress activated protein kinase
SDS – sodium dodecylsulphate
SDS-PAGE – sodium dodecylsulphate polyacrylamide gel electrophoresis
sec – seconds
SEM – standard error of mean
SH3 - Src homology 3
SIK – salt-inducible kinase
siRNA – small interfering RNA
somCRE – somatostatin CRE
$TAF_{II}130$ - TATA-box-binding protein associated factor
TAK – tumour growth factor β activated protein kinase
TBP – TATA-box binding protein
TFIID – transcription factor II D
TFIIB - transcription factor II D
TNF alpha – Tumour Necrosis Factor alpha
TORC – transducer of regulated CREB
vol - volume
wt – wild-type
ZPK – (human) Zipper Protein Kinase

1. INTRODUCTION

1.1 General principles of the signal transduction

Signal transduction is a process that the living organisms use to coordinate all biochemical reactions in their cells in order to respond to extracellular signals. The cell reactions may result in short- or long-term changes not only in the metabolism and/or in the cell function but also in processes such as proliferation, differentiation, apoptosis and immune defense. In order for a cell to express a response, first the external signal must be recognized by a cell-specific membrane receptor protein and transferred to a cell-understandable syntax. Second, the signal is passed over suitable effector proteins through intracellular signal molecules. Finally, a specific biochemical process is triggerd (Lodish et al., 2004; Pollard and Earnshaw, 2002).

Fundamental components of the intracellular signal transduction comprise of effector proteins and small molecule messengers. An incoming signal is passed on from its specific membrane receptor to downstream proteins, which in turn have other effector proteins. By this way, more proteins are involved in the signal chain (Krauss, 2003). The small molecule messengers play a role as connectors among effector proteins.

One of the predominant principle of the intracellular signal transduction is the change in concentration of diffusible messenger substances, so-called second messengers, which bind to and activate effector proteins (Krauss, 2003). Calcium (Ca^{2+}) and the cyclic nucleotide cAMP (cyclic Adenosin-3', 5 ' - mono phosphate) are well-known representatives of these signal molecules; they diffuse among cell compartments and work by binding to a certain “switch” proteins and/or - enzymes and lead to the activation of the enzymes e.g. the Ca^{2+}-binding protein calmodulin or cAMP-dependent protein kinase PKA (Pollard and Earnshaw, 2002).

A second universal principle relies on the cascade of sequential enzymes; here the signal is passed on and amplified from membrane receptors to sequentially-activated enzymes. In eucaryotic cells the so-called MAPK (mitogen-activated protein kinase) cascade is best examined. The MAPK cascade is often activated by mitogenic signals, which promote cell division activities. The MAPK pathway is composed of modules containing at least three types of protein kinases, which transmit the signal by sequential phosphorylation in a hierachical way. The MAPKKKs (MAP Kinase Kinase Kinase) standing top in the hierarchy are Serine/Threonine-specific protein kinases. They phosphorylate the subordinate MAPKKs (MAP Kinase Kinase) downstream of the module at two serine

residues, which are separated by 3 other amino acids. The MAPKKs are dual-specificity protein kinases, which phosphorylate the down-stream MAPKs at Tyrosine and Threonine residues in the T-X-Y (Tyrosine-X-Threonine) motif. The MAPKs are divided into different subgroups depending on their sequence homology, input signals, and the preceeding MAPKKs. MAPKs designate their own downstream substrate proteins. As serine/threonine kinases they phosphorylate a number of cytosolic and nuclear proteins. Of the at least six different MAPK pathways that have been identified to date in mammalian cells, the best investigated are ERK, JNK/SAPK and p38 (Widmann et al., 1999; Garrington and Johnson, 1999; Pearson et al., 2001; Kyriakus and Avruch, 2001; Krauss, 2003).

Effector molecules transfer new demands to the cell e.g. protein production through the functional proteins, enzymes. The function and morphology of a cell are determined by expression of specific genes. Furthermore, the cellular processes e.g. development, differentiation, metabolism are characterized by a variable pattern of gene expression (Krauss G. 2003). By this view, transcription factors like the CREB (cAMP response element binding protein) are especially important due to their influence on the gene expression. Most importantly, an effector is not assigned to only one signal pathway. The transcription factor CREB is, for this reason, a good example. Originally, CREB was identified as a substrate of the cAMP signal pathway. Today it is known that numbers of extracellular factors affect the CREB-mediated gene transcription by at least three separate signal pathway (Shaywitz and Greenberg, 1999; Lodish et al., 2004; Pollard and Earnshaw, 2002).

1.2 The transcription factor CREB

The ubiquitously expressed transcription factor CREB, cAMP-response element binding protein, is involved in numerous cell signalling pathways (Shaywitz and Greenberg, 1999; Tardito et al., 2006). CREB binds to its recognition sequence, CRE, with the consensus motif 5'-TGACGTCA-3' and mediates the activation of cAMP-responsive genes (Shaywitz and Greenberg, 1999). CREB target genes include, for instance, metabolic enzymes (Lactate dehydrogenase, Phosphoenolpyruvate carboxylkinase (PEPCK), Pyruvate carboxylase etc.), transcription factors (c-Fos, STAT3, c-Maf etc.), cell cycle or survival (Proliferating cellular nuclear antigen PCNA, Cyclin A, Cyclin D1, Bcl-2 etc.), growth factors (insulin, TNFα, etc.), immune regulators (T-cell receptor-α, Interleukine-6, etc.), signalling proteins (Mitogen-activated protein kinase kinase phosphatase MKP-1, Glucose-regulated protein 78, etc.) and many others (Mayr and Montminy, 2001).

1.2.a. Structure of CREB

In mammals, the CREB family is composed of CREB, CREM and ATF-1, which have the basic-leucine zipper (bZip) in the structure (Mayr and Montminy, 2001). The CREB gene comprises 11 exons, which form 2 main spliced products designated CREB-α (341) and CREB-δ (327). CREB-α comprise 14 amino acids more than the δ-form (**Fig. 1**). These two forms function equally.

The primary structure of CREB includes a kinase inducible domain (KID) which is centrally located and composed of 60 amino acids. The domains Q1 and Q2 (constitutive activators) are glutamine-rich, which flank the KID. The leucine zipper domain is located in the C-terminus of CREB, which mediates CREB dimerization. The basic domain which is responsible for DNA binding is positioned between Q2 and leucine zipper domains (Mayr and Montminy, 2001).

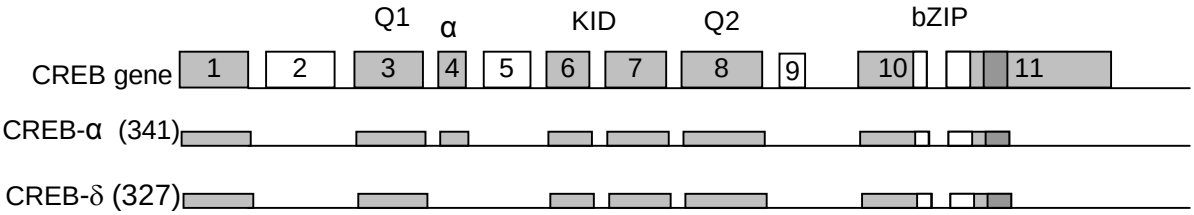

Figure 1: CREB structure (Mayr and Montminy, 2001).
The CREB gene includes 11 exons. Post-transcription splicing forms 2 main proteins designated CREB-α (341) and CREB-δ (327). Both have the same function because important domains - such as KID, Q1 and 2, and bZIP - are conserved. The difference is only that CREB-α includes 14 amino acids more than the δ-form.

1.2.b. Characteristics and functions of CREB

The bZip domain of CREB binds as a dimer to the CRE site on the promoter of target genes (Montminy et al., 1986). CREB activates gene transcription when the serine 133 in the KID is phosphorylated and CREB interacts with other co-factors (Mayr and Montminy, 2001). Besides the Mitogen-Activated Protein Kinase (MAPK) ERK1/2 and p38, an increase of the intracellular concentration of cAMP which activated protein kinase A (PKA) and membrane depolarization with elevation of intracellular calcium concentration and stimulation of calcium-calmodulin dependent protein kinases (CaMK I, II, and IV) lead to the phosphorylation of CREB at Ser-133 (in CREB-341) (Tan et al., 1996; Gonzalez et al., 1989; Sun et al., 1994; Mayr and Montminy, 2001). This phosphorylation is essential for the recruitment of the CREB co-activator, CREB binding protein, CBP which has histone

acetylase activity and associates with RNA-polymerase II complexes (Mayr and Montminy, 2001; Shaywitz and Greenberg, 1999; Nakajima et al., 1997). Besides CBP, the CREB-directed gene transcription depends also on its interaction with other proteins. Among these, the interaction of the CREB-Q2 domain with $TAF_{II}130$ of the TFIID complex which belongs to the general transcriptional machinery (Nakajima et al., 1997) plays an important role in the process since TFIID complex integrates with TBP- TATA-box binding protein- to stabilize the whole transcriptional machinery on the promoter of target genes.

Additionally, some findings showed that the phosphorylation of CREB at Ser119 (corresponding to Ser-133 in CREB- α) which recruits CBP to involve in transcription is not sufficient for transcriptional activity. The stimulated CREB-directed gene transcription is inhibited by the immunosuppressive drugs cyclosporin A and FK506 independent of the phosphorylation of Ser119 (Oetjen et al., 2005; Schwaninger et al., 1995; Schwaninger et al., 1993a). Recently, a new co-activator of CREB named transducer of regulated CREB (TORC) was identified (Iourgenko et al., 2003). TORC promotes CREB-directed gene transcription through phosphorylation-independent interaction with the bZip DNA binding/dimerization domain of CREB (Conkright et al., 2003a, b).

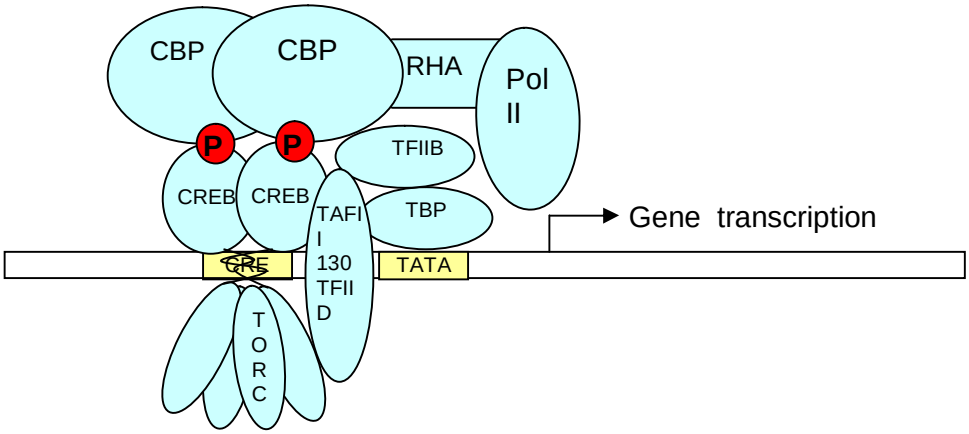

Figure 2: CREB-directed gene transcription (described following Conkright et al. 2003, Screaton et al. 2004, Ravnskjaer et al. 2007)

Homodimerised CREB binds to the cAMP-responsive element and is phosphorylated at Ser 119 by some stimuli. CBP is recruited to KID domain of CREB after this phosphorylation. The complex TAFII 130/TFII D interacts with the Q2 domain of CREB, which integrates with TFIIB and TATA-box binding protein (TBP) and enhance the CREB binding to the promoter of target gene. Besides, TORC binding to the bZip domain of CREB as tetramer also enhance the interaction between CREB and TAFII 130 component of TFIID. The glutamine-rich region of C-terminal TORC also binds to TAFII 130 component. RNA-Polymerase II associates with CBP through RNA-Helicase A (RHA), which activates the CREB target gene transcription.

CREB has diverse functions in different tissues. For instance, it regulates the growth-factor-dependent cell survival (Mayr and Montminy, 2001). CREB-/- mice have a lower

number of developing T cells than the control littermates (Rudolph et al., 1998). The transgenic mice expressing a non-phosphorylatable CREB in pituitary or a dominant-negative A-CREB in chondrocytes had dwarfish phenotype, which was shown to be partly due to blockage of proliferation (Struthers et al., 1991; Long et al., 2001; Inoescu et al., 2001). Some genes involved in this process include cyclinD1 and cyclin A, which are probably regulated by CREB (Desdouets et al., 1995; Lee et al., 1999; D'Amico et al., 2000). Overexpression of the anti-apoptotic Bcl2 gene reduced the cell death caused by dominant-negative CREB expression (Riccio et al., 1999, Bonni et al., 1999).

Especially, a quarter of CREB-dependent genes are involved in metabolic regulation (Mayr and Montminy, 2001). Glucose homeostasis is also regulated by hepatic enzymes which are CREB-dependent (Herzig et al., 2001, 2003; Mayr and Montminy, 2001). CREB modulates glucagon production in the pancreas (Schwaninger et al., 1993), which in turn, glucagon enhances glucose output from the liver during fasting by stimulating the transcription of gluconeogenic genes via the cyclic AMP-inducible factor CREB (Koo et al., 2005).

CREB appears to have a special meaning for the function and the mass of the β-cells: It binds to the promotor of rat insulin I gene and the promotor of human insulin gene and activates their transcription (Oetjen et al., 1994; Eggers et al., 1998; Oetjen et al. 2003a, b). Transgenic mice, which overexpress a dominant-negative mutant of CREB in the β-cells, become diabetic because of apoptotic β-cell death (Jhala et al., 2003). These evidences emphasize the crucial role of CREB in metabolism and cell survival.

1.3 Transducer of regulated CREB (TORC), a CREB coactivator

The transducer of regulated CREB 1 (TORC1) was first identified in 2003 as coactivator of the transcription factor CREB, which potently induces known CREB1 target genes (Iourgenko et al., 2003). A number of TORC1-related proteins were discovered, such as two human genes hTORC2 and hTORC3 which are 32% identical to TORC1, or a single drosophila gene dTORC1 with 20% idendical to TORC1 (Iourgenko et al., 2003). In mice, the orthologs of TORC1, TORC2, and TORC3 were found. The fugu and drosophila have only TORC1 orthologs (Iourgenko et al., 2003). The protein sequences include a highly conserved N-terminal coil-coil domain (residues 8-54 of hTORC1) (Iourgenko et al., 2003).

TORC isoforms are expressed differently in distinct tissues. TORC1 is present abundantly in the prefrontal cortex and the cerebellum of the brain, and TORCs 2 and 3 are highly expressed in B- and T-lymphocytes (Conkright et al., 2003a). TORC1 was shown to be

involved in hippocampal long-term synaptic plasticity (Kovacs et al., 2007; Zhou et al., 2006), whereas TORC2 is involved predominantly in the regulation of glucose homeostasis (Dentin et al., 2008; Dentin et al., 2007; Koo et al., 2005; Liu et al., 2008; Screaton et al., 2004).

1.3.a. Structure of TORC

TORC proteins have a highly conserved N-terminal predicted coiled-coil domain, a so-called CREB binding domain (CBD), (**Fig. 3**) which interacts with the bZip domain of CREB. The coiled-coil structure of TORC1 is located at aa 1-42 (Conkright et al., 2003a). Additionally, a protein kinase A (PKA) phosphorylation consensus sequence is also present in all TORC isoforms (Iourgenko et al., 2003).

TORC 2 has a nuclear localizing sequence (NLS) at aa 56-144 and two nuclear export sequence (NES1 and 2) within aa 145-320. Both NLS and NES motifs are conserved in all three isoforms of the TORC family (Screaton et al., 2004).

By fusing the C-terminus of TORC isoforms with DNA-binding domain of GAL4 and applying reporter gene assays with minimal promoter linked to GAL4-binding sites, Iourgenko et al. discovered that all TORC isoforms have a transactivation domain at the C-terminus (**Fig. 3**) (Iourgenko et al., 2003).

A study on the phosphorylation of TORC2 showed that it has twelve independent phosphorylated serine residues in which seven residues are in the central region (aa 300-500), and the Ser-171 is dephosphorylated by elevation of Ca^{2+} influx and cAMP levels (Screaton et al., 2004). TORC2 has two motifs which mediate the binding of calcium/calmodulin-dependent phosphatase calcineurin and two multiple phosphorylated regions which interact with the 14-3-3 protein (Screaton et al., 2004).

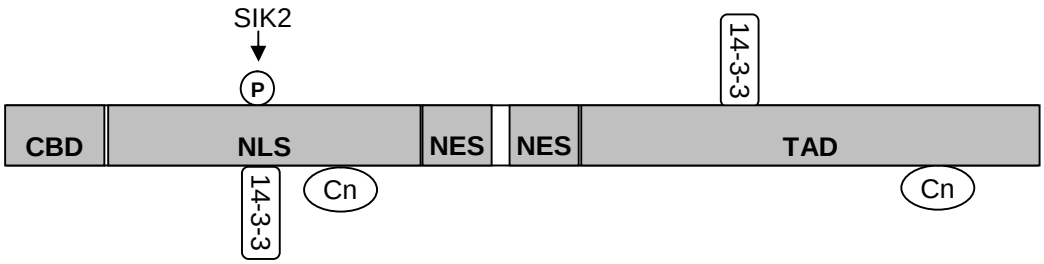

Figure 3: Structure of TORC (modified from Screaton et al., 2004)

The CREB binding domain (CBD) is a highly conserved predicted coiled-coil structure, located at the N-terminus of TORC. TORC has a nuclear localisation signal (NLS) and two nuclear export sequences (NES). The transactivation domain (TAD) is located C-terminal.

1.3.b. Regulations and functions of TORC

The nuclear translocation of TORC is pivotal to their role in CREB-directed gene transcription. In the basal condition, TORC2 and 3 are phoshorylated on Ser-171 and Ser-163, respectively, by the salt-inducible kinase-1(SIK1), a member of the family of AMP-activated protein kinases (AMPK). However, phosphorylation of TORC1 on Ser-167 may be due to SIK1 and as yet unidentified kinases (Screaton et al., 2004; Katoh et al., 2006). SIK1 is found to repress CREB activity in both nucleus and cytoplasm, and enhance Phospho-TORCs relocation from the nucleus to the cytoplasm where they are sequestered via phosphorylation-dependent association with 14-3-3 proteins (Screaton et al., 2004; Katoh et al., 2004). SIKs are activated by the tumour suppressor kinase LBK1 through phosphorylation at a threonine in the A-loop of SIKs (Katoh et al., 2006).

Besides SIKs, AMPKs (5'-AMP activated protein kinases) were also identified as kinases of TORC proteins. Activated AMPK kinases phosphorylate TORC2 at Ser-171 which results in inhibition of O-glycosylation, interaction with 14-3-3 proteins, sequestration in the cytoplasm, and prevention of transcriptional activation (Koo et al., 2005; Takemori et al., 2007a; Dentin et al., 2008). LKB1 can also phosphorylate and activate AMPK (Shaw et al., 2005).

Recently, Ser-275 on TORC2 (equivalent to Ser-261 on TORC1) was indentified as another regulatory phosphorylation site (Jansson et al., 2008). In beta cells, the phosphorylation of TORC2 on Ser-171 responds primarily to cAMP signals (Koo et al., 2005; Screaton et al., 2004), whereas Ser-275 phosphorylation of TORC2 is induced by low level glucose and is blocked by glucose influx-induced calcineurin (Jansson et al., 2008). MARK2 (MAP/microtubule affinity-regulating kinase) specifically phosphorylates TORC2 at both Ser-171 and Ser-275, leading to TORC2 interaction with 14-3-3 proteins and attenuation of CREB-dependent gene transcription (Jansson et al., 2008). Despite Ser-369 of TORC2 is the interaction site with 14-3-3 proteins, it does not control the nuclear localization of TORC2 (Jansson et al., 2008).

In contrast with the other studies whereby phosphorylation of TORCs leading to their cytosolic accumulation and transcriptional reduction, MEKK1 (a MAPKKK) induces the transcriptional activity of TORC1 by direct phosphorylation on as yet unidentified sites of its C-terminal 220 aa which results in its nuclear localization.

Another mechanism that downregulates TORC activity was found due to proteosome-dependent degradation. Dentin et al. (2007) showed that on Ser-171 phosphorylated

TORC2 sequestered in the cytoplasm undergoes polyubiquitination at K628 leading to its degradation.

TORC nuclear localization increases under elevation of intracellular cAMP or Ca^{2+}, signals enhancing CREB-directed gene transcription, (Bittinger et al., 2004; Screaton et al., 2004). Indeed, cAMP and Ca influx work in different ways and converge on the dephosphorylation of TORCs at regulatory sites and shuttle between nuclear and cytoplasm.

An increase in calcium influx activates the calcium/camodulin-dependent phosphatase calcineurin which binds directly to and dephosphorylates TORCs at regulatory phosphorylation sites leading to TORC nuclear localization (Bittinger et al., 2004; Screaton et al., 2004),

Distinctly, elevation of intracellular cAMP by treatment with forskolin, a bicyclic diterpene activating the enzyme adenylyl cyclase, inhibits TORC phosphorylation activity of SIK by activating PKA which was shown to phosphorylate SIK1 at Ser-577 (Katoh et al., 2004; Takemori and Okamoto, 2008).

In the nucleus, TORC binds to the leucine zipper of CREB and activates the CREB-dependent gene transcription (Screaton et al., 2004). p300/CBP recruitment of TORC to CREB is not dependent on phosphorylation of CREB at Ser-133, as p300/CBP does. However, TORCs enhance the association of $TAF_{II}130$ with CREB independent of Ser-133 phosphorylation (Conkright *et al.*, 2003). In the nucleus, TORC is shown to interact directly with CBP and they together mediate CREB target gene transcription (Ravnskjaer et al., 2007; Xu et al., 2007).

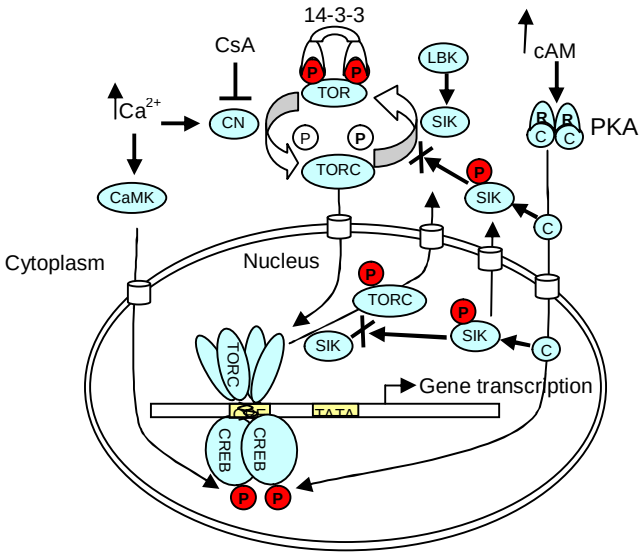

Figure 4: The nucleo-cytoplasmic shuttling of TORC (Screaton et al., 2004, Gonzalez et al., 1989, Takemori and Okamoto, 2008, Katoh et al., 2004 and 2006; Sun, P. et al, 1994).
In basal conditions TORC proteins are phosphorylated (at Ser171 of TORC2 or Ser163 of TORC3) by salt inducible kinase (SIK). The phospho-TORCs translocate from the nucleus to the cytoplasm where they are sequestered through interaction with 14-3-3 proteins.
Under stimulated condition, such as with Forskolin, the elevation of intracellular cAMP activates protein kinase A (PKA) and release the C subunit from tetramers of PKA. Diffusion of the C subunit into the nucleus leads to phosphorylation of CREB at Ser133, which activates CREB-directed transcription. In addition, PKA phosphorylates SIK1 and 2 at Ser577 and Ser587, respectively, which inhibit the phosphorylation of TORCs by SIKs. The PKA-induced phosphorylation of SIK also enhances SIK cytoplasmic redistribution.
In the calcium-dependent pathway, the increase of intracellular Ca^{2+} level activates the calcium/calmodulin-dependent phosphatase leading to dephosphorylation of TORCs and to accumulation of TORCs in nucleus where they enhance the phospho CREB-independent gene transcription. High Ca^{2+} levels also activate calcineurin (CN), calcium/calmodulin-dependent kinase (CaMK), which phosphorylates CREB at S133 and activates CREB-directed transcription.

TORC coactivators have been shown to be involved in many physiological and pathological processes. Regarding cell metabolism, TORC 2 modulates the signals of insulin and gluconeogeneis (Canettieri *et al.*, 2005; Koo *et al.*, 2005; Dentin *et al.*, 2007, 2008). TORCs regulate mitochondrial biogenesis and energy metabolism through activation of peroxisome proliferators-activated receptor γ coactivator 1α (PPAR1α) gene transcription (Wu *et al.*, 2006). TORCs are also transcriptional activators of steroidogenic acute regulatory protein (StAR), a mitochondrial protein involved in cholesterol metabolism (Takemori *et al.*, 2007b).

In addition, TORCs have also some roles in cell development and death. TORC2 regulates the development of B-cells (Kuraishy *et al.*, 2007) or induces the expression of antiapoptotic BCL2 gene (Kim et al., 2008). In the hippocampus TORC1 is necessary for late-phase long-term synaptic potentiation (Zhou *et al.*, 2006; Kovács *et al.*, 2007).

Other findings demonstrated the role of TORCs in tumorigenesis (Siu and Jin, 2007). TORC1 fused with MAML2, an oncoprotein found in malignant salivary gland tumor, promotes oncogenesis through activating CREB and its target genes (Coxon *et al.*, 2005; Wu *et al.*, 2005). TORCs are also essential coactivators of the Tax oncoprotein of human T-cell leukemia virus type 1 (HTLV-1) in the activation of viral long-terminal repeats (Koga *et al.*, 2004; Siu *et al.*, 2006). This coactivation is inhibited by BCL3 (Hishiki *et al.*, 2007).

1.4 Dual leucine zipper bearing kinase

The Dual leucine zipper bearing kinase (DLK) was first characterized from embryonic mouse kidney by Holzman *et al.* (1994) using degenerate oligonucleotide-based polymerase chain reaction cloning. DLK homologs identified in human and rat cell lines were termed ZPK (human zipper protein kinase) and MUK (MAPK upstream kinase), respectively. (Reddy and Pleasure 1994; Blouin *et al*. 1996; Hirai *et al*. 1996)

A DLK transcript is expressed in a tissue-specific and developmentally regulated pattern: it was identified in aldult ovary and most abundant in adult brain and all developmental stages of embryonic brain, kidney, lung, and heart (Holzman *et al.*, 1994); by studies on embryonic mice, DLK transcripts have been found in other organs such as skin, intestine, pancreas (Nadeau *et al*. 1997); DLK transcripts were detected in some organs of the adult mouse, most abundant in the central nervous system, as well as in the epithelial compartment of the stomach, intestine, liver and pancreas (Blouin *et al*. 1996).

At the protein level, DLK protein is predominantly present in synaptic termini of neurons, where it is bound to both the plasma membrane and cytosolic compartments (Mata *et al.* 1996); DLK protein and mRNA were also observed in mouse brain, human skin, (Germain *et al*. 2000; Hirai *et al*. 2005; Robitaille *et al*. 2005), mouse pancreatic islets of Langerhans (Oetjen *et al*. 2006) and in mesenteric white adipose and brown adipose tissue of mature mice (Couture *et al*. 2009).

In the nuclei of neurons, DLK was also detected in a small quantity (Merritt *et al*. 1999). DLK was shown to associate with the Golgi apparatus in fibroblasts (Douziech *et al*. 1999).

1.4.a Structure of DLK

The ZPK gene, a homolog of DLK, is located on human chromosome 12, which encodes a protein of 859 amino acids (Reddy *et al*. 1995). In the mouse, DLK gene is located on mouse chromosome 15 (Watanabe *et al*. 1997).

The mouse DLK protein is composed of 888 amino acids, which is recognized as a protein with an apparent molecular mass of 130 kDa through immunoblot by the anti-DLK immune serum. It has a kinase catalytic domain, a leucine zipper domain which includes two leucine/isoleucine motifs with a short spacer region in between, and the glycine- and proline- rich domains at both N-terminal and C-terminal ends (**Fig. 5**) (Holzman.L.B *et al.*1994).

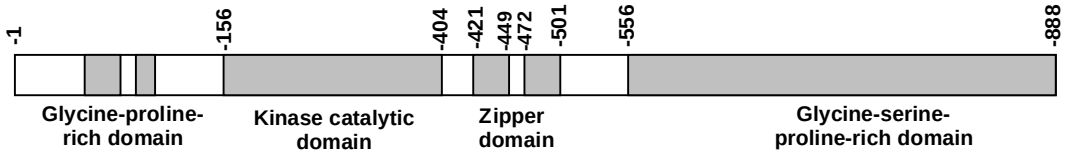

Figure 5: The structure of DLK protein (Holzman.L.B *et al.*, 1994).
DLK composes of two glycine-proline rich domains at both C- and N-termini. The kinase catalytic domain located from residue 156 to 405 includes 11 subdomains typical of serine/threonine and tyrosine protein kinase families. Two heptad repeats of nonaromatic hydrophobic amino acids of leucine zipper motifs located from residue 421 to 501 are separated by a spacer of 25 amino acids.

Sequence alignment showed that DLK is closely similar to the members of the Mixed Lineage Kinase family, a subfamily of Mitogen-activated protein kinase kinase kinase MAPKKK (Gallo and Johnson 2002). They share two common structural features: their catalytic domain has amino acid sequence similar to those of serine/threonine-specific and tyrosine-specific protein kinases; and they contain two Leucine/Isoleucine zipper motifs, which are separated by a short spacer region, located C-terminally near the catalytic domain (Dorow et al., 1993, Holzman et al., 1994). However, the catalytic domains of MLK members are more identical to each other than that of DLK. The zippers of DLK have 24% sequence identity and 46% sequence similarity to the zippers of MLK3, whereas MLK3 zippers are 61% identical and 76% similar to MLK1 and 2 (Holzman, L.B *et al.*, 1994).

DLK and LZK (leucine zipper bearing kinase, characterized by Sakuma et al., 1997), which share 90% identity in catalytic and leucine zipper domains, are suggested as a distinct subgroup of MLK subfamily. They lack both CRIB (Cdc42/Rac interactive binding)-motifs and a N-terminal SH3 (Src homology 3)-domains which are contained within the MLK1/2/3 proteins. Additionally, both have C-terminal sequences which are different from

each other and from those of MLK1/2/3 (Holzman et al., 1994, Sakuma et al., 1997, Nihalani et al., 2000).

Wallenda *and* DLK-1, two orthologs of DLK identified in *Drosophila melanogaster* and *Caenorhabditis elegans, respectively,* share sequence identity of 23% and 31% to mouse DLK, respectively.

1.4.b Characteristics and function of DLK

MLK members are characterized by an autocatalytic activity and leucine zipper-based homodimerization (Dorow et al. 1993, Gallo et al. 1994, Tanaka and Hanafusa, 1998). Given such features, Mata et al. (1996) experimented on COS7 cell line and showed that DLK autophosphorylates *in vivo* and migrate at 260 kDa on nonreducing SDS-PAGE, and the Flag-tagged DLK immunoprecipitated with the Myc-tagged DLK. This led to conclusion that DLK is able to autophosphorylate and homodimerize (Mata et al. 1996).

MLK members are composed of hybrid structures of catalytic domains and exhibit mostly serine/threonine-specific autocatalytic activity *in vitro* (Gallo et al., 1994). Likewise, DLK was shown to autophosphorylate on serine and threonine, but not tyrosine (Holzman et al., 1994). Additionally, DLK phosphorylates β-casein and myelin basic proteins on serines and threonines (Mata et al., 1996).

Studies on the ATP binding site of DLK showed that lysine-185 is important for kinase activity of DLK. The DLK K185A mutant, lysine-185 is mutated to alanine, has no autocatalytic activity and unable to phosphorylate β-casein. DLK homodimerization does not depend on its kinase catalytic activity (Mata et al. 1996).

Regulation of DLK activity by oligomerization and phosphorylation

About the mechanism that relate to the activation and regulation of DLK in mammalian cells is little known. The oligomerization and dimerization of DLK are suggested as important processes leading to DLK activation. The leucine zipper domain of DLK with an α-helical structure is necessary for DLK homodimerization. DLK P-P point mutant with disrupted α-helical structure in which the Leu-437 and Leu-463 were replaced by proline residues did not interact with the leucine zipper domain of DLK (Nihalani *et al*. 2000).

Homodimerization of DLK takes place through its leucine zipper domain, which leads to its autophosphorylation and the activation of JNK pathway (Nihalani *et al*. 2000). By binding

to the scaffold protein JIP-1 (JNK interacting protein) and MBIP (MAPK upstream kinase (MUK)-binding inhibitory protein) DLK remains in its monomeric and inactive form (Nihalani *et al*. 2000, Fukuyama *et al*. 2000). Especially, DLK leucine zipper domain interacts with only the leucine zipper of DLK, not other MLKs (Nihalani *et al*. 2000).

In addition, the phosphorylation status of DLK also regulates its activation. Oligomerization-dependent autophosphorylation of DLK results in activation of JNK signal pathway (Nihalani *et al*. 2000). Recently, Daviau et al. (2009) have observed that treatment of cells with vanadate, a tyrosine phosphatase inhibitor, or PDGF (platelet-derived growth factor) results in tyrosine phosphorylation of DLK and enhances DLK enzymatic activity.

In basal condition, phosphorylation of DLK is regulated by the serine/threonine phosphatase PP1 and PP2A: by treatment of cells with okadaic acid, an inhibitor of protein phosphatases PP1 and 2A, phosphorylated DLK is accummulated (Mata *et al*. 1996). Under basal condition, phosphorylation status of DLK is not effected by the calcineurin inhibitor Cyclosporin A (CsA). However, CsA inhibits the membrane depolarization-dependent dephosphorylation of DLK. By this way, increased intracellular calcium enhances dephosphorylation of DLK via calcineurin activation-related pathway (Mata et al. 1996).

Regulation by interaction and degradation

Several studies demonstrated that overexpressed DLK induces JNK activation in different cell lines (Fan *et al*. 1996; Hirai *et al*. 1996; Robitaille *et al*. 2005). In addition, DLK was observed to activate MKK4 (Mitogen-activated protein kinase kinase 4) and MKK7, which are upstream activators of JNK. Therefore, it is possible that JNK activation is modulated by DLK through MKK 4 and MKK7 (Hirai *et al*. 1997; Merritt *et al*. 1999). It is unclear how DLK induce MKK4 activation, however, MKK7 was shown to directly interact with DLK (Merritt *et al*. 1999).

In the kidney cell line COS-7, DLK remains in its monomeric, none-phosphorylated and inactivated form by the interaction with the scaffold protein IB/JIP-1 (islet brain/JNK interacting protein-1) (Nihalani et al., 2001; 2003). Phosphorylation of IB/JIP-1 by JNK results in the dissociation of DLK from the complex. DLK in its homodimerized and autophosphorylated form become catalytic active and phosphorylate MKK7, which activate the downstream Kinase JNK (Nihalani et al., 2001; 2003).

JNK contributes to the stability of DLK by a positive feedback loop mechanism. Apoptotic stimuli-induced stabilization of DLK (or JIP, MLK) is prevented by inhibition of JNK expression or activation (Xu *et al*. 2001; Xu *et al*. 2005).

Beside regulation by interaction, DLK was shown to undergo ubiquitination-mediated degradation.

In mouse fibroblasts, DLK stability is regulated by interaction with the stress-inducible heat shock protein Hsp70 and its co-chaperone CHIP, an E3 ubiquitin ligase. Okadaic acid-activated DLK wild type, not the kinase-deficient mutant, is proteasomally degraded by CHIP associated with Hsp70 (Daviau *et al*. 2006). The same regulatory process is conserved with DLK orthologs. In *Drosophila melanogaster* and *Caenorhabditis elegans*, DLK orthologs Wallenda and DLK-1, respectively, are downregulated by Highwire/RPM-1, an E3 ubiquitin ligase (Nakata *et al*. 2005; Collins *et al*. 2006; Wu *et al*. 2007).

In addition, DLK expression is also downregulated through proteasomal degradation by Phr1, the mammalian homolog of Highwire/RPM-1, (Lewcock *et al*. 2007); however, it is not clear yet because Phr1 mutant mice exhibited no increase in DLK detected in the central nervous system (Bloom *et al*. 2007).

Phenotypes

DLK -/- mice exhibit abnormal brain development and die perinatally due to the absence of anterior commissure and defects in axon growth and radial migration of neocortical pyramidal neurons (Hirai *et al*. 2006; Bloom *et al*. 2007). Axon degeneration induced by nerve injury is blocked by a gene-trap mutation of DLK in mice (Miller *et al*. 2009).

By mutation of DLK-1, an ortholog of DLK, in *C. elegans*, the axon regeneration of injured neurons was impaired (Hammarlund *et al*. 2009). Wallenda, another DLK ortholog, was also found to be involved in normal axon degeneration (Miller *et al*. 2009) and axonal transport (Horiuchi *et al*. 2007).

Protein Function

Like other members of MLK, DLK is an upstream activator of JNK (Rana *et al*. 1996; Tibbles *et al*. 1996; Cuenda *et al*. 1998; Hirai *et al*. 1998; Merritt *et al*. 1999). DLK has been shown to be involved in various pathway and processes in different cell lines. A number of studies showed that DLK activates JNK signalling pathway probable by phosphorylation of MKK4 and MKK7 (Fan *et al*. 1996; Hirai *et al*. 1996; Robitaille *et al*.

2005; Hirai *et al*. 1997; Merritt *et al.* 1999). After membrane depolarization in the HIT T15 cell line, DLK inhibits the transcriptional activity of CREB (Oetjen *et al*. 2006). In mouse NIH 3T3 fibroblasts, suppression of DLK by siRNA inhibits platelet derived growth factor (PDGF)-stimulated extracellular signal-regulated kinase (ERK) and causes Akt kinase activation (Daviau *et al*. 2009). DLK activates p46^{SAPK} and P38 ^{MAPK}, but not ERK2 (Fan *et al.*, 1996).

By overexpression of DLK, it has been shown that DLK is involved in apoptosis of pancreatic beta cells (Plaumann et al. 2008) and of neurons (Xu *et al*. 2001; Hirai *et al*. 2002; Chen *et al*. 2008). The terminal differentiation of human epidermal keratinocytes is regulated by DLK (Germain *et al*. 2000; Robitaille *et al*. 2005). Knockdown of DLK by siRNA blocks calphostin C-induced apoptosis of NIH 3T3 cells (Robitaille *et al*. 2008) or prevents adipocyte differentiation of 3T3-L1 cells (Couture *et al*. 2009).

DLK regulates radial migration and axon projection via modulating JNK activity (Hirai et al. 2006). DLK was demonstrated to promote degradation of injured neurons in adult mice (Miller *et al*. 2009). Two orthologs of DLK in *Drosophila melanogaster* and *Caenorhabditis elegans* exhibit the same feature: the DLK-deficient mutants protect injured neurons from degradation (Miller *et al*. 2009; Hammarlund *et al*. 2009). Additionally, a new regulatory feature of DLK has been indentified that it is involved in the viability of cancer cells (Schlabach *et al*. 2008).

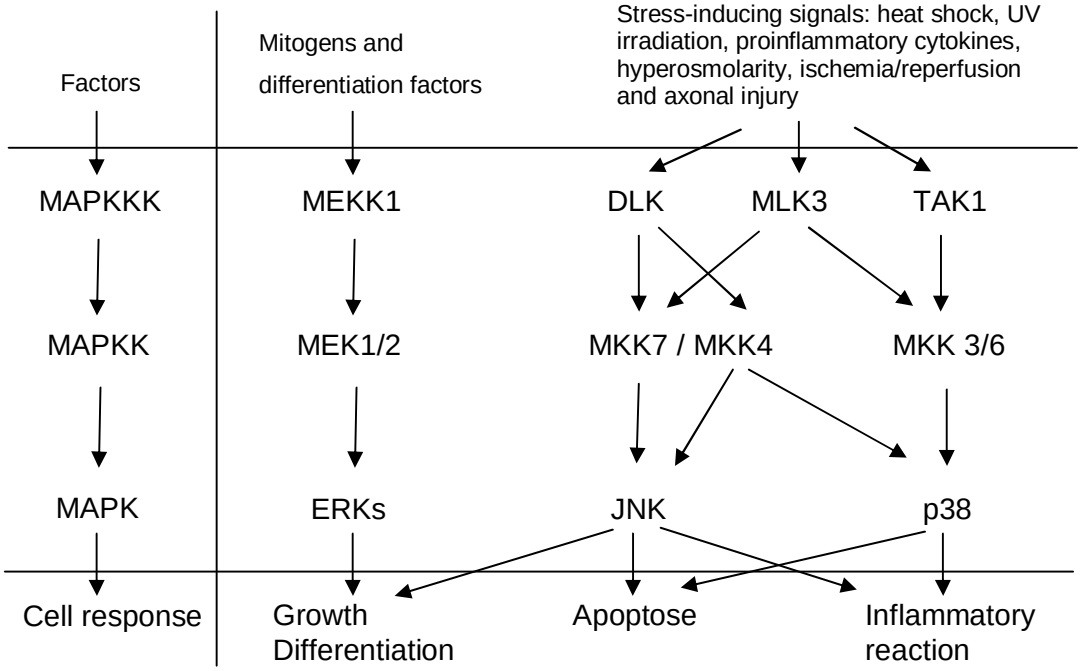

Figure 6: The role of DLK in MAPK signaling pathway (Garrington and Johnson 1999)
DLK is upstream in the MAPK pathway. By activating MKK7 DLK induces JNK-dependent pathways which confer different responses of the cells. Abbreviations were mentioned in the Abbreviation list.

Previous studies demonstrated that DLK reduces CRE- and CREB-directed transcription after membrane depolarization in the electrically excitable cell line HIT (Oetjen et al. 2006). Since DLK decreased CBP transcriptional activity either stimulated by membrane depolarization or under basal conditions, it was proposed that DLK inhibits membrane depolarization-induced CREB activity at least in part through inhibition of CBP (Oetjen et al. 2006). Given that in addition to CBP the recruitment of TORC is required for CREB transcriptional activity (Screaton et al. 2004), besides CBP TORC might be a target of DLK action. Therefore, in the present study the regulation of TORC by DLK was investigated.

1.5. Objectives of the study

The present study aimed to elucidate the molecular mechanism through which DLK regulates the activity of TORCs

To obtain this purpose the effects of DLK on TORCs have been investigated in aspects such as: the transcriptional activity, the nuclear accumulation, the phosphorylation and the recruitment to the promoter. Moreover, the interaction between DLK and TORC was examined *in vitro* and *in vivo*.

MATERIAL AND METHODS

2. MATERIAL

2.1. Equipments & Consumables

2.1.a. Equipment

Autoclave	Bioclav, Schütt Labortechnik, Göttingen, Germany
Balances	Sartorius AG, Göttingen, Germany
Cell culture hood	Lamin Air, Heraeus, Hanau, Germany
Centrifuge rotors	JA-20/JA-17/JA-14, Ti 70, Beckamnn GmbH, Krefeld, Germany
Centrifuges	Beckmann centrifuge GS-6 –Beckmann GmbH, München, Germany Beckmann J2HS centrifuge – Beckmann GmbH, München, Germany Beckmann L8-70M Ultracentrifuge – Beckmann GmbH, München, Germany Biofuge 15R – Heraeus / Thermo Electron Corp. Langenselbold, Germany Biofuge pico – Heraeus / Thermo Electron Corp., Langenselbold, Germany Eppendorf 5417R, Eppendorf GmbH, Hamburg, Germany Megafuge 1.0 – Heraeus Sepatech, Langenselbold, Germany
Cell Disrupter	Branson Sonifyer® B15 – Heinemann Ultraschall- u. Labortechnik, Schwäbisch Gmünd, Germany Dounce homogenizer (1 ml) – Kontes Glas Co., Vineland, USA
DNA Sequencer	ABI PRISM 3100 Genetic Analyzer – Applied Biosystems, Darmstadt, Germany ABI PRISM 7900 HT Sequence Detection System – Applied Biosystems, Darmstadt, Germany
Electrophoresis power supplier	Biometra® Standard Power Pack P25 – Whatman Biometra, Göttingen, Germany
Electrophoresis chamber (DNA)	Roth, Karlsruhe, Gemnany
Electrophoresis (proteins)	Electrophoresis chamber SE 600 – Hoefer Scientific Instruments, San Francisco, USA Mighty Small SE 250/SE 260, Hoefer Scientific Instruments, San Francisco, USA Mighty Small SE245 Dual Gel Caster, glasses, spacer, combs – Hoefer Scientific Intsruments, San Francisco, USA
Gel Dryer	DryGel Sr Slab Gel Dryer, SE1160 - Hoefer Scientific Instruments, San Francisco, USA
Incubators	Bacteria Incubator – Heraeus / Thermo Electron Corp., Langenselbold, Germany Innova™4300 Incubator – New Brunswick Scientific GmbH, Nürtingen,

	Germany Incubator STERI CULT 200 – Forma Scientific Inc., San Bruno, USA
Luminometer	AutoLumat LB 953, Berthold Technologies GmbH & Co.KG, Bad Wildbad, Germany
Micro pipettes	Gilson, France
Micro plate reader for GFP	Fusion™, Packard, Switzerland
Microscope	Zeiss Axiovert 200 microscope – Carl Zeiss AG, Oberkochen, Germany
Microwave oven	Phillips, Whirlpool, UK
PCR cycler	PCR cycler T-Gradient – Biometra, Göttingen, Germany PTC-200 Peltier Thermal Cycler – Biozym, Hess.-Oldendorf, Germany
pH meter	pH 523, Schütt Labortechnik, Göttingen, Germany
Phospho Image Scanner	BAS-MS 2325 phosphor-imager screen – FUJIFILM, purchased from raytest Isotopenmess-geräte GmbH, Straubenhardt, Germany BAS-1800II phosphor-imaging device – FUJIFILM, purchased from raytest Isotopenmess-geräte GmbH, Straubenhardt, Germany
Pipetus akku	Hirschmann Laborgeräte, Göttingen, Germany.
Rocking platform	Biometra, Göttingen, Germany Rocking platform Polymax 1040 – Heidolph Instruments GmbH & Co.KG, Schwabach, Germany
Rolling platform	TRM-V – IDL, Nidderau, Germany
Rotator	Rotator GFL 3025 – Gesellschaft für Labortechnik GmbH, Burgwedel, Germany
Spectrophotometer	Shimadzu UV-160, Duisburg, Germany
Semi-dry transfer device	Bender & Hobein, Switzerland
Shaking platform	Certomat®R shaking platform – Sartorius, Göttingen, Germany
Temperature regulator	Certomat®HK temperature-regulating device – Sartorius, Göttingen, Germany
Thermomixer	Eppendorf, Hamburg, Germany
Tube Sealer	Beckmann Tube Sealer – Beckmann GmbH, München, Germany.
Vacuum Pump	KnF Laboport, Neuberger, Germany
Waterpump	Schütt Labortechnik, Göttingen, Germany

Waterbath	W. Krannich GmbH, Göttingen, Germany
X-ray Cassettes	Eastman KODAK Company, New York, USA

2.1.b. Consumables

Cell culture dishes	Falcon™ 6 cm cell culture dishes and BD Falcon™ 15 cm cell culture dishes – Schuett24 GmbH, Göttingen, Germany
Coverslips	Nunc™ Thermanox Plastic Coverslips, 25 mm diameter – Nunc, Roskilde, Denmark
Disposable cell scraper	Sarstedt, Nümbrecht, Germany
Dialysis tubes	GIBCO BRL, Karlsruhe, Germany
ECL- X ray films	Amersham Biosciences, Freiburg, Germany
Eppendorf tubes	Eppendorf, Hamburg, Germany
15, 50 ml tubes	Greiner Bio-one, Solingen, Germany
Filter units	Sartolab, Biofiltronic GmbH, Nörten-Hardenberg, Germany
Glass pipettes	WU, Mainz, Germany
Glassware	Schott Duran, Mainz, Germany
Gloves	Paul Hartmann AG, Heidenheim, Germany
Microscope slides 76x26mm	Roth, Karlsruhe, Germany
Microplates	96-well microplates, U-shaped bottom – Sarstedt, Nümbrecht, Germany 96-well Millipore plates (Millipore-MAHV N45) – Millipore GmbH, Schwalbach, Germany 384-well PCR plate – Applied Biosystems, Darmstadt, Germany
Nitrocellulose membrane (0.45µm)	Hybond™, ECL™, Amersham Biosciences Freiburg, Germany
Parafilm	Parafilm® M – Brand GmbH & Co KG, Wertheim, Germany
Pasteur pipettes	Brand, Wertheim / Main, Germany
Plates (agar)	Greiner, Frickenhausen, Germany
Pipette tips	Sarstedt, Nümbrecht, Germany
Plastic tubes for luminometer (5 ml)	Sarstedt, Nümbrecht, Germany

Quick Seal Tubes	Beckmann GmbH, Munich, Germany
Spectrophotometer cuvettes (plastic)	Sarstedt, Nümbrecht, Germany
Spectrophotometer cuvettes (quartz)	Sarstedt, Nümbrecht, Germany
Syringes	BD Discardit II, Beckton Dickinson, Spain
Syringe filters	Sartorius, Göttingen, Germany
Syringe needles	Sterican, B/BRAUN, Melsungen, Germany
Tips	Tips (10 µL) - Eppendorf AG, Hamburg, Germany Tips (200 µL, 1 mL) - Sarstedt, Nümbrecht, Germany
Ultracentrifuge tubes	Beckman GmbH, Krefeld, Germany
Whatman paper P81	Whatman, Maidstone, UK
6-well plates	Nunc, Roskilde, Denmark

2.2. Chemicals

2.2.a. Substances

Amersham Biosciences GmbH (Freiburg, Germany): DEAE-Dextran, Sephadex G50

AppliChem GmbH (Darmstadt, Germany): Albumin fraction V, Acetic acid, Acrylamide, Agar, Ampicillin, Ammoniumpersulfate (APS), Aprotinin, ATP, Bis-acrylamide, Boric acid, Bromide, Bovine serum albumin (BSA), Chlorophorm, Cesium chloride, Dimethyl sulfoxide (DMSO), Dithiothreitol (DTT), D-saccharose, EDTA, EGTA, Ethanol, 37% formaldehyde, Glucose, 87% glycerol, Glycine, Glycylglycine, HEPES, Hydrochloric Acid (HCl), Imidazol , Iso-amylalcohol, Iso-propanol, Isopropyl-β-D-thiogalactoside (IPTG), Leupeptin, Low fat milk, Lysozyme, Magnesium chloride ($MgCl_2$), Magnesium sulphate ($MgSO_4$), Manganese chloride $MnCl_2(H_2O)_4$, Methanol, β-Mercaptoethanol, Pepton from casein, Potassium chloride (KCl), Potassium diphosphate, Potassium-di-hydrogenphosphate (KH_2PO_4), Di-potassium-hydrogenphosphate (K_2HPO_4), Pepstatin A, Pepton from casein, Phenylmethylsulfonylfluorid PMSF, Ponceau S solution, Potassium di-hydrogen phosphate (KH_2PO_4), Polyethylene glycol 6000 (PEG 6000), Skim milk, Sodium acetate, Sodium borohydrate, Sodium carbonate (Na_2CO_3), Sodium bicarbonate, Sodium chloride, Sodium-dodecylsulfate (SDS), Sodiumhydrogencarbonate ($NaHCO_3$), Sodiumhydroxide (NaOH), Sodium-di-hydrogenphosphate ($NaH_2PO_4 \cdot 2H_2O$), Di-Sodium-hydrogenphosphate (Na_2HPO_4), TEMED, Tris base, Tween 20, Tween 80, β-mercaptoethanol, Zinc chloride.

Biomol GmbH (Hamburg, Germany): Phenol (liquefied and Tris saturated)
Biontex (München, Germany): Metafectene
Hartmann Analytics (Braunschweig, Germany): [^{32}P]- γ-ATP, L-[^{35}S]-Methionine
Invitrogen (Karlsruhe, Germany): Agarose (Electrophoresis Grade)
Kodak AG (Stuttgart, Germany): GBX Fixation solution, LX24 x-ray developer
MANAC Incorporated (Fukuyama, Hiroshima, Japan): Phos-tag™ Acrylamide AAL-107
Merck (Darmstadt, Germany): n-Butanol, Nonidet-P40
Promega GmbH (Mannheim, Germany): D-Luciferin
Qiagen: Ni-TNT-Agarose beads
Roche (Mannheim, Germany): ATP, GTP, CTP, TTP
Sigma-Aldrich Chemie GmbH (Harmburg, Germany): Bromphenolblue, Sepharose CL-4B, Coomassie brilliant blue, Cyclosporin A, Deoxycholic acid, Ethidium bromide, Forskolin Glutathione-agarose beads, L-Glutathione, Lithiumchloride (LiCl), Chloroamphenicol, 25 % glutaraldehyde, Okadaic acid, Protein A agarose, Sodium fluoride, Sodium orthovanadate, Triton X-100, Xylene cyanol FF

2.2.b. Stock solutions and buffers

2.2.b.I. Stock solutions

All stock solutions were prepared in double-destilled H_2O if not stated differently.

Ampicillin	5 % (w/v)	0.5 g / 10 ml
Aprotinin	50 μg/μl	5mg/100 μl of 10 mM Tris/HCl pH8.0
APS	10 % (w/v)	1 g / 10 ml
ATP	200 μM	1.1 g / 9.075 ml distilled water
Chloroform / isoamylalcohol	1/24 (v/v)	1ml / 24 ml
Chloramphenicol		34 mg /ml 99% EtOH
Cyclosporin A (CsA)	830μM	1mg in 0.1ml 99% EtOH, plus 20 μl Tween 80, drop in 1ml RPMI
Dithiothreitol (DTT)	1 M	1.542 g / 10 ml
EDTA pH 8.0	0.5 M	46.53 g / 250 ml
EGTA pH 7.8 – 8.0	180 mM	3.423 g / 50 ml
Ethidium Bromide		100 mg / 10 ml
Forskolin	10 mM	1 mg / 243.6 µl DMSO
Hepes pH 7.5	1 M	59.58 g / 250 ml
Glucose	0.5 M	9 g / 100 ml
Glycine	1 M	7.507 g / 100 ml
Glycylglycine pH 7.8	0.5 M	3.303 g / 50 ml

Kanamycin	5 % (w/v)	0.5 g / 10 ml
KCl	2 M	2.98 g / 20 ml
K_2HPO_4	0.5 M	4.35 g / 50 ml
KH_2PO_4	100 mM	3.402 g / 250 ml
LiCl	4 M	1.696 g / 10 ml
Leupeptin	50 μg/μl	5 mg / 100 μl of 10 mM Tris/HCl pH8.0
$MgCl_2$	1 M	5.08 g / 25 ml
$MgSO_4$	1 M	12.324 g / 50 ml
$MnCl_2$	10 mM	0.1 g of $MnCl_2$ $(H_2O)_4$ / 50 ml
NaCl	0.5 M	0.292 g / 10 ml
Na_2HPO_4	75 mM	1.33 g / 100 ml
NaH_2PO_4	75 mM	1.33 g / 100 ml
NaOH	1 N	4 g / 100 ml
Phos-tag™ AAL solution	5 mM	10 mg / 3.3 ml
Penicillin/Streptomycin	10,000 U/ml / 10,000 μg/ml (ready to use solution-GIBCO)	
PMSF	200 mM	348 mg / 10 ml 99%-ethanol
Pepstatin	50 μg/μl	5 mg / 100 μl of 10 mM DMSO
RNase	0.01% (w/v)	0.1 mg / ml
SDS	10% (w/v)	25 g / 250 ml
Tris/HCl	1 M	60.57 g / 500 ml

(pH of Tris/HCl was adjusted to 6.8, 7.4, 7.5, or 8.0 with 6 N HCl)

The following stocks were aliquoted and stored at -20°C: Aprotinin, APS, ATP, DTT, Forskolin, Leupeptin, Pepstatin, Penicillin/Streptomycin. Cyclosporin A was kept at 4°C. The others were stored at room temperature.

2.2.b.II. Buffers

Routinely used buffers and media were prepared as follows:

Stocks of Tris-base and HEPES were adjusted to different pH using hydrochloric acid (HCl).

PBS pH 7.4	*1x*	*1 L*
NaCl	140 mM	8.00 g
KCl	2.5 mM	0.20 g
Na_2HPO_4	8.1 mM	1.44 g
KH_2PO_4	1.5 mM	0.24 g

The buffer was autoclaved and stored at room temperature.

2.3. Biological Material

2.3.a. Kits

Big Dye® Terminator v1.1 Cycle Sequencing Kit – *Applied Biosystems, Darmstadt, Germany*

Bradford Dye Reagent for Protein Assays – *Biorad, München, Germany*

Easy Pure® DNA purification kit – *Biozym, Hess.-Oldendorf, Germany*

ECL Western Blotting Analysis System – *Amersham Biosciences, Freiburg, Germany*

TaqMan® Gene Expression Master Mix – *Applied Biosystems, Darmstadt, Germany*

TNT T7 Coupled Reticulocyte Lysate System – *Promega, Mannheim, Germany*

Vectashield® Mounting Medium with DAPI – *Vector Laboratories, Burlingame, USA*

2.3.b. Procaryotic and eukaryotic cell lines

Prokaryotic cell lines

Chemically competent *Escherichia coli* strain DH5α was used for plasmid amplification. Chemically competent *Escherichia coli* strain BL-21 was used for expression of recombinant GST-fusion proteins and His-tagged proteins.

Eukaryotic cell lines

Hamster insulinoma tumor cells, clone HIT-T15 (Santerre et al., 1981), were used for all experiments in this thesis.

2.3.c. Media and material for cell cultures

Gibco BRL (Karlsruhe, Germany): Agar, fetal calf serum, horse serum, Penicillin / Streptomycin, Trypsin / EDTA, RPMI medium

AppliChem GmbH (Darmstadt, Germany): Yeast extract

LB medium		*1000 ml*
NaCl	1 % (w/v)	10 g
Pepton	1 % (w/v)	10 g
Yeast extract	0.5 % (w/v)	5 g
Ampicillin (or Kanamycin)	50 µg / ml	1000 µl 5 % stock solution (added after autoclaving of the LB medium)

The LB medium was autoclaved and stored at room temperature. Ampicillin or kanamycin was added freshly to the LB medium before use. LB medium was used for the culture of bacteria.

RPMI complete medium		*500 ml*
RPMI Medium		450 ml
Fetal calf serum	10 % (v/v)	50 ml
Horse serum	5 % (v/v)	25 ml
Penicillin / streptomycin	1 % (v/v)	5 ml

The RPMI complete medium was prepared under sterile condition and stored at 4°C. RPMI medium was used for culture of eukaryotic cell line.

2.3.d. Plasmids

2.3.d.I. Expression vectors

The coding sequence for human CREB is deposited in the GenBank database under GenBankAccession Number M27691.

The coding sequence for mouse DLK is deposited in the GenBank database under GenBankAccession Number NM009582.

The coding sequences for full lengths or fragments of human TORC1, TORC2, and TORC3 are based on the sequences provided kindly by Mark Labow (Novartis Pharmaceuticals, Suffern, NY, USA) and deposited in the GenBank database under GenBankAccession Numbers AY360171, AY360172, and AY360173, respectively.

The coding sequences for full lengths of mouse TORC1 is deposited in the GenBank database under GenBankAccession Numbers NM_001004062.

Mammalian expression vectors

The plasmids for mammalian expression used in this work include: pcDNA3.1 (Invitrogen, Karlsruhe, Germany), pSG424 (Sadowski and Ptashne, 1989), pHA.CMV (Clontech, kindly given by Dr. Tran Ngoc Tuoc, Göttingen).

The expression vectors for flag-TORC1 wild-type and flag-TORC1 S151A in which Ser-151 was changed to alanine (both have mouse origin) were kindly given by Dr. Robert A. Screaton (University of Ottawa, Canada). Mouse TORC1 contains 630 amino acids.

The construct *TORC1* encodes for the full-length human TORC1 comprising 651 amino acids. The coding sequence was cloned into the mammalian expression vector pcDNA3.1 by use of the restriction sites *Bam*HI and *Xba*I (Heinrich et al., 2009).

The plasmids *GAL4-TORC1, GAL4-TORC1*$_{1-44}$*, GAL4-TORC1*$_{\Delta 44}$, GAL4–TORC1 S167A encode the full-length human TORC1, the first 44 amino acids of TORC1, the truncated form of TORC1 without the first 44 amino acids and the full-length TORC1 with one point mutation where the serine at 167 was substituted by alanine, respectively, fused C-terminally to the DNA-binding domain of the yeast transcription factor GAL4 (amino acids 1-147). The coding sequence of TORC1, either full-length, the first 44 amino acids, the truncated form of TORC1 without the first 44 amino acids or the point mutation TORC1 S167A was subcloned into the mammalian expression vector pSG424 by use of the restriction sites *BamH*I and *Xba*I.

The construct HA-TORC1 encodes for the full-length human TORC1 containing a hemagglutinin (HA) epitope (YPYDVPDYA) between the first and the second amino acid of TORC1. The HA epitope was inserted by use of a modified primer. The coding sequence was subcloned into pHA.CMV vector using restriction sites *EcoRI* and *Xho*I.

The expression construct GAL4-*TORC2* and GAL4-*TORC2* S171A encodes the full-length human TORC2 comprising 694 amino acids and the full-length TORC2 with one point mutation where the serine at 171 was substituted by alanine fused C-terminally to the DNA-binding domain of the yeast transcription factor GAL4 (amino acids 1-147). The coding sequence of TORC2 wild-type and TORC2 S171A was subcloned into the mammalian expression vector pSG424 by use of the restriction sites *Kpn*I and *Xba*I (for TORC2 wild-type), and *EcoR*I and *Xba*I (for TORC2 S171A).

The construct *GAL4-TORC3* encodes the human full-length TORC3 protein comprising 620 amino acids fused C-terminally to the DNA-binding domain of GAL4 (amino acids 1-147). The coding sequence was subcloned into the vector pSG424 using the restriction sites *Kpn*I and *Xba*I.

The plasmid flag-DLK wild-type encodes the full-length mouse-DLK comprising 888 amino acids. The coding sequence was cloned into the mammalian expression vector pcDNA3.1 by use of the restriction sites *HindIII* and *Xba*I (Holzman et al., 1994).

Flag-DLK K185A encodes the full-length mouse-DLK with one point mutation where the lysine at 185 was substituted by alanine. The coding sequence was cloned into the mammalian expression vector pcDNA3.1 by use of the restriction sites *HindIII* and *Xba*I (Mata et al., 1996).

The plasmid Flag-DLK P-P encodes the full-length mouse-DLK with two point mutations where the leucines at 437 and 463 were substituted by prolines. The coding sequence was cloned into the mammalian expression vector pcDNA3.1 by use of the restriction sites *HindIII* and *Xba*I (Nihalani et al., 2000).

The coding sequences of CREB wild-type and CREB R300A were used as templates in the TNT system-based protein synthesis.

The pGFPtpz-cmv® control vector (Caberra-Packard, Dreieich, Germany) was used to check for transfection efficiency in luciferase reporter gene assays. This expression vector codes for the green fluorescent protein (GFP) variant topaz under control of the cyto-megalo-virus promoter.

The pBluescript (Stratagene, La Jolla, CA, USA) was used to adjust the amount of DNA in all transient transfection.

Bacterial expression vectors

The vectors for bacterial expression used in this work include: pGEX2T (GE Healthcare, Munich, Germany) and pET28b(+) (Novagene, kindly given by Prof. Dr. Frauke Melchior, Heidelberg).

The construct His-TORC1 wild-type, His-TORC1Δ44, His-TORC1 S167A, His-TORC2 wild-type and His-TORC2 S171A were used to express recombinant His-tagged proteins in E.coli. The coding sequences of TORC1 and TORC2 wild-type or mutants were amplified by PCR and subcloned into the bacterial expression vector pET28b (+) vector using restriction sites *Xba*I and *Xho*I.

The expression construct *GST-TORC1$_{1-44}$ was* used to express recombinant GST-fusion protein of TORC1 (1-44) in *E.coli*. The coding sequences of TORC1 (1-44) was subcloned into the bacterial expression vector pGEX-2T using restriction sites *BamH*I and *XbaI*.

Table 1: Mammalian and bacterial expression constructs.

The table lists all constructs used in the present work. The constructs kindly given by other authours were put in “provided by” column. The other constructs were generated newly using PCR cloning with primers and templates as indicated in table 2.

Name of constructs	Source	Vector	Notes	provided by
TORC1	homo sapiens	pcDNA3.1	full length	Annette Heinrich
HA-TORC1	homo sapiens	pHA.CMV	HA-tag	
Flag-TORC1	Mus musculus			Rob Screaton
Flag-TORC1 S151A	Mus musculus			Rob Screaton
GAL4-TORC1	homo sapiens	pSG424	full length	Ulrike Böer
GAL4-TORC1 S167A	homo sapiens	pSG424	full length	
GAL4-TORC1$_{\Delta 44}$	homo sapiens	pSG424	aa 45-651	
GAL4-TORC1$_{1-44}$	homo sapiens	pSG424	aa 1-44	Ulrike Böer
His-TORC1	homo sapiens	pET28b(+)	His-tag	
His-TORC1 S167A	homo sapiens	pET28b(+)	His-tag	
His- TORC1$_{\Delta 44}$	homo sapiens	pET28b(+)	His-tag	
GST- TORC1$_{1-44}$	homo sapiens	pGEX2T	GST-fusion	
GAL4-TORC2	homo sapiens	pSG424	full length	Ulrike Böer
GAL4-TORC2 S171A	homo sapiens	pSG424	full length	
His-TORC2	homo sapiens	pET28b(+)	His-tag	
His-TORC2 S171A	homo sapiens	pET28b(+)	His-tag	
GAL4-TORC3	homo sapiens	pSG424	full length	Ulrike Böer
CREB	homo sapiens	pcDNA3.1	aa 1-327	Ulrike Böer
CREB-R300A	homo sapiens	pcDNA3.1	Arg300 --> Ala	Ulrike Böer
Flag-DLK	Mus musculus	pcDNA3.1	full length	Lawrence Holzman
Flag-DLK K185A	Mus musculus	pcDNA3.1	Lys300 --> Ala	Lawrence Holzman
Flag-DLK P-P	Mus musculus	pcDNA3.1	Leu437 --> Ala Leu463 --> Ala	Lawrence Holzman

2.3.d.II. Luciferase reporter gene constructs

The expression vector *4xsomCRE-Luc* (Oetjen et al., 1994) includes four repeats of the CRE-containing region -58 to -31 of the rat somatostatin gene in front of the truncated thymidine kinase promoter (-81 to +52) of the herpes simplex virus (Nordeen, 1988).
The plasmid *G5E1B-Luc* (Kruger et al., 1997) contains five repeats of an enhancer element, identified in yeast as binding site for the yeast transcription factor GAL4 (Webster et al., 1988), in front of the viral E1B TATA box (Lillie and Green, 1989; Liu and Green, 1990).
The plasmid -65SMSLuc (Schwaninger et al. 1993) includes the somatostatin gene sequence of -65SMSCAT (Powers et al., 1989) which was subcloned into the BamHI-SmaI sites of pXP2 plasmid (Nordeen, 1988).

2.3.e. Oligonucleotides

2.3.e.I. Oligonucleotides used for PCR cloning

The primers used to generate new constructs in the present work are listed in table 3. Synthetic oligonucleotides were purchased from Eurofins MWG Operon (Ebersberg, Germany). The sequences in 5' – 3' direction of the primer used for PCR cloning procedures (3.1.a.I) and site-directed mutagenesis (3.1.a.II) are indicated.

Table 2: The primer pairs (forward and reverse) used to generate the constructs in the present work.

The names of plasmids are given in the *construct* column. Sequences of oligonucleotides are presented in 5' – 3' direction. The primer direction is indicated: forward (for) and reverse (rev). The restriction sites are underlined and are indicated in the column *restr. site*. The sequences complemented with templates were shown in bolds and italics. The point mutation was made by substitution of nucleotides showed in bolds and shade. Templates were shown in the right column.

Constructs	Direction	Primers	Restr. site	Templates
HA-TORC1	For	GCG G GAA TTC CC ***ATG GCG ACT TCG AAC AAT CCG***	*Eco*RI	TORC1 wild-type
	Rev	GCG CTC GAG TTA ***CAG GCG GTC CAT CCG GAA GG***	*Xho*I	
GAL4-TORC1 S167A (*)	For	GCG GGA TCC CC ***ATG GCG ACT TCG AAC AAT CCG CGG***	*BamH*I	TORC1 S167A
	Rev	GCG TCT AGA TTA ***CAG GCG GTC CAT CCG GAA GGT***	*Xba*I	
GAL4-TORC1$_{\Delta 44}$	For	GCG GGA TCC CC ***CAG CTC CAG AAA TCC CAG TAC***	*BamH*I	TORC1 wild-type
	Rev	GCG TCT AGA TTA ***CAG GCG GTC CAT CCG GAA GGT***	*Xba*I	
His-TORC1	For	GCG G TCT AGA ***ATG GCG ACT TCG AAC AAT CCG***	*Xba*I	TORC1 wild-type
	Rev	GCG CTC GAG ***CAG GCG GTC CAT CCG GAA GG***	*Xho*I	
His-TORC1 S167A	For	GCG G TCT AGA ***ATG GCG ACT TCG AAC AAT CCG***	*Xba*I	TORC1 S167A
	Rev	GCG CTC GAG ***CAG GCG GTC CAT CCG GAA GG***	*Xho*I	
His-TORC1$_{\Delta 44}$	For	GCG G TCT AGA ***CAG CTC CAG AAA TCC CAG TAC***	*Xba*I	TORC1 wild-type
	Rev	GCG CTC GAG ***CAG GCG GTC CAT CCG GAA GG***	*Xho*I	
GST- *TORC1$_{1-44}$*	For	GC GGG ATC CCC ***ATG GCG ACT TCG AAC AAT CCG CGG***	*BamH*I	TORC1 wild-type
	Rev	GCG CTC GAG ***CTG GAG CCG CGC GGC CCG C***	*Xho*I	
GAL4-TORC2 S171A (**)	For	GCG GAA TTC CCC ***ATG GCG ACG TCG GGG GCG AAC***	*Eco*RI	TORC2 wild-type
	Rev	CAG AGT C**AG C**GC TTG TCC TGT TAA GTG CAG		
	For	CAG GAC AAG C**GC T**GA CTC TGC CCT TCA TAC		
	Rev	GCG TCT AGA TTA ***TTG GAG CCG GTC ACT GCG GAA***	*Xba*I	
His-TORC2	For	GCG G TCT AGA ***ATG GCG ACG TCG GGG GCG AAC***	*Xba*I	TORC2 wild-type
	Rev	GCG CTC GAG ***TTG GAG CCG GTC ACT GCG GAA***	*Xho*I	
His-TORC2 S171A	For	GCG G TCT AGA ***ATG GCG ACG TCG GGG GCG AAC***	*Xba*I	TORC2 S171A (above)
	Rev	GCG CTC GAG ***TTG GAG CCG GTC ACT GCG GAA***	*Xho*I	

(*)The template TORC1 S167A was kindly given by Robert Screaton

(**)The construct which was generated by site directed mutagenesis.

Synthetic oligonucleotides used for site-directed mutagenesis by primerless PCR (3.1.a.II) were designed complementarily to each other. The mutation TORC2 S171A was made by substitution of the serine residue (S) at position 171 in the coding sequence of human TORC2 with alanine residue (A): codon TCT (S) changed to GCT (A).

2.3.e.II. Oligonucleotides used for quantitative real-time PCR

Primers used for quantitative real-time PCR in ChIP-assays as well as the TaqMan™ probes are listed in table 7. Primers CRE_ChIP_f and CRE_ChIP_r and the TaqMan™ probe CRE were designed to quantify amounts of 4xsomCRE-Luc plasmid (2.3.d.II) by quantitative real-time PCR (3.14). The primer CRE_ChIP_f anneals upstream of the inserted oligomerized CRE-promoter sequence to the bases 6071 – 6086 of the pT81 vector. The primer CRE_ChIP_r anneals downstream of the oligomerized CRE-promoter sequence to the bases +1 – -14 of the thymidine kinase promoter. The TaqMan™ probe CRE anneals to bases -46 – -24 of thymidine kinase promoter.

Table 3: Oligonucleotides and TaqMan™ probes for quantitative real-time PCR.

Sequences of synthetic primers and TaqMan™ probes are presented in 5' – 3' direction. The direction of the primer with respect to the coding sequence to be analyzed is indicated: forward (for) and reverse (rev). Labelling of the TaqMan™ probe with fluorophore and quencher is indicated.

Name	**Direction**	**Sequence**
CRE_ChIP-f	for	GCAATAGCATCACAAATTTCACAAA
CRE_ChIP-r	rev	CCGCCCCGACTGCAT
TaqMan™ probe CRE	for	CGAATTCGCCGGATCTCGAGCTC modifications: 5'–Fluorescein; 3'–TAMRA

2.3.f. Enzymes and buffers

All the enzymes and buffers were purchased from Fermentas Life Sciences Ltd., St. Leon-Rot, Germany

Restriction enzymes

The restriction enzymes were used in the present work include: *BamH*I, *EcoR*I, *Hind*III, *Kpn*I, *Xba*I and *Xho*I. Each has an activity of 10 U/µl. The buffer Tango™ yellow was used in combination with these enzymes according to the instructions of the manufacturer.

Modifying enzymes

Modifying enzymes were used in the present work include: *Pfu* DNA Polymerase (2.5 U/µl), T4 DNA Ligase (1 U/µl), RNase A (10 mg/ µl), Proteinase K (10 µg/µl). Corresponding buffers were used together with these enzymes according to the instructions of the manufacturer.

2.3.g. DNA and protein markers

All DNA and protein markers were purchased from Fermentas Life Sciences (St. Leon-Rot, Germany).

DNA-ladders and loading buffer include: GeneRuler™ 100bp DNA Ladder, GeneRuler™ 1kb DNA Ladder, 6x DNA loading buffer

Protein markers: PageRuler™ Prestained Protein Ladder, PageRuler™ Plus Prestained Protein Ladder

2.3.h. Antibodies

The antibodies used in the present work are listed in **Table 4**

Table 4: Primary and secondary antibodies.

The basic information of antibodies used in the present work. The dilutions or amounts of the primary and secondary antibodies as used in the present work are given for the different application.

Name of antibodies	**Source**	**Clone**	**Application**	**Dilution/amount**	**Company / reference**
panTORC (1-42)	rabbit	polyclonal	Immuno-Cytochemistry and Western blot	1:1,500	Calbiochem, Darmstadt, Germany
TORC1	rabbit	polyclonal	Western blot	1:2,000	Cell signaling, Beverly, MA, USA
Phospho TORC1 (Ser-151)	rabbit	polyclonal	Western blot	1:2,000	Cell signaling, Beverly, MA, USA
DLK	rabbit	polyclonal	Western blot	1:2,000	(Holzman et al. 1994)
FLAG M2	mouse	monoclonal	CoIP	10 µg	Sigma Aldrich, Hamburg, Germany
anti-HA	rabbit	polyclonal	ChIP	10 µg	Sigma Aldrich, Hamburg, Germany
GAPDH (FL-335)	rabbit	polyclonal	Western blot	1:1,000	Santa Cruz Biotechnology, Heidelberg, Germany
mouse IgG-HRP (linked to horseradish peroxidase)	sheep		Western blot	1:10,000	Amersham Biosciences, Freiburg, Germany
rabbit IgG-HRP (linked to horseradish peroxidase)	donkey		Western blot	1:10,000	Amersham Biosciences, Freiburg, Germany
mouse IgG-TRITC (linked to tetramethylrhodamin-5-isothiocyanate)	rabbit	polyclonal	Immuno-cytochemistry	1:50	Invitrogen, Karlsruhe, Germany
rabbit IgG-Alexa®488 (linked to AlexaFluor® 488)	goat	polyclonal	Immuno-cytochemistry	1:50	Invitrogen, Karlsruhe, Germany

The panTORC (1-42) antibody is directed against the first 42 amino acids of TORC. These amino acids are highly conserved among the three isoforms. Therefore, all TORCs are recognized by this antibody.

The TORC1 antibody was raised specifically against TORC1.

The Phospho-TORC1 (Ser151) antibody detects specifically TORC1 phosphorylated on serine 151 (mouse-TORC1). In the present work, this antibody is used to detect phosphorylation of human-TORC1 at serine-167 (equivalent as serine-151 of mouse-TORC1).

The DLK antibody was raised against the C-terminal 223 amino acids of mouse DLK.

The FLAG M2 antibody detects the proteins tagged with the FLAG epitope DYKDDDDK.

The anti-HA antibody detects the proteins tagged with the hemagglutinin (HA) epitope YPYDVPDYA.

The antibody GAPDH (FL-335) is used to detect full-length human glutaraldehyde-3-phosphate dehydrogenase (amino acids 1-335).

The mouse and rabbit IgG-HRP antibodies are used as secondary antibodies for immunolabelling in Western blots. These antibodies detect the primary ones with mouse and rabbit source, respectively.

The rabbit IgG-Alexa®488 antibody was used as secondary antibody for immunocytochemistry assay. This antibody detects primary antibodies raised in rabbit.

3. METHODS

3.1. Generation of Plasmid DNA

3.1.a. PCR cloning and site-directed mutagenesis

3.1.a.II. Polymerase chain reaction (PCR)

The DNA sequence of interest is amplified by a polymerase chain reaction (PCR) using specific primers and a heating program. First, by heating to 95°C, the double-strands of template DNA are separated. By lowering the temperature closely to the melting point of primers, the primers anneal with the template. Afterwards, the temperature is increased to 72°C, the temperature at which thermostable DNA polymerase starts synthesizing new DNA sequences based on the template. The process is repeated several times, thereby amplifying the DNA exponentially.

The PCR programme is:

Step	Reactions	Time	Temperature
1.	Initial denaturation	5 min	95°C
2.	Denaturation	1 min	95°C
3.	Annealing	45 sec	depending on melting temperature of the primers
4.	Elongation	30 sec – 2min (depending on the length of desired DNA)	72°C
5.	Final elongation	10 min	72°C
6.	Store	∞	4°C

Steps 2 to 4 were repeated 25 - 35 times.

In the present work, *Pfu* DNA polymerase was used. PCR was performed using the gradient cycler T-Gradient.

DNA templates were diluted to a concentration of 50 ng / µl using sterile H_2O. The primers were diluted to concentration of 10 mmol / µl.

Prepare the dNTP-mix as below:

dNTPs	*10 mM*	*400 µl*	
dATP	10 mM	40	µl of 100 mM dATP
dGTP	10 mM	40	µl of 100 mM dGTP
dCTP	10 mM	40	µl of 100 mM dCTP
dTTP	10 mM	40	µl of 100 mM dTTP
ddH_2O		add 400 µl	

Aliquots of 10 µl were prepared and stored at -20°C.

The PCR mixture for one reaction was as follows:

Template DNA	(50 ng/µl)	1 µl
Forward primer	(10 pmol/µl)	1 µl
Reverse primer	(10 pmol/µl)	1 µl
DMSO		2 % (v/v)
10x reaction buffer (plus $MgCl_2$)		5 µl
Pfu Turbo DNA-Polymerase		1 µl
dNTP-Mix	(10 mM)	1 µl
ddH_2O		add 50 µl

The PCR mixture was briefly vortexed and centrifuged before starting the PCR program. The PCR products were electrophoresed on agarose gels (3.1.b) to detect the size of the DNA and the desired DNA fragment was purified from the gel for cloning of plasmids.

3.1.a.II. Site-directed mutagenesis primerless PCR

In order to generate point mutation in the gene of interest, the primerless PCR was used. Mutations at specific sites in the coding sequence of interest are introduced by designing primers with the substituted nucleotides. Two sets of primer pairs were designed for two independent PCRs. Two different fragments were amplified by PCR, each fragment including an overlapping region containing the substituted nucleotides. The PCR products were electrophoresed on agarose-gel (3.1.b) and the fragments were purified from the gel (3.1.c). 1 µl of these fragments were used in a second PCR, so-called primerless PCR whereby the fragments served as primers and as templates. Finally, the whole DNA fragment is amplified by using the primers complementary at the two ends of template. (**Fig. 7**).

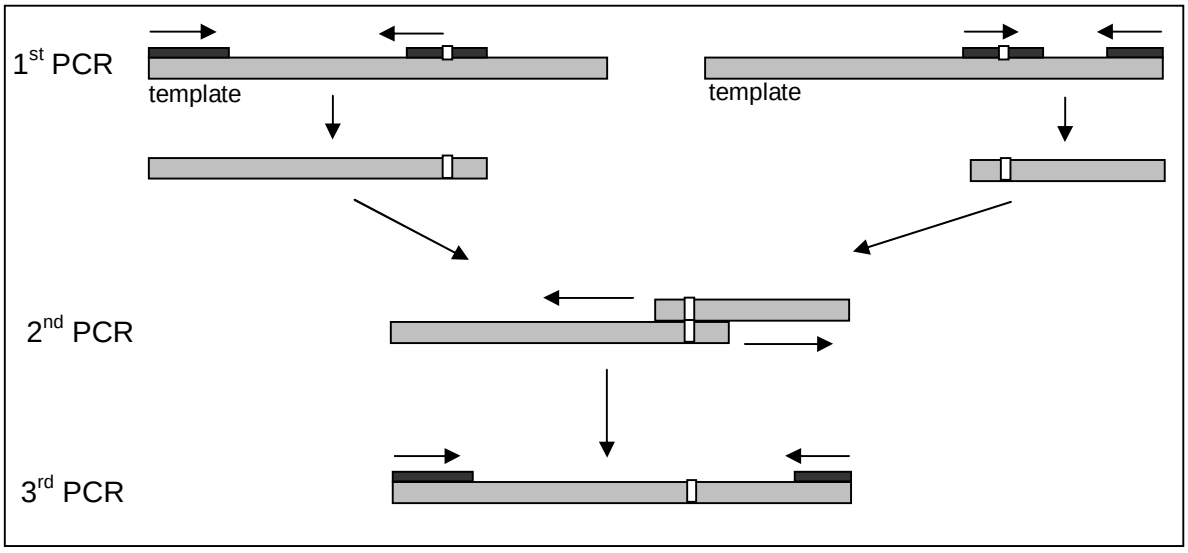

Figure 7: Site-directed mutagenesis by primerless PCR.
Site-directed mutation was generated by independent PCRs. The first PCR generated 2 fragments with overlapping region and mutation sites. The second PCR, so-called primerless PCR, was performed using 2 fragments as primers. The third PCR was done to amplify the primerless-PCR products which carried the desired mutations.

3.1.b. DNA gel electrophoresis

The buffers used in DNA gel electrophoresis are described as follows:

TAE-buffer	*1x*	*1 l*
Tris	40 mM	4.84 g
EDTA	1 mM	2 ml of 0.5 M stock
Acetic acid	20 mM	1.14 ml

Loading buffer (blue)	*6x*	*10 ml*
Glycerol	30% (v/v)	3.39 ml of 87 % glycerol
Bromophenolblue	0.25% (w/v)	0.025 g
Xylene Cyanol FF	0.25% (w/v)	0.025 g

These buffers were stored at room temperature.

Gel preparation and electrophoresis

During agarose gel electrophoresis, DNA fragments are separated according to their size and percentage of agarose (see the table bellows) (Sambrook et al., 1989)

Percentage of agarose	**DNA fragments separated**
0.3 %	60 – 5 kb
0.6 %	20 – 1 kb
0.7 %	10 – 0.8 kb
0.9 %	7 – 0.5 kb
1.2 %	6 – 0.4 kb
1.5 %	4 – 0.2 kb
2.0 %	3 – 0.1 kb

An appropriate concentration of agarose was dissolved in 1 x TAE by heating. The solution was cooled and ethidium bromide was added at a final concentration of 1 µg /ml. The solution was poured into a gel chamber with a comb and let to solidify at room temperature. The gel was placed in an electrophoresis chamber and covered with TAE buffer.

DNA samples were mixed with the corresponding volume of 6x loading buffer and loaded into the wells of the gel, which were formed by the comb. Electrophoresis of DNA was performed by applying a constant electric field of 80V (Biometra® Standard Power Pack P25).

Ethidium bromide is a fluorescent dye, which intercalates between the stacked bases of the DNA. This causes the dye, bound to DNA, to display an increased fluorescence yield compared to that of the dye in free solution under the UV-light of 366 nm wavelength. Analysis was perfomed using the BioDocAnalyze system including the transilluminator Biometra Ti1 and the software BioDocAnalyze 2.0.

3.1.c. DNA purification from agarose gels

After electrophoresis, the bands corresponding to the DNA of interest were cut out of the gel and purified by using the Easy Pure® Purification Kit according the instructions of the manufacturer. In brief, the agarose-gel was melted in 3 volumes of SALT-solution (100 µl solution per 100 mg of agarose-gel) at 55°C for 5min (Thermomixer compact) in an 1.5 ml Eppendorf tube; the mixture was incubated with a DNA binding solution (silica-matrix) to extract the DNA and pelleted by centrifugation; the pellet was washed twice with the WASH-solution; finally the pellet was dried in a Speed Vac, resuspended in 20 µl sterile

H_2O and incubated for 5 min at room temperature to elute the DNA. After centrifugation, the supernatant containing the purified DNA was transferred to a new Eppendorf tube.

3.1.d. Restriction enzyme digest of DNA

Purified PCR-products or the corresponding vector were digested with the appropriate restriction endonucleases. Restriction endonucleases digest DNA specifically at recognized nucleotide sequences. The whole amount of purified PCR-products or 2 µg of plasmid DNA were digested and used in cloning. Reaction volume for digestion as follows:

	Total PCR-products	Plasmid DNA (2 µg)
10x buffer Tango™ (yellow)	2.5 µl	1 µl
Restriction endonuclease	1 µl (each)	1 µl (each)
Sterile H_2O	add to 25 µl	add to 10 µl

The solutions were mixed in an Eppendorf tube by vortexing and spun down shortly. The digestion was carried out for 2 h in a waterbath at 37°C. To prepare DNA for ligation, the digest was carried out overnight. The samples were analyzed by agarose gel electrophoresis and re-purified to use for ligation.

3.1.e. Ligation of DNA

Ligation of DNA fragments was performed with the T4 DNA ligase. The T4 DNA ligase catalyzes the formation of a phosphodiester bond between juxtaposed 5'-phosphate and 3'-hydroxyl termini in double-stranded DNA.

To estimate the amounts of DNA needed for the ligation, 3 µl aliquots of the purified and digested DNA samples were analysed by DNA gel electrophoresis. The insert DNA was employed in a ~4-fold excess over the corresponding linearized vectors. Pipeting scheme for the ligation reaction as follows:

Reaction volumes:

10x ligation buffer	1 µl
T4 DNA ligase	1 µl
Insert	appropriate volume (4-fold molecular excess over vector)
Vector (linearized)	~ 0.5 µg
H_2O	add 10 µl

The solutions were mixed in an Eppendorf tube by vortexing and centrifuged briefly. The ligation reaction was carried out in a water bath at 16°C over night.

The whole amount of the reaction was used to transform competent *E.coli* to amplify the plasmid.

3.2. Amplification of plasmid DNA

3.2.a. Preparation of competent E.coli

Solutions and reagents

LB medium (2.3.c)

Liquid nitrogen

50 mM $CaCl_2$	100 ml
$CaCl_2$	0.735 g
Add to 100 ml with distilled water	
Autoclave 20 min at 120 ^oC, 15 psi.	

50 mM $CaCl_2$ + 15 % glycerol	
87 % Glycerol	5.62 ml
50 mM $CaCl_2$	26.5 ml
0.2 µm sterile filtered	

LB-agar plates (without antibiotics)		*500 ml*
Agar	1.5 % (w / v)	7.5 g
Add to 500 ml with LB medium		
Autoclave 20 min at 120 ^oC, 15 psi.		

The LB-agar was cooled to 50°C and poured into 10 cm dishes. After hardening, the agar plates were stored at 4°C.

Procedure

E. coli competent cells were prepared following the calcium chloride ($CaCl_2$) procedure. Briefly, one colony of DH5α cells was inoculated overnight in 10 ml of LB media. From this pre-culture, a 100 ml LB culture was inoculated and grown at 37 ^oC (200 rpm) until the OD_{600} reached a value of 0.6. Cells were centrifuged for 10 min at 3,000 rpm and the supernatant was disposed. The pellet was resuspended in 50 ml of a cold sterile 50 mM $CaCl_2$ solution and kept on ice for 30 min. The cells were centrifuged again under the same conditions and the pellet was now resuspended in a cold solution of 50 mM $CaCl_2$ containing 15 % glycerol. Cells were aliquoted into 100 µl aliquots in 1.5 ml eppendorf tubes. Cells were immediately frozen in liquid N_2 and stored at - 80 ^oC.

3.2.b. Transformation of competent E.coli

Media

LB medium (2.3.c)

LB-agar plates (with antibiotics)	*Final concentration*	*for 500 ml*
Agar (add to 500 ml with LB medium autoclave for 20 min at 120°C 15 psi)	1.5 % (w / v)	7.5 g
Ampicillin (or Kanamycin) (added when the agar was cooled to 50°C)	50 µg / ml	500 µl of 5% stock solution

The LB-agar was cooled to 50°C and poured into 10 cm dishes. When hardened the agar plates were stored at 4°C.

Procedure

The plasmid DNA was transformed into competent *E.coli* by applying heat shock. Principally, the temperature rises quickly during the heat shock making the cell walls of the bacteria fragile and the plasmid DNA can be taken up. First, 30 µl of competent *E.coli* was thawed on ice. The whole amount of ligated samples or 200 ng of DNA was used in transformation. The DNA and bacteria were mixed and incubated on ice for 30min. After incubation, the heat shock at 42°C was performed for 90 sec (Thermomixer compact). The suspension was quickly immersed on ice for 2 min. 500 µl of LB-medium (without ampicillin) was added to the suspension. The mixture was incubated for 2 h at 37°C (Thermomixer compact, agitating at 500 rpm). Afterwards 200 µl of suspension were plated on a LB-agar plate (with appropriate antibiotic) and incubated over night at 37°C in an incubator.

3.2.c. Small scale DNA preparation (Mini-prep)

Buffers and solutions

Buffer M1		*100 ml*
Tris/HCl pH 8.0	25 mM	2.5 ml of 1 M Tris/HCl pH 8.0 stock solution
Glucose	50 mM	10 ml of 0.5 M Glucose stock solution
EDTA pH 8.0	10 mM	2 ml of 0.5 M EDTA pH 8.0 stock solution
add fresh before use:		
Lysozyme		2 mg / 1 ml buffer M1

Buffer M2		*5 ml*
NaOH	0.2 N	1 ml 1 N NaOH stock solution
SDS	1%	500 µl 10%-SDS stock solution
H_2O sterile		3.5 ml

Buffer M3		*20 ml*
Na acetate pH 4.8	3 M	8.165 g / 20 ml

Procedure

Mini preparation of plasmid DNA was used to confirm the identity of the construct. The process was performed with several colonies of every construct. The single colonies were picked and grown over night in 3 ml LB media using 15 ml blue-cap tubes (Greiner bio-one, Solingen, Germany) at 37°C, shaking 200 rpm. 1.5 ml of the over-night bacteria culture was centrifuged in an Eppendorf tube for 2 min at 6000 rpm at 4°C. After discarding the supernatant the pellet was resuspended in 150 µl buffer M1 and kept on ice for 10 min. Next, addition of 200 µl buffer M2 was done quickly to lyse the cells. The suspension was inverted several times for mixing and left for 5 min on ice. 150 µl of buffer M3 was added and the suspension was stored on ice for 5 min to neutralize the lysate. The sample was centrifuged for 10 min at 14,000 rpm at 4°C. The resulting supernatant was transferred to a new Eppendorf tube and the plasmid-DNA was extracted by addition of 200 µl phenol plus 200 µl chloroform-isoamylalcohol (24:1). The suspension was mixed by vortex and different phases were separated by centrifugation at 14,000rpm at 4°C for 5 min. The DNA-containing aqueous phase was transferred to a new Eppendorf tube. DNA was precipitated by addition of 1/10-sample volume buffer M3 and 2-sample volumes ice-cold 99 %-ethanol and storage at -20°C for 15min. Subsequently, the DNA was centrifuged for 30 min at 14000 rpm, 4°C. After discarding the supernatant the pellet was washed with 500 µl cold 70 %-ethanol and again centrifuged for 5 min at 14,000 rpm at 4°C. The acquired pellet was dried and solved in RNase solution. The RNase-digest was applied for 30 min in a water bath at 37°C.

The DNA products from mini-prep were digested with the appropriate restriction enzymes and applied on an agarose electrophoresis to analyse.

3.2.d. Large scale DNA preparation (Maxi-prep)

Buffers and solutions

0.5M EDTA pH 8.0 (2.2.b.I)

LB medium (2.3.c)

Ethidium bromide	10 mg/ml
CsCl	10.9 g
STE Buffer	100 ml
1 mM EDTA	0.2 ml / 0.5 M
25% Saccharose	25 g
50 mM Tris-HCl pH 8.0	5 ml / 1 M

Triton-Mix	100 ml
60 mM EDTA pH 8.0	12 ml / 0.5 M
50 mM Tris-HCl pH 8.0	5 ml / 1 M
0.1 % Triton X-100	0.1 ml

PEG solution	100 ml
1.5 M NaCl	30 ml / 5 M
30% PEG 6000	30 g

TNE Buffer	100 ml
1 mM EDTA	0.2 ml / 0.5 M
10 mM NaCl	0.2 ml / 5 M
10 mM Tris-HCl pH 8.0	1 ml / 1 M

TE Buffer	1L
1 mM EDTA pH 8.0	2.0 ml / 0.5 M
10 mM Tris-HCl pH 8.0	10 ml / 1 M

Lysozyme	7 ml
60 mg/ ml Lysozyme	420 mg
Add to 7 ml of STE buffer	

Maxi-preparation procedure

After identification of the desired plasmid by mini-prep, a maxi-preparation of DNA was performed by using ultracentrifugation of bacterial lysate in a cesium chloride (CsCl) gradient. The process was performed as described by Sambrook et al. (1989). Briefly, the

culture given high yield of desired plasmid was inoculated into 30 ml LB medium containing a final concentration of 50 μg/ml ampicillin or kanamycin (depending on the antibiotic resistance of the plasmid). The bacteria were grown overnight at 37°C with agitation (225 rpm). In the next morning, the suspension was inoculated in 1 L LB medium containing the appropriate antibiotics. The culture was grown under the same condition until it reached an OD_{600} around 0.6-0.8. Chloramphenicol was added to a final concentration of 200 mg/L of the culture. After growing for 12 h, the bacteria were harvested by centrifugation (15 min at 6,000 rpm at 4°C). From now on, all steps were conducted on ice. After discarding the supernatant the pellet was resuspended in 45 ml ice-cold STE buffer. Lysis of the bacteria was carried on in 3 ml of a lysozyme solution for 20 min. The lysis was stopped by adding 3.6 ml of 0.5 M EDTA and incubating for 5 min. In the next step, the suspension was incubated with 28.8 ml of Triton mix solution for 30 min (shaking the mixture every 5 min). After centrifugation of the mixture for 1 h at 14,000 rpm at 4°C, the supernatant was transferred into a new tube and incubated for 1 h with 40 ml of a 30% PEG solution. Centrifugation for 10 min at 10,000 rpm at 4°C followed and the supernatant was removed. The pellet was dried and resuspended in 10 ml of TNE buffer together with 10.9 g of CsCl and 150 μl of a 10 mg/ml ethidium bromide solution. The suspension was transferred to ultracentrifuge tubes which were weighted (the difference between the weights were not more than 0.05 g) to keep balance before centrifugation. The samples underwent ultracentrifugation for 20 h at 60,000rpm at 20°C. After ultracentrifugation the band containing plasmid DNA was sucked out with a needle and a syringe. The samples were washed with isoamylalcohol to remove ethidium bromide (until the solution was colorless). CsCl was removed by dialyzing each sample in 2 L of TE buffer during 24 h at 4°C. Afterwards, the DNA concentration and purity were measured (OD_{260}, OD_{280}) (3.2.f) and the identity of plasmids were checked by enzymatic restriction (3.1.d)

3.2.e. Sequencing

The newly generated expression vector was sequenced. The DNA sequence was determined by the chain-termination method (Sanger et al., 1977) using the sequencing kit Big Dye® Terminator v1.1 Cycle Sequencing Kit. This kit contains fluorescently labeled didesoxynucleotides (ddATP, ddGTP, ddCTP and ddTTP) which lead to a termination of the DNA synthesis after incorporation. These ddNTPs are mixed with dNTPs in a relation that statistically allows the synthesis of fragments of all possible sizes. The PCR for sequencing was performed using the PTC-200 Peltier Thermal Cycler.

The following components were used for the reaction:

DNA	300 ng
Primer	10 pmol
BigDye® Mix	1.8 µl
DMSO	0.5 µl
dd H_2O	ad 10 µl

The PCR program used for the sequencing as follows:

1. 2 min of initial denaturation 94°C
2. 15 sec of denaturation 96°C
3. 15 sec of annealing 56.5°C
4. 4 min of elongation 60°C
5. 7 min of final elongation 72°C

Steps 2 – 4 were repeated 24 times.

After amplification of DNA the PCR fragments were purified by gel filtration chromatography. The samples were filled with dd H_2O to a final volume of 40 µl. The Sephadex (Sephadex G50, Amersham Biosciences) was preswollen in a 96-well Millipore plate (Millipore-MAHV N45) and washed once with H_2O. The samples were added on top of the sephadex and were purified by centrifugation for 5 min at 150x*g* (Beckmann GS-6). Afterwards the samples were analyzed by capillary electrophoresis with respect to their size and the nucleotides were determined by fluorescence analysis using the ABI PRISM 3100 Genetic Analyzer.

3.2.f. Quantification of DNA concentration

The concentration and purity of DNA was determined by UV-absorption at 260 nm using a UV-visible recording spectrometer (Shimadzu UV-160). The measurement was performed in quartz cuvettes in a total volume of 1 mL TE-buffer (3.2.d)
Following is the formula used to calculate DNA concentration

c (µg / µL) = OD_{260} x 50 x dilution factor of DNA

The ratio between the absorption at 260 nm and at 280 nm gives a measure of the purity of the plasmid DNA. The ratio should range between 1.8 and 2.0.

3.3. Analysis of proteins

3.3.a. Quantification of proteins

3.3.a.I. Bradford assay

The Bradford assay was used to determine the concentration of proteins in solution. In this assay, the Dye Reagent For Protein Assays (Biorad) containing the Coomassie Brilliant Blue G-250 is red. When binding to a protein, the dye changes its colour to blue. The intensity of blue colour correlates with the amount of the protein in solution (Bradford, 1976). Briefly, the Dye Reagent was diluted 1:5 in H_2O. BSA was used to generate a standard curve ranging from 0.5 µg to 20 µg. 1 µl of the protein solution was added to 1 ml of diluted reagent. The mixture was vortexed in a cuvette. The OD value of the protein solution was determined by photometric measurement at 550 nm using a spectrophotometer (Shimadzu UV-160, Duisburg). The concentration of protein was calculated based on a standard curve.

3.3.a.II. Semi-quantitative SDS-PAGE

Different volumes of protein solutions and defined amounts of BSA (100 – 2,000 ng) were denatured in sufficient amount of 2x Laemmli loading buffer (Laemmli, 1970). The samples were electrophoresed by SDS-PAGE (3.3.b) and the gel was stained with Coomassie (3.3.c).

3.3.b. SDS-PAGE

Buffers and solutions

Stacking-gel buffer		*200 ml*
Tris/HCl pH 6.8	0.5 M	12.144 g
SDS	0.4 % (w/v)	8 ml 10 %-SDS solution

Resolving-gel buffer		*200 ml*
Tris/HCl pH 8.8	1.5 M	36.342 g
SDS	0.4 % (w/v)	8 ml 10 %-SDS solution

Acryl-amide solution		*250 ml*
Acryl amide	29.2 % (w/v)	73 g
Bis-acryl amide	0.8 % (w/v)	0.82 g

Tank buffer		*1L*
Tris	25 mM	3.09 g
Glycine	192 mM	14.41 g
SDS	0.1 % (w/v)	10 ml 10 %-SDS solution

Lämmli-loading buffer	*2x*	*100 ml*
Tris/HCl pH 6.8	160 mM	16 ml 1 M Tris/HCl pH 6.8 stock
SDS	4 % (w/v)	4 g
Glycerol	10 % (v/v)	11.4 ml 87.5-% solution
Bromphenolblue	0.05 % (w/v)	50 mg
β-Mercaptoethanol	10 % (v/v)	10 ml

Gel preparation

The gel caster Mighty Small SE245 Dual Gel Caster and the corresponding glasses, spacer and combs were used to cast the gels.

8% and 10%-acryl amide resolving gels and 4%-acryl amide stacking gels were prepared as follows:

Resolving gel:	1 gel (10%)	1 gel (8%)	Stacking gel:	1 gel
Separating-gel buffer	2.5 ml	2.5 ml	Stacking-gel buffer	1.25 ml
H2O	4.2 ml	4.8 ml		3.13 ml
Acryl-amide solution	3.3 ml	2.7 ml		620 µl
Temed	15 µl	15 µl		7.5 µl
APS-stock solution	100 µl	100 µl		50 µl

After casting the resolving gel n-butanol was applied to the upper layer to release air bubbles and to smooth the edge between resolving gel and stacking gel. n-butanol was removed after gel polymerisation. The stacking gel was cast on top of the resolving gel; the comb was inserted.

To separate the phospho-proteins from their isotypes, the Phos-tag SDS-PAGE was used. The acrylamide gel was supplemented with 50 µM Phos-tag^{TM} AAL-107, a ligand of acrylamide which is able to bind to the phospho groups of the proteins, thereby retarding the migration of phosphorylated proteins (Kinoshita et al., 2008).

Electrophoresis of proteins

Proteins were separated by SDS-poly-acrylamide gel electrophoresis. The comb was removed from the gel. The gel was placed in gel-electrophoresis chamber (Mighty Small SE250/SE260 Mini Vertical Unit) filled with tank buffer. Equal amounts of protein from different samples were used. The proteins were denatured by boiling the samples for 10 min at 95°C (Thermomixer compact) in 2x Lämmli-loading buffer. Denatured proteins were loaded onto the gel. Electrophoresis of proteins through the stacking gel was conducted by applying a current of 15 mA per gel using the power supply Biometra® Standard Power Pack P25. As the lowest migrated band of bromphenolblue reached the resolving gel the current was adjusted to 25mA per gel until the samples passed the whole length of the gel. 4 µl of the PageRuler™ Prestained Protein Ladder was loaded onto the gel to estimate the molecular weight.

3.3.c. Detection of proteins with Coomassie stain

Buffers and solutions

Coomassie-stain solution		*1 L*
Bromphenolblue	0.25 % (w/v)	2.5 g
Methanol	40 % (v/v)	400 ml
Acetic acid	10 % (v/v)	100 ml

Destain solution		*1 L*
Iso-propanol	25 % (v/v)	250 ml
Acetic acid	10 % (v/v)	100 ml
Methanol	10 % (v/v)	100 ml

Procedure

After electrophoresis, the stacking gel was removed and the resolving gel containing proteins was stained for 20 min in coomassie-stain solution and destained over night with destain solution.

3.3.d. Western blot

Buffers and solutions

Buffer A		*1 L*
Tris, pH 11.3	300 mM	36.3 g
Methanol	20% (v/v)	200 ml
H_2O		add to 1L

Buffer B		*1 L*
Tris, pH 10.5	25 mM	3.03 g
Methanol	20% (v/v)	200 ml
H_2O		add to 1L

Buffer C		*1L*
Tris, pH 9.0	25 mM	3.03 g
Methanol	20% (v/v)	200 ml
Adjust pH with boric acid		
H_2O		add to 1L

TBS-T	10x	*1 L*
NaCl	1.5 M	80 g
Tris	100 mM	24.2 g
Adjust pH to 7.5		
H_2O		add to 1L

TBS-T	1x	*1 L*
TBS 10x		100 ml
Tween 20	0.1 % (v / v)	1 ml
H_2O		add to 1L

Blocking solution		*50 ml*
Skim milk powder	5% (w/v)	2.5 g
TBS-T		add to 50 ml

Antibody solution		*10 mL*
Skim milk powder	1% (w/v)	0.1 g
TBS-T		add to 10 ml

Blotting

After SDS-PAGE was performed, the resolving gel was incubated for 20 min in buffer C and the nitrocellulose membrane was incubated for 10 min in buffer B. Proteins were transferred from the gel to the membrane using a semi-dry electroblotting chamber. The arrangement of the blotting stacks was as follows (starting from the cathode- bottom to the anode-top): 2x whatman papers in buffer A, 2x whatman papers in buffer B, membrane in buffer B, gel in buffer C and finally 4x whatman papers in buffer C. A roller was used to avoid formation of bubbles. The transfer was done for 1 h 10 min at a constant current of 1.2 mA / cm^2.

Immunodetection

In order to avoid unspecific protein binding, after blotting, the membrane was blocked for 1 h at RT in blocking solution under constant rocking. After three washing steps, 5 min each, with TBS-T, the required dilution of the primary antibody was added in a 5 % skim milk-TBS-T solution. The membrane in the solution of primary antibody was incubated overnight at 4^{o}C with gentle rocking. Next day, the membrane was washed three times, 5 min each, with TBS-T at room temperature. Then the membrane was incubated for 1 h at room temperature with the secondary antibody (anti-rabbit or mouse horseradish peroxidase-HRP) at 1: 10,000 dilution. After three washing steps of 5 min with TBS-T, the membrane was ready for protein detection. The antibody-antigen complex was detected with Immun-Star WesternC Kit (Bio-Rad Laboratories, Munich, Germany) using the VersaDoc system.

3.3.e. Analysis of radioactively labeled proteins

In case radioactively labelled proteins were to be detected, after electrophoresis, the stacking gels were removed. The separating gels were placed on Whatman paper and covered with plastic film. The gels were dried by heating to 60°C and applying vacuum using a gel dryer (DryGel Sr Slab Gel Dryer SE1160). To analyse radioactively labeled proteins the dried gels were exposed to a phosphor-imager screen (BAS-MS 2325, FUJIFILM). The exposure time was from overnight to several days depending on the incorporated isotope. The phosphor-imager screen was scanned using the phosphor-imager device BAS-1800II (FUJIFILM) and the software AIDA Version 4.15.025.

3.4. Purification of GST-fusion and His-tagged proteins

3.4.a. Screening for inducible clones expressing GST- and His-fusion proteins

The coding sequences of interest were subcloned into the bacterial expression vector pGEX2T or pET28b downstream of the lac operon to result in the expression of

glutathione S-transferase (GST) or His-fusion proteins, respectively. In *E.coli* the lac operon controls the expression of sugar-metabolizing enzymes, which depend on the presence of lactose in the media. In case that there is no lactose in the media, the lac operon encoding protein called repressor which in turn binds to the site of transcription initiation on the lac operon. This inhibits transcription. The lac operon genes expression can be induced by lactose or other structurally similar molecules, like isopropyl-β-D-thiogalactoside (IPTG), added to the media. These molecules bind to the lac repressor, which results in its release from the DNA; and therefore the gene transcription under the control of lac operon is activated. By using IPTG as inducer, the production of GST-fusion or His-tagged proteins can be enhanced.

To screen for the colonies expressing high yield of interested proteins nine colonies containing the same transformed construct were picked and left for growing over night at 37°C in 2 ml LB-media. Next morning, 100 µl of every bacteria suspension was inoculated in another 2 ml LB-media. The bacteria were cultured again for about 2 h at 37°C, until the OD_{600} reaches 0.6-0.8. Then 500 µl per sample was collected and stored on ice. To the remaining 1.5 ml bacteria suspension 1 mM IPTG was added and incubated for further 3 h at 37°C to produce the GST- or His-fusion proteins. From every sample, 200 µl was taken and the remaining suspension was stored at 4°C. The samples taken before and after induction were centrifuged for 2 min at 7,000 rpm (4,000x*g*) at 4°C (Eppendorf centrifuge 5417R). The supernatant was discarded and the pellet was denatured in 50 µl 2x Lämmli-loading buffer. The samples were analysed by SDS-PAGE and coomassie-staining to identify the potentially inducible clones.

3.4.b. Purification of GST- and His-fusion proteins

Buffers and solutions

Buffer A1		*1 L*
HEPES pH 7.5	20 mM	20 ml of 1 M Hepes pH 7.5 stock
NaCl	1 M	58.44 g
add fresh before use from stock-solutions:		
DTT	1 mM	10 µl 1 M DTT / 10 ml buffer A
PMSF	1 mM	50 µl 200 mM PMSF / 10 ml buffer A

Buffer A2		*1 L*
Tris-HCl pH 8.0	20 mM	20 ml of 1 M Tris-HCl pH 8.0 stock
NaCl	1 M	58.44 g
Glycerol	20% (v/v)	200 ml
Tween 20	0.1% (v/v)	1 ml

$ZnCl_2$	10 µM	10 ml of 1 mM $ZnCl_2$
Imidazol	40 mM	40 ml of 1 M Imidazol
add fresh before use from stock-solutions:		
DTT	1 mM	10 µl 1 M DTT / 10 ml buffer A
PMSF	1 mM	50 µl 200 mM PMSF / 10 ml buffer A

Buffer A2-plus: contains all the components with the same concentration as buffer A2, except NaCl 2M

Reaction buffer		*1 L*
NaCl	100 mM	5.844 g
EDTA	1 mM	2 ml of 0.5 M EDTA pH 8.0 stock
Tris/HCl pH 7.5	20 mM	20 ml 1 M Tris/HCl pH 7.5 stock
Nonidet-P40	0.5 % (v/v)	5 ml
add fresh before use from stock-solutions:		
DTT	1 mM	10 µl 1 M DTT / 10 ml Na^+- Buffer
PMSF	1 mM	50 µl 200 mM PMSF / 10 ml Na^+- Buffer

Preparation of glutathione- and NTA-Ni-agarose beads

Relying on the affinity of the beads described in the protocols supplied by the producers sufficient amounts of glutathione-agarose or NTA-Ni-agarose beads were employed for purification of GST- or His-proteins, respectively. The agarose beads were pre-swollen overnight in 8 ml PBS at 4°C. The suspension was centrifuged in the next day for 3 min at 900 rpm (150x*g*) at 4°C using the centrifuge Sigma 4K1. After discarding the supernatant the beads were washed with 10 ml buffer A1 or A2, for glutathione- or NTA-Ni-agarose, respectively, followed by 3 min centrifugation at 900 rpm (150x*g*) at 4°C. The washing step was repeated once. Afterwards, 0.5 ml buffer A1 or A2 was added to the glutathione- or NTA-Ni-agarose, respectively, making a total volume of 1 ml.

Purification of GST-fusion and His-tagged proteins

The colony given highest yield of GST- or His-proteins was inoculated overnight at 37°C in 100 ml of LB media. The next morning, the suspension was spun down for 2 min at 3,000 rpm. The bacteria pellet was inoculated in 1 L of LB-media and grown until an OD 600 of 0.5 – 0.6. At this phase the bacteria were growing logarithmically and were induced by adding 1 mM IPTG. The culture was grown overnight at 25°C. Afterwards, the bacteria pellet was obtained by 15 min centrifugation at 3,500 rpm (2,000x*g*) at 4°C (Beckmann centrifuge J2-HS), followed by discarding the supernatant.

The obtained pellets were resuspended in 10 ml buffer A1 or A2, corresponding to GST- or His-proteins, respectively. Corresponding samples were pooled in a 50 ml tube (Greiner bio-one, Solingen, Germany) and kept on ice. The bacteria walls were disrupted by sonication using the Branson Sonifyer® Cell Disrupter B15, applying 5 cycles of 10 s sonication and 20 s break at 70 % duty cycle. To prevent overheating and protein degradation during sonication the tube was kept in an ice-methanol bath.

The suspension of disrupted bacteria was centrifuged for 10 min at 10000 rpm (12000x*g*) at 4°C (Beckmann centrifuge J2-HS). The supernatant was transferred into a new 50 ml blue cap tube which contained 1 ml prepared glutathione-agarose or NTA-Ni-agarose beads. To promote binding the mixture was slightly rotated for 2h at 4°C on a rolling platform (TRM-V). Subsequently, the samples were centrifuged 3 min at 900 rpm (150x*g*) at 4°C (Sigma 4K1), the supernatant was discarded and the pellets were washed 4 times in 10 ml buffer A1 or buffer A2-plus, corresponding to GST- or His-proteins, respectively. Afterwards, the GST- or His-fusion proteins bound to glutathione-agarose beads or NTA-Ni-agarose beads were added with reaction buffer to form slurry of 50 % and stored on ice at 4°C.

3.5. Labelling of proteins with [^{35}S]-Methionine

The [^{35}S]-labeled proteins were synthesized *in vitro* by using the TNT® T7 Coupled Reticulocyte Lysate System following the manufacturer's instructions and using the delivered solutions.

The synthesis reaction was performed in an Eppendorf tube, as follows:

TNT® Rabbit Reticulocyte Lysate		25 µl
TNT® Reaction Buffer		2 µl
TNT® RNA Polymerase T7		1 µl
Amino acid mixture minus methionine	1 mM	1 µl
Template		1 µg
Redivue™ L-[^{35}S] methionine	10 µCi / µl	3 µl
H_2O sterile	add to	50 µl

The reaction solution was mixed by vortex and incubated for 90 min at 30°C with agitating at 900 rpm in a heat block (Thermomixer compact). Afterwards the synthesized proteins were stored on ice at 4°C for later use in GST- and His-pull down assays.

3.6. GST- and His- pull-down assay

The coding sequences of the proteins of interest were used as templates for *in vitro* transcription/translation with TNT® T7 coupled reticulocyte lysate system. 30 µCi of L-[^{35}S] methionine was used to label the *in vitro* transcribed / translated proteins in a 50 µl reaction mixture (3.5).

To exclude unspecific binding, NTA-Ni-agarose or glutathion-S-transferase (GST) was used as control in His- or GST- pulldown assay, respectively. Equal amount of the His-tagged or GST-fusion proteins and GST were employed in the assay (controlled by SDS-PAGE analysis (3.3.a.II)); equal volumes were achieved by filling with corresponding agarose beads which were pre-washed and equilibrated to reaction buffer (3.4.b). The samples were centrifuged for 2 min at 800 rpm (70x*g*) at 4°C (Eppendorf centrifuge 5417R). After discarding the supernatant the pellet was washed with 200 µl of the reaction buffer. Pellet and solution were mixed by tipping on the Eppendorf tube. The supernatant was discarded after applying again 2 min centrifugation at 800 rpm (70x*g*) at 4°C (Eppendorf centrifuge 5417R). In the final reaction, the proteins bound to beads were incubated with 250 µl of reaction buffer and 4 µl of [^{35}S] radioactively labelled proteins overnight at 4°C on a rocking platform (Polymax 1040). Next day, the proteins bound to beads were centrifuged 2 minutes at 800 rpm (60x*g*) at 4°C (Biofuge 15R). The samples were washed 4 times, each with 400 µl reaction buffer followed by 2 min centrifugation at 800 rpm (60x*g*) at 4°C (Biofuge 15R) and discarding of the supernatant. Finally, SDS-sample buffer was added to the samples, boiled at 95^{0}C for 5 minutes and loaded on a SDS-PAGE for analysis. 1 µl of [^{35}S] proteins (25%) were used as inputs for analysis. The gels were dried and the radioactively labelled proteins were visualized by exposure to a phosphor-imager screen (3.3.e). The bands corresponding to [^{35}S] proteins recovered from GST alone, GST fusion protein or His-tagged proteins were evaluated by densitometric analysis (3.3.e).

3.7. Culture of HIT-T15 cells

HIT-T15 cells were cultured under sterile conditions. Filter- or autoclave-sterilized solutions were pre-warmed in water bath at 37^{o}C before use. All glassware items were autoclaved. Before putting equipment or handling in the sterile hood, all outside surfaces were wiped with 70 % isopropanol solution.

The culture of HIT-T15 cells monolayers was performed in 30 ml of RPMI complete medium (2.3.c) on 15-cm (150 x 25 mm) plates. The cells were incubated at 37^{o}C in a 5 % CO_2, 95 % humidity atmosphere (Steri-Kult Incubator, Labotect GmbH, Göttingen). Once a week, the cells were propagated when they reach 80-90 % confluence (~35 x 10^6 cells).

The propagation process was performed as follows: the plate was washed with 10 ml 1X PBS solution. The cells were incubated in 3 ml of Trypsin/EDTA solution (GIBCO BRL, Karlsruhe) for 2-3 min at 37°C. The plates were shaken to detach the cells. Cells were resuspended in 7 ml of RPMI medium and transferred into a 50 ml tube (Blue Max, Falcon, Becton). The suspension was centrifuged for 2 min at 310x*g* (Megafuge 1.0) and washed once with RPMI complete medium. The cells were seeded at a density of ~0.5 x 10^6 cells / cm^2. After three days the medium was changed.

3.8. Transient transfection of HIT-T15 cells

Buffers and solution

RPMI complete medium (2.3.c)

RPMI uncomplete medium (without supplement of serum and antibiotics)

DEAE-Dextran solution (30 ml)

60 mg/ml DEAE-Dextran	1.8 g
Add to 30 ml with distilled water	
Filtrate through a 0.45 μm syringe filter	

TD Buffer	*500 ml*
0.7 mM K_2HPO_4	0.35 ml of 1 M stock solution
5 mM KCl	2.5 ml of 1 M stock solution
140 mM NaCl	70 ml of 1 M stock solution
25 mM Tris-HCl pH 7.4	12.5 ml of 1 M stock solution
dd H_2O	Add to 500 ml
Autoclave 20 min at 120°C at 15 psi.	

3.8.a.Transfection using DEAE Dextran

First, the medium was sucked off and the plate was washed with 10 ml 1X PBS solution. The cells were incubated with trypsin-EDTA for 3 min at 37°C and the plate was shaken to detach the cells. The cells were resuspended in 7 ml of uncomplete RPMI. The suspension was centrifuged and the medium was disposed. Cell pellets were washed twice in 10 ml TD buffer. After centrifugation, cells were resuspended in 1 ml of TD buffer/dish and 5 μl/dish of a 60 mg/ml DEAE-Dextran solution was added. This cell suspension was then mixed with the desired plasmids. 2 μg of DNA plasmid/dish was used. To estimate the transfection efficiency, 0.5 μg of the plasmid pGFPtpz-cmv[R] /dish was used. After 15 min incubation of the mixture at room temperature, the transient transfection was stopped by adding complete RPMI medium. The cells were centrifuged and the supernatants were removed. This washing step was repeated twice with complete

RPMI medium. Finally, appropriate volumes of complete RPMI medium (5 ml/dish) were added and 5 ml of cell suspension were seeded into 60 x 15 mm polystyrene tissue culture dishes. Incubation of cells was performed at 37^{o}C under 5 % CO_2 atmosphere until treatment and harvest were performed.

3.8.b. Transfection using Metafectene

In order to get high transfection efficiency for further experiments, transfection with a polycationic transfection reagent, Metafectene (Biontex, Munich), was performed according to the manufacturer's protocol. This method was used to transfect the HIT-T15 cells once they reached 80-90% confluency.

DNA mixture and Metafectene mixture were separately prepared in the Eppendorf tubes with 300 µl of RPMI uncomplete medium (without serum and antibiotics). The ratio of DNA:Metafectene was 1:2 (w/v). The HIT-T15 cells on 15-cm plate were washed with 15 ml of 1 x PBS, then 3 ml of trypsin / EDTA solution was applied. After incubation for 2 - 3 min at 37°C, the plate was shaken to detach the cells. The cells were washed with RPMI uncomplete medium and transferred to a 50 ml tube. After centrifugation, the cell pellet was resuspended in the appropriate amount of RPMI complete medium and plated out (4.5 ml per 6-cm plate). Subsequently, DNA/medium mix was added to the metafectene/medium mix and incubated for 25 min at RT. The DNA/Metafectene complex was added to the 6 cm plate.

3.9. Treatment of HIT-T15 cells

Depending on the purpose of different experiments, HIT-T15 cells were treated with KCl, Forskolin, a combination of KCl and Forskolin, or Cyclosporin A (an immunosuppressive agent) in different concentration and time course. The basic principles were as follows:

Treatment with KCl leads to membrane depolarization of HIT-T15 cells and opening of voltage-gated calcium channels of the L-type resulting in an increase in the intracellular calcium concentration.

The treatment of cells with forskolin (FSK) increased the intracellular cAMP level as FSK is a potent activator of the adenylyl cyclase.

By treatment with Cyclosporin A, the phosphatase calcineurin was inhibited.

In luciferase reporter-gene assays, the cells were treated with a final concentration of 45 mM KCl, 10 µM FSK, or the combination of 45 mM KCl and 10 µM FSK. These treatments were performed for 6 h before harvest of cells and measuremet of luciferase activity.

For immunocytochemistry experiments, cells were treated with 45 mM KCl for 30 min.

For analysis of *in vivo* phosphorylation of the proteins of interest, HIT-T15 cells were treated with 5 µM CsA for 15 min, or with the combination of 45 mM KCl and 10 µM FSK

for 15 min.

For chromatin immunoprecipitation assays, HIT-T15 cells were treated for 30 min with the combination of 45 mM KCl and 10 µM FSK.

3.10. Preparation of cell lysates for Western blot

Cell lysis buffer		50 ml
HEPES pH 7.5	50 mM	2.5 ml of 1 M stock
NaCl	150 mM	1.5 ml of 5 M stock
$MgCl_2$	1.5 mM	75 µl of 1 M stock
EGTA	1 mM	50 µl of 1 M stock
Triton X-100	1 % (v/v)	500 µl
NP-40	0.5 % (v/v)	250 µl
The following inhibitors was added freshly before use		
phosphatase inhibitors		
Na_3VO_4	0.1 mM	5 µl of 1 M stock
β-glycerophosphate	20 mM	2 ml of 0.5 M stock
NaF	1 mM	50 µl of 1 M stock
PMSF	1 mM	250 µl of 0.2 M stock
protease inhibitor		
Pepstatin	1 µg/ml	1 µl of 50 µg/µl stock
Leupeptin	1 µg/ml	1 µl of 50 µg/µl stock
Aprotinin	1 µg/ml	1 µl of 50 µg/µl stock

Procedure

The cell lysates were prepared for Western blot to analyze proteins. In brief, the cells were harvested 48 h after transfection. Cells in 6 cm-dishes were washed with cold 1X PBS. To each dish 100 µl of cell lysis buffer was added. Cells were scraped from the plates and transferred to 1.5 ml eppendorf tubes. Cells were mechanically disrupted 4 to 5 times with a syringe and a needle (27 G x ¾", Sterican, B/BRAUN). The suspensions were incubated on ice for 30 min. After centrifugation for 10 min at 13,000 rpm, the supernatant was transferred to new eppendorf tubes. Protein concentration was measured using Bradford assay (3.3.a.I). Equal amounts of proteins from different samples were aliquoted for analysis. Equal volumes of 2X Laemmli buffer (pre-heated at 95^{o}C) were added and samples were then heated on a thermo block at 95^{o}C for 5 min. SDS-PAGE analysis was performed (3.3.b).

3.11. Immunocytochemistry

Buffers and solutions

Quenching buffer		*50 mL*
Sodium borohydride	0.1% (w/v)	0.05 g
PBS		50 mL

Blocking buffer		*50 mL*
BSA	1% (w/v)	0.5 g
Horse Serum	10% (v/v)	5 mL
PBS		44.5 mL

Antibody-dilution buffer		*1.4 mL*
BSA	1% (w/v)	0.014 g
PBS		1.4 mL

Staining procedure

To investigate the effect of DLK on the location of endogenous TORC proteins under basal or KCl-treated condition, immunocytochemistry experiments were performed. Cells were grown on coverslips in 6-well plates (0.962cm² per well) and plated ~2 x 10^6 cells per well. Cells were transfected by metafectene (with ratio µl metafectene: µg DNA = 2:1). 48 h after transfection, cells were treated for 30 min with 45 mM KCl. After that, the coverslips were transferred to new 6-well plates and washed once with 4 ml 1x PBS per well at room temperature. PBS was aspirated off completely and the cells were immediately fixed by immersing the coverslips in 4 ml per well of -20°C precooled 100 % methanol, for 10 min. Next, the coverslips were rinsed 3 times for 5 min each with 4 ml PBS per well at room temperature, agitating gently. The cells were quenched in 4 ml (per well) fresh 0.1 % sodium borohydride in PBS (quenching buffer) for 5 min while agitating. Subsequently, the coverslips were washed 3 times for 5 min each with 4 ml PBS per well at RT, agitating. The PBS was aspirated off completely. Incubation of coverslips in 4 ml blocking buffer per well was performed for 45 min. To reduce background by removing any aggregated material, before staining the cells, the antibodies were centrifuged for 20 min at 12000 x g. The primary antibodies were diluted with antibody-dilution buffer (flag mouse antibody 1:50, pan TORC antibody 1:1,500). A sheet of parafilm was placed in a 15-cm dish. 50 µl of diluted antibodies mixture was pipetted on the parafilm and the coverslip was placed on (the surface containing cells was turned bottom). The 15-cm dish was covered with aluminium foil and cells were incubated with primary antibody overnight at 4°C (paper

soaked with PBS was also placed in the dish to keep the environment humid). On the next day, the coverslips were placed again into the 6-well plate (the cell-containing surface was on top). A washing step was carried on 3 times with all coverslips using 4 ml PBS per coverslip, agitating for 5 min each. Next, the secondary antibodies were diluted in antibody-dilution buffer (TRITC-tetramethylrhodamin-5-isothiocyanate- linked anti-mouse IgG 1:200;and fluorophore Alexa488®-linked rabbit IgG antibody 1:50). The cells were incubated with the diluted secondary antibody on parafilm as performed with the primary antibody. This incubation was carried out for 30 min at room temperature in the dark (cover the plate with aluminium foil). Afterwards, the coverslips were washed 3 times with 4 ml PBS at room temperature, agitating for 5 min each. Finally, the coverslips were mounted on slides using the Vectashield® Mounting Medium with DAPI (4',6-Diamidino-2-phenylindol) and were sealed with nail polish. The samples were kept in the dark at 4°C for later microscopic analysis.

Fluorescence microscopic analysic

The cells were observed at 63x magnification (Zeiss, LD Achroplan 63x) using the Zeiss Axiovert 200 microscope. The Software OpenLab™ 3.1 (Improvision Ltd.) was used to operate the device. Excitation/emission wavelengths for the fluorophores were: 495 nm / 519 nm for AlexaFluor® 488; 555 nm / 580 nm for TRITC; and 360 nm / 460 nm for DAPI.

3.12. Co-immunoprecipitation assay

Immunoprecipitation

HIT cells were transfected with expression vectors as indicated using metafectene (Biontex, Germany). 48 h after transfection, cells were lysed for 30 min in lysis buffer (3.10). Lysates were centrifuged for 10 min at 13,000 rpm, 4°C. The concentration of total protein in the supernatant was quantified using Bradford protein assay (Bio-Rad Laboratories, München). 500 µg of protein extract was incubated overnight on a rotator, at 4°C with the primary antibody and protein A-agarose beads. The proteins bound to the beads were collected by centrifugation (13,000 rpm, 4°C for 1 min) and washed three times with the lysis buffer. The immunoprecipitates were used for *in vitro* kinase assays or co-immunoprecipitation assays.

Co-immunoprecipitation assays

To investigate the interaction between DLK and TORC in HIT-T15 cell, the HIT cells were co-transfected with expression vectors for flag-tagged DLK wild-type or mutants and a vector expressing TORC1 wild-type. The immunoprecipitation was performed 48 h after

transfection using the anti-flag M2 antibody (Sigma, Taufkirchen, Germany). The Western blot was performed to investigate whether flag-tagged DLK co-immunoprecipitated TORC 1 wild-type.

3.13. In vitro kinase assay

Buffers and solutions

Kinase buffer			*50 ml*
HEPES pH 7.5	1 M	25 mM	1.25 ml of 1M HEPES pH 7.5
NaCl	5 M	100 mM	1 ml of 5 M NaCl
$MgCl_2$	1 M	10 mM	0.5 ml of 1M $MgCl_2$
Na_3VO_4	1 M	0.1 mM	5 µl of 1M Na_3VO_4
Add freshly before use			
PMSF	200 mM	1 mM	250 µl of 200 mM PMSF
ATP	200 mM	50 µM	125 µl of 200 mM ATP
protease inhibitor			
Pepstatin	5 mg/ml	1 µg/ml	1 µl of 50 µg/µl stock
Leupeptin	5 mg/ml	1 µg/ml	1 µl of 50 µg/µl stock
Aprotinin	5 mg/ml	1 µg/ml	1 µl of 50 µg/µl stock

His-tagged TORC proteins were prepared as described in (3.4.b)

HIT cells were transfected with expression vectors for flag-tagged DLK wild-type or DLK K185A, respectively. The flag epitope-tagged DLK or its mutant were immunoprecipitated as described above (3.12). Immunoprecipitated flag-tagged DLK was washed three times with kinase buffer. The immunocomplex was incubated in kinase buffer for 3 h at room temperature with 25 µmol/l ATP, 2 µg of dephosphorylated casein (Sigma, Taufkirchen, Germany) as control or equal amount of His-tagged TORCs bound to Ni-agarose beads which have been washed 3 times with kinase buffer, and 3 µCi γ-[^{32}P]-ATP (3,000 Ci/mmol) in a total volume of 200 µl, gently shaking. The reaction mixture was centrifuged for 1 min at 2000 rpm. After discarding the supernatants SDS-sample buffer were added to the pellets and boiled at 95^{0}C for 10min. Samples were subjected to SDS-PAGE. The phosphorylation of proteins was detected by a PhosphorImager. For the determination of the amount of immunoprecipitated DLK, a Western blot was performed using the antibody against C-terminal 223 amino acids of mouse DLK.

3.14. Chromatin-immunoprecipitation (ChIP)

Buffers and solutions

Cell lysis buffer		*100 ml*
Tris/HCl pH 8.0	10 mM	1 ml of 1 M stock
NaCl	10 mM	200 µl of 5 M stock
Nonidet-P40	0.2 % (v/v)	2 ml of 10% Nonidet-P40
Protease inhibitors	1x	200 µl of 50x protease inh. mix / 10 ml

Nuclei lysis buffer		*100 ml*
Tris/HCl pH 8.0	50 mM	5 ml of 1 M stock
EDTA	10 mM	2 ml of 0.5 M stock
SDS	1 % (w/v)	10 ml of 10% SDS
Protease inhibitors	1x	200 µl of 50x protease inh. mix / 10 ml

Wash buffer I		*50 ml*
Tris/HCl pH 8.0	20 mM	1 ml of 1 M stock
NaCl	150 mM	1.5 ml of 5 M stock
EDTA	2 mM	0.2 ml of 0.5 M stock
SDS	0.1 %	0.5 ml of 10% SDS
Triton X100	1% (v/v)	0.5 ml

Wash buffer II		*50 ml*
Tris/HCl pH 8.0	20 mM	1 ml of 1 M stock
NaCl	500 mM	5 ml of 5 M stock
EDTA	2 mM	0.2 ml of 0.5 M stock
SDS	0.1 %	0.5 ml of 10% SDS
Triton X100	1% (v/v)	0.5 ml

Wash buffer III		*50 ml*
Tris/HCl pH 8.0	10 mM	0.5 ml of 1 M stock
EDTA	1 mM	0.1 ml of 0.5 M stock
LiCl	0.25 M	3.125 ml of 4 M stock
Nonidet-P40	1 % (v/v)	0.5 ml
Deoxycholic acid	1 % (w/v)	500 mg

Elution buffer I		*10 ml*
Tris/HCl pH 8.0	10 mM	100 µl of 1 M stock
EDTA	1 mM	20 µl of 0.5 M stock
SDS	1 % (w/v)	1 ml of 10 % SDS

Elution buffer II		*10 ml*
Tris/HCl pH 8.0	10 mM	100 µl of 1 M stock
EDTA	1 mM	20 µl of 0.5 M stock
SDS	0.67 % (w/v)	670 µl of 10 % SDS

TE buffer		*50 ml*
Tris/HCl pH 8.0	10 mM	0.5 ml of 1 M stock
EDTA	1 mM	0.1 ml of 0.5 M stock

Chromatin immunoprecipitation assay

To investigate the effect of DLK on the recruitment of TORC to a CRE-containing promotor, the chromatin immunoprecipitation assay was performed. The assay was performed as described by Heinrich et al., 2009.

HIT cells on 10-cm plates were co-transfected using Metafectene with expression vectors for DLK wild-type/K185A/NLS1 or NLS2 and HA-tagged TORC1, and with p4xsomCRE. 48h after transfection, cross-linking of proteins and DNA was achieved by adding 1 % formaldehyde to the plates and agitating for 20 min at room temperature. The cross-linking reaction was stopped by addition of glycine to a final concentration of 0.125 M and agitating the plates for 5 min at room temperature. The media was discarded and cells were rinsed twice with 5 ml of ice-cold PBS. Cells were scraped in 1.5 ml PBS and centrifuged for 2 min at 1,700x*g*, 4°C. Cell pellets were lysed in 800 µl cell lysis buffer. Samples were frozen and thawed (in liquid N_2 and 37°C waterbath, respectively) 3 times. Disrupted cells were homogenized in a 1 ml douncer 20 times. After leaving on ice for 10 min, the samples were centrifuged 5 min at 2,700x*g*, 4°C. The pellets were added with 300 µl nuclei lysis buffer, mixed and incubated 10 min on ice. Samples were applied to sonication 5 times (each 5 seconds, 30 sec break with output control 6, duty cycle 50 %). The disrupted nuclei were centrifuged 10 min at 18,000x*g*, 4°C. 10 % of the supernatants were used as input. The remaining supernatants were incubated on a rotator overnight at 4°C with 30 µl protein A agarose slurry (containing 50 % beads) which were already equilibrated overnight with nuclei lysis buffer plus 0.1 % BSA and with 10 µg (2 µl) anti-HA antibody (Sigma). Subsequently, the samples were centrifuged 1 min at 18,000x*g*, 4°C.

The washing steps were performed as follows: twice with washing buffer 1, once with washing buffer 2, once with washing buffer 3 and once with TE buffer. Each washing step was repeated with 5 min rotation, 2 min centrifugation at 1,700x*g*, 4°C and followed by discarding the supernatants. Afterwards, the agarose pellets were added to 100 µl elution buffer 1 and incubated for 15 min at 65°C. The samples were centrifuged 3 min at 18,000x*g*, 4°C. The supernatants were transferred into new eppendorf tubes. To the pellets 150 µl elution buffer 2 were added and the incubation and centrifugation were repeated. The supernatants were transferred into the corresponding eppendorf tubes. The inputs were added with 10 % SDS and filled up to 250 µl with TE buffer. All samples and inputs were incubated overnight at 65°C while agitating. In the next day, to each sample 250 µl TE buffer plus 100 µg Proteinase K was added and incubated for 2 h at 37°C. After addition of 55 µl 4 M LiCl, the DNA was extracted twice with 500 µl Phenol and once with 500 µl chloroform/isoamylacohol (24/1), each step was performed with 2 min centrifugation at 18,000x*g*, room temperature and taking the upper phase. The DNA was precipitated by addition of 1 µl glycogen and 900 µl 100 %-EtOH, cooled down at -20°C for 30 min. The samples were centrifuged 30 min at 18,000x*g*, 4°C. The pellets were washed with 500µl 70% EtOH and centrifuged 10 min at 13,000 rpm, 4°C. Afterwards, the pellets were dried and resuspended in 20 µl TE buffer. The samples were used for quantitative real-time PCR using the ABI PRISM 7900 HT Sequence machine and the primers described before (2.3.e.II)

Quantitative real-time PCR

The DNA samples resulting from ChIP assays were analyzed quantitatively by real-time PCR using TaqMan™ probes. The oligonucleotide TaqMan™ probe is labeled with a fluorescent dye at its 5’ end and carries a quencher at its 3’ end. The probe is complementary to the nucleotides of the sequence of the specific DNA template. Normally, the fluorescene of the probe is quenched. The probe is disabled from 3’ extension by a 3’ phosphate. During the PCR, the probe hybridized to the DNA is digested by the polymerase due to its 5’-3’ exonuclease activity. The digestion of quencher-nucleotides leads to the enhancement of fluorescence intensity (Lee et al., 1993). Spectrophotometric measurement of the fluorescence during PCR determines the amounts of DNA template present in the sample.

3.15. Luciferase reporter-gene assay

Buffers and solutions

Scraping Buffer (500 ml)

1 mM EDTA	1 ml of 0.5 M EDTA
150 mM NaCl	75 ml of 1 M NaCl
40 mM Tris HCl pH 7.5	20 ml of 1 M Tris-HCl pH 7.5

Potassium phosphate buffer pH 7.8 (500 ml)

Solution 1: 100 mM K_2HPO_4	8.71 g in 400 ml water
Solution 2: 100 mM KH_2PO_4	1.36 g in 100 ml water

Adjust the pH of solution 1 to pH 7.8 with solution 2. Add to 500 ml with distilled water.

Potassium phosphate buffer + DTT (5 ml)

Phosphate buffer pH 7.8	5 ml
1 mM DTT	5 µl of 1 M DTT

0.5 M Glycylglycin (100 ml)

Glycylglycin	6.6 g

Add to 100 ml with distilled water

Glycylglycin Buffer (100 ml)

4 mM EGTA	2.22 ml of 180 mM EGTA
25 mM Glycylglycine (pH 7.8)	5 ml of 0.5 M Glycylglycin
15 mM $MgSO_4$	1.5 ml 1 M $MgSO_4$

Adjust pH to 7.8 with NaOH

Keep at 4°C

Luciferin

10 mM DTT	275 mg
Glycylglycin buffer	178.5 ml
1 mM Luciferin	50 mg

Dissolve DTT with glycylglycin buffer on ice

Add the luciferin in the dark

Make 1.4 ml aliquots and freeze at -80°C

Luciferase assay mix (LAM) Buffer (for 25 samples)

2 mM ATP	100 µl of 200 µM ATP
1 mM DTT	10 µl of 1 M DTT
82.4 % (v/v) Glycyglycin buffer	7.5 ml
16.5 mM Potassium phosphate buffer pH 7.8	1.5 ml

Luciferin Mix (LM) Buffer (for 25 samples)

10 mM DTT	56 µl
Glycyglycin buffer	5.6 ml
1 mM Luciferin	1.4 ml

Cell extract preparation procedure

Cells were harvested 48 h after transfection. Briefly, the cells were washed once with 1X PBS solution. The cells were detached in 750 µl/dish of scraping buffer using a scraper. Cell suspensions were pipetted into 1.5 ml eppendorf tubes (on ice). The dish was washed with another 750 µl/dish of scraping buffer and the suspension was collected into the same tube. Cells were centrifuged for 5 min at 5,200 x g and the supernatant was sucked off using a water pump. Cell pellets were resuspended in 150 µl of potassium buffer containing DTT and were subjected to 3 times freezing with liquid N_2 followed thawing in water bath at 37^{o}C. The suspensions were centrifuged for 5 min at 20,800 *x g*. The supernatant was used as cell extract for luciferase reporter and GFP assays.

Luciferase assay procedure

In the presence of ATP the substrate luciferin is adenylated by the enzyme luciferase isolated from the firefly *Photinus pyralis*. The luciferyl-adenylate undergoes an oxidative decarboxylation which produces light. As long as the substrate luciferin is present in excess, the production of light is proportional to the amount of luciferase in the reaction mixture (de Wet et al., 1987). By determining the luciferase activity in luciferase reporter-gene assays the promoter activity is estimated.

Luciferase activity from cell extracts prepared from transiently transfected cells was measured. Briefly, 50 µl of every cell extracts was pipetted into 5 ml plastic tube (75 x 12 mm diameter - Sarstead, Nümbrecht) and 368 µl of the LAM buffer were added. 50 µl of the potassium phosphate buffer containing DTT were used as a blank. The samples were shortly vortexed and placed in a Luminometer (AutoLumat LB 953, E&G Berthold). The luciferin mix (LM) was stored in the dark and was placed in the automatic injector of the luminometer. 200 µL of the luciferin solution were injected automatically to the samples

and the light emission was measured at 560 nm for 20 sec. The raw data were expressed as relative light units.

GFP reporter gene assay procedure

Green fluorescent protein (GFP) containing a chromophore possessing visible absorption and fluorescence under aerobic conditions was isolated from the jellyfish *Aequorea Victoria.* GFP topaz (GFPtpz) is a variant of GFP containing 4 point mutations which modify the chromophore and thereby change the emission spectrum to yellow (Tsien, 1998). To control for transfection efficiency during luciferase reporter-gene assay the pGFPtpz-cmv® control vector was cotransfected. The expression of GFPtpz is under control of a potent CMV-promoter.

Micro plate reader for GFP (Fusion^{TM}, Packard, Switzerland) was used for measurement of GFP. 50 μl of the cell extract were pipetted into every other well of a 96 U-shaped well plate. 50 μl of the potassium phosphate buffer containing DTT were used as a blank. The fluorometer Fusion (Canberra-Packard) performed 1 sec measurement at excitation wavelength of 485 nm and emission at 530 nm. The device was operated using the software Fusion InstrumentControl Application version 3.50 (Canberra-Packard). The final GFP values are the result of the subtraction of the GFP measurements from the average of three blank values.

3.16. Statistics

The data were analyzed by one-way or two-way analysis of variance (ANOVA) followed by Student's *t*-test using the software STATISTICA (Statsoft, Hamburg, Germany). Significance level was set at $p \leq 0.05$.

4. RESULTS

4.1. Effect of DLK on the transcriptional activity conferred by the three TORC isoforms

TORC transactivating capacity of CREB directed gene transcription is regulated by its cellular localization and presumably by its own transcriptional activity (Bittinger et al. 2004; Screaton et al. 2004; Heinrich et al. 2009). To examine the effect of DLK on TORCs transcriptional activity, the GAL4 system was used. An expression vector encoding either TORC1, TORC2 or TORC3 fused to the DNA binding domain (DBD) of the yeast transcription factor GAL4 (GAL4-TORC) was transiently co-transfected (§3.8.a) into the electrically excitable β-cell line HIT-T15 together with a luciferase reporter gene, consisting of five copies of the GAL4 DNA binding sites placed in front of a minimal viral E1B promotor (pG5E1B) (**Fig. 8**). Through the GAL4-DBD GAL4-TORC fusion proteins are tethered to the promoter of the G5E1B-Luc, thereby activating transcription of the luciferase gene. Thus, luciferase activity can be considered as a measure of TORC transcriptional activity. Cells were also co-transfected with expression vectors of DLK wild-type or DLK K185A. In this mutant, lysine-185 is changed to alanine resulting in the loss of ATP binding and thus enzymatic activity. 48 h after transfection cells were harvested and luciferase assay was performed (§3.15) to determine the transcriptional activity of TORC.

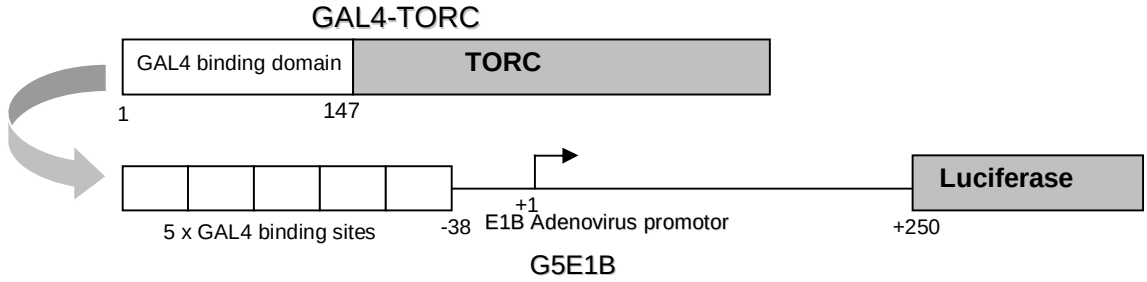

Figure 8: The sketch of plasmid 5xGal4E1BLuc and expression vector of GAL4-TORC

Under the basal condition, DLK wild-type and DLK K185A reduced the transcriptional activity of TORC1 to 18.2 ± 0.6% (n=6, p<0.0029) and 41.5 ± 4.6% (n=6, p<0.01), respectively (**Fig. 9A**). They reduced TORC2 activity to 59.5 ± 2.8% (n=6, p<0.001) and to 80 ± 4.5% (n=6, p<0.01), respectively (**Fig. 9B**). The transactivating capacity of TORC3 was decreased by DLK wild-type and the kinase dead DLK mutant to 41.6 ± 1.7% (n=6, p<0.001) and 73.7 ± 4.7% (n=6, p<0.0026), respectively (**Fig. 9C**). In all cases, DLK wild-type and DLK K185A significantly inhibited all three TORC isoforms (**Fig. 9A-C**).

In each group, the inhibitions of TORC transcriptional activities caused by DLK wild-type or by its kinase dead mutant were significantly different. The enzymatic dead DLK mutant had less inhibitory effect than the wild-type form of DLK (**Fig. 9A-C**). In the presence of overexpressed DLK K185A TORC1 and 3 activities were about 2-fold higher than their

activities in the presence of overexpressed DLK wild-type (n=6, p<0.0038 and n=6, p<0.001, respectively) (**Fig. 9A, C**). TORC2 activity was also significantly different between DLK wild-type presenting group and the group of kinase dead DLK mutant (60% and 80% (n=6, p<0.004), respectively) (**Fig. 9B**).

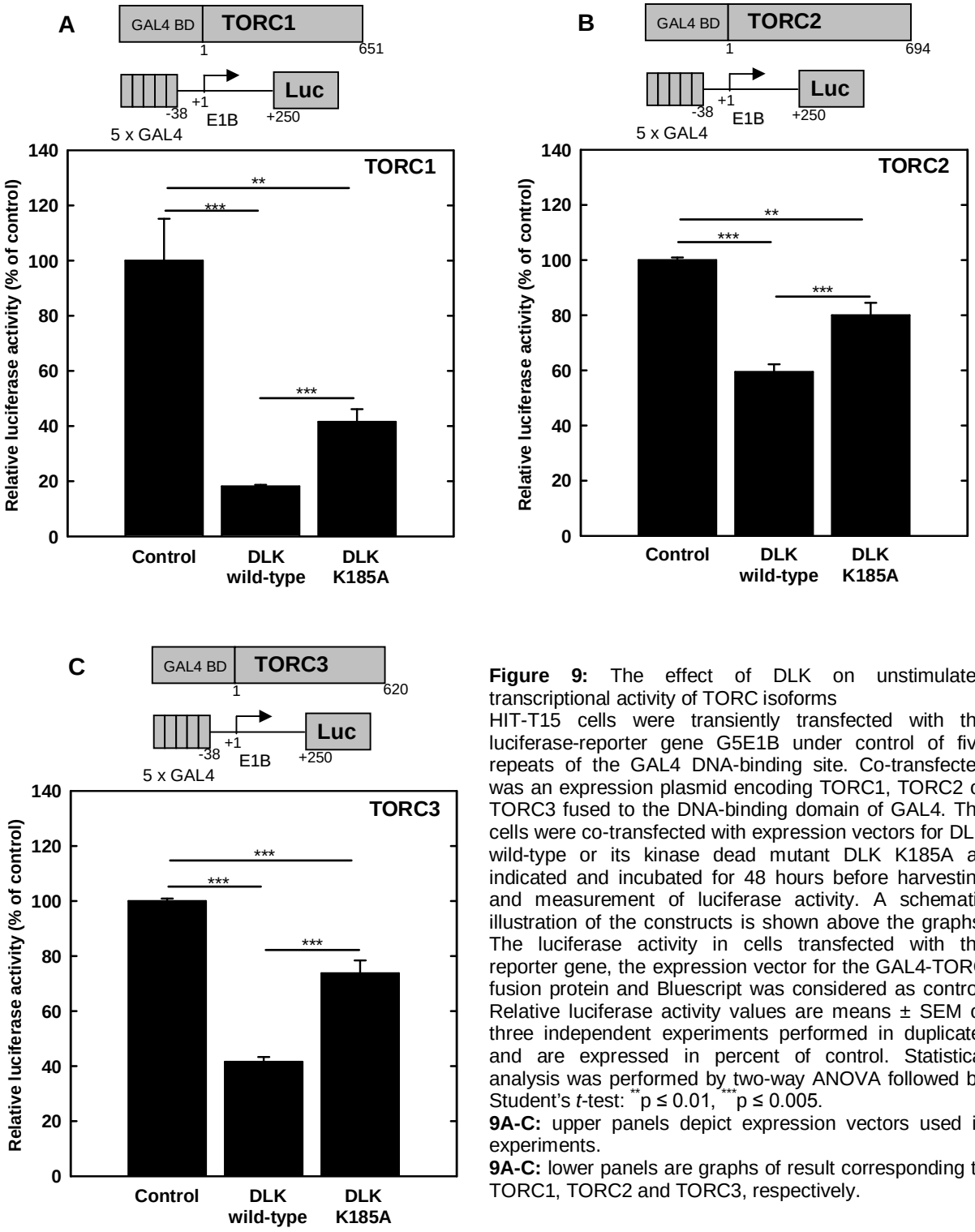

Figure 9: The effect of DLK on unstimulated transcriptional activity of TORC isoforms
HIT-T15 cells were transiently transfected with the luciferase-reporter gene G5E1B under control of five repeats of the GAL4 DNA-binding site. Co-transfected was an expression plasmid encoding TORC1, TORC2 or TORC3 fused to the DNA-binding domain of GAL4. The cells were co-transfected with expression vectors for DLK wild-type or its kinase dead mutant DLK K185A as indicated and incubated for 48 hours before harvesting and measurement of luciferase activity. A schematic illustration of the constructs is shown above the graphs. The luciferase activity in cells transfected with the reporter gene, the expression vector for the GAL4-TORC fusion protein and Bluescript was considered as control. Relative luciferase activity values are means ± SEM of three independent experiments performed in duplicate, and are expressed in percent of control. Statistical analysis was performed by two-way ANOVA followed by Student's *t*-test: $^{**}p \leq 0.01$, $^{***}p \leq 0.005$.
9A-C: upper panels depict expression vectors used in experiments.
9A-C: lower panels are graphs of result corresponding to TORC1, TORC2 and TORC3, respectively.

CREB-directed gene transcription is regulated by nucleo/cytosolic shuttling of TORC. Under resting conditions phosphorylated TORC is sequestered in the cytoplasm by binding to 14-3-3 proteins. By an increase of intracellular Ca^{2+} and cAMP levels TORC is dephosphorylated and translocated to the nucleus (Bittinger et al., 2004; Screaton et al., 2004). The effect of DLK on the transcriptional activity of TORC proteins after treatment with KCl and forskolin (a bicyclic diterpene) was examined using reporter gene assays. KCl treatment of cells results in its membrane depolarization thereby increasing intracellular Ca^{2+} levels by activation of the voltage-gated calcium channel of the L-type.

The calcium/calmodulin-dependent phosphatase calcineurin is activated by high concentration of Ca^{2+}, which was shown to dephosphorylate TORC (Bittinger et al., 2004; Screaton et al., 2004). Forskolin treatment of cells activates the enzyme adenylyl cyclase thereby increasing intracellular cAMP level and activation of PKA. PKA inhibits SIK, thereby reducing the phosphorylation of TORC (Katoh et al., 2004; Takemori and Okamoto, 2008). To understand the effect of DLK on TORCs under the stimulated condition, HIT-T15 cells were transiently co-transfected with the luciferase reporter gene G5E1B and expression vectors encoding GAL4-TORC1, -TORC2 or -TORC3 fusion proteins. The cells were co-transfected with expression vectors for DLK wild-type or its kinase dead mutant DLK K185A as indicated and cultured for 48 hours before harvesting and the measurement of luciferase activity. Cells were treated with 45 mM KCl, 10 µM forskolin, or a combination of both 6 hours prior to harvest. The same principle of GAL4 system and luciferase reporter gene assay (§3.15) was applied.

Forskolin and KCl enhanced the transcriptional activity of TORC1 approximately 4.5-fold, each, and the combined stimuli increased the activity 8-fold (**Fig. 10A**). TORC2 activity was enhanced by KCl, Forskolin and their combination 1.7-, 2- and 2.3-fold, respectively (**Fig. 10A**). TORC3 activity was not enhanced by KCl and slightly increased by treatment of forskolin or the combination of KCl and forskolin (**Fig. 10A**).

As seen in **Fig. 10B-D**, under the treatment with KCl, DLK wild-type reduced the transcriptional activities of TORC1, TORC2 and TORC3 to 35.3 ± 4.1% ($p<0.001$), 54.3 ± 1.6% ($p<0.001$) and 44.4 ± 1.8% ($p<0.001$), respectively. TORC1, TORC2 and TORC3 activities were reduced by DLK K185A to 67.5 ± 1.4% ($p<0.001$), 81.4 ± 2.6% ($p<0.001$) and 73.2 ± 4.8% ($p<0.001$), respectively. In the condition of membrane depolarization, the inhibition effected by DLK K185A on TORC1, 2 and 3 were significantly different from the effect caused by DLK wild-type (**Fig. 10B-D**).

After treatment with forskolin, TORC1, TORC2 and TORC3 activities were decreased in the presence of DLK wild-type to 43.1 ± 1.8% (n=6, p<0.001), 66.7 ± 3.9 (n=6, p< 0.001) and 52.5 ± 0.9% (n=6, p<0.001), respectively, whereas DLK K185 reduced the activities of TORC1, TORC2 and TORC3 to 54.7 ± 1.6% (n=6, p<0.001), 75.3 ± 4.7% (n=6, p<0.0036) and 80.4 ± 5.5 (n=6, p<0.017), respectively (**Fig. 10B-D**). Under these experimental conditions, the inhibitory effects caused by DLK wild-type on TORC1 or 3 were significantly different from the effects resulted from overexpression of DLK K185A (**Fig. 10B-D**). After treatment with forskolin DLK wild type reduced TORC2 activity more than DLK K185 did, even though their effects were not significantly different in these experiments.

The combined treatment with KCl plus forskolin did not change much the inhibitory effect on three TORC isoforms caused by DLK wild-type or its enzymatic dead mutant, as compared to other single treatments. In this condition, only on TORC3 DLK wild-type and its mutant exerted significantly different inhibition (**Fig. 10D**). The transcriptional activity of TORC1 was reduced by DLK wild-type and DLK K185A to 55.3 ± 3.1% (n=6, p<0.001), 61.0 ± 2.2% (n=6, p<0.001), respectively (**Fig. 10B**). The presence of overexpressed DLK wild-type and DLK K185A also resulted in a reduction of TORC2 or TORC3 transcriptional activities to 69.5 ± 4.5% (n=6, p<0.001) and 75.6 ± 2.3% (n=6, p<0.001) or 52.9 ± 2.8% (n=6, p<0.001) and 69.8 ± 4.8% (n=6, p<0.001), respectively (**Fig. 10C, D**).

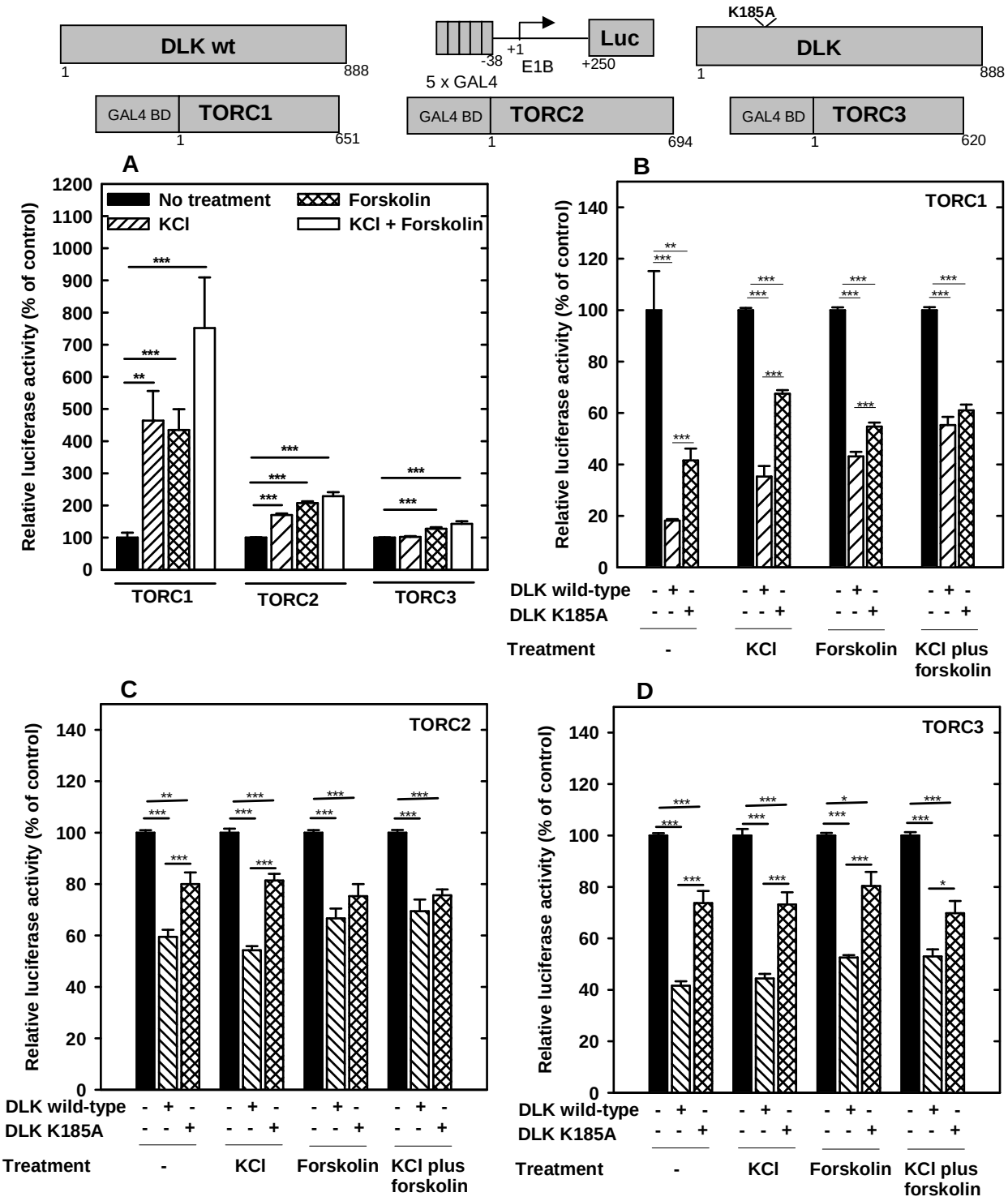

Figure 10: Effect of DLK on the stimulated transcriptional activity of TORC isoforms
A luciferase reporter fusion gene under the control of five DNA binding sequences for the yeast transcription factor GAL4 (plasmid G5E1B.Luc) was transiently co-transfected into HIT cells with an expression vector for fusion proteins consisting of DNA binding domain of GAL4 and TORC1, TORC2 or TORC3. The cells were co-transfected with expression vectors for DLK wild-type (wt) or DLK K185A as indicated and incubated for 48 hours. Treatment of cells with 40 mM KCl or 10 µM forskolin was performed 6 hours prior to harvesting and measuring luciferase activity. The luciferase activity in cells transfected with the reporter gene, the expression vectors for GAL4-TORC fusion protein and Bluescript was considered as control. Relative luciferase activity values are means ± SEM of three independent experiments performed in duplicate, and are expressed in percent of control. Statistical analysis was performed by two-way ANOVA followed by Student's *t*-test: $^{*}p \leq 0.05$, $^{**}p \leq 0.01$, $^{***}p \leq 0.005$.
The most upper panel depicts a scheme of the expression vectors used in experiments
10A: Effect of KCl and forskolin on the transcriptional activities of TORC1, TORC2 and TORC3. The control groups under basal condition were set as 100%.
10B-D: Effect of DLK on stimulated transcriptional activity of TORC isoforms (B: TORC1; C: TORC2; D: TORC3).

4.2. Comparison of the inhibitory effect of DLK on the transcriptional activity of three TORC isoforms

In order to investigate which TORC isoform was most inhibited by DLK, the reporter gene assay using the GAL4 system was used. HIT-T15 cells were transiently co-transfected (§3.8a) with the reporter gene plasmid pG5E1B and GAL4-TORC 1, -TORC2 or -TORC3. Increasing amounts of the expression vector for DLK were transiently co-transfected as indicated. Cells were harvested and luciferase assays (§3.15) were performed after 48h.

Increasing amounts of the expression vector for DLK showed that TORC1 activity was most intensively inhibited as compared to TORC2 and 3 activities (**Fig. 11**). The amount of expression vector for DLK wild-type from 0.6µg to 2µg significantly decreased transcriptional activity of TORC1 from 30% to 55%. Meanwhile the similar amounts of DLK expressing vector significantly inhibited TORC3 and TORC2 activities from 20% to 40% and 15% to 35%, respectively (**Fig. 11**). The results indicated that the inhibitory action of DLK on the transcriptional activity of TORC was enforced by increasing amounts of the expression vector for DLK wild-type. Inhibition of TORC1 transcriptional activity was the most pronounced.

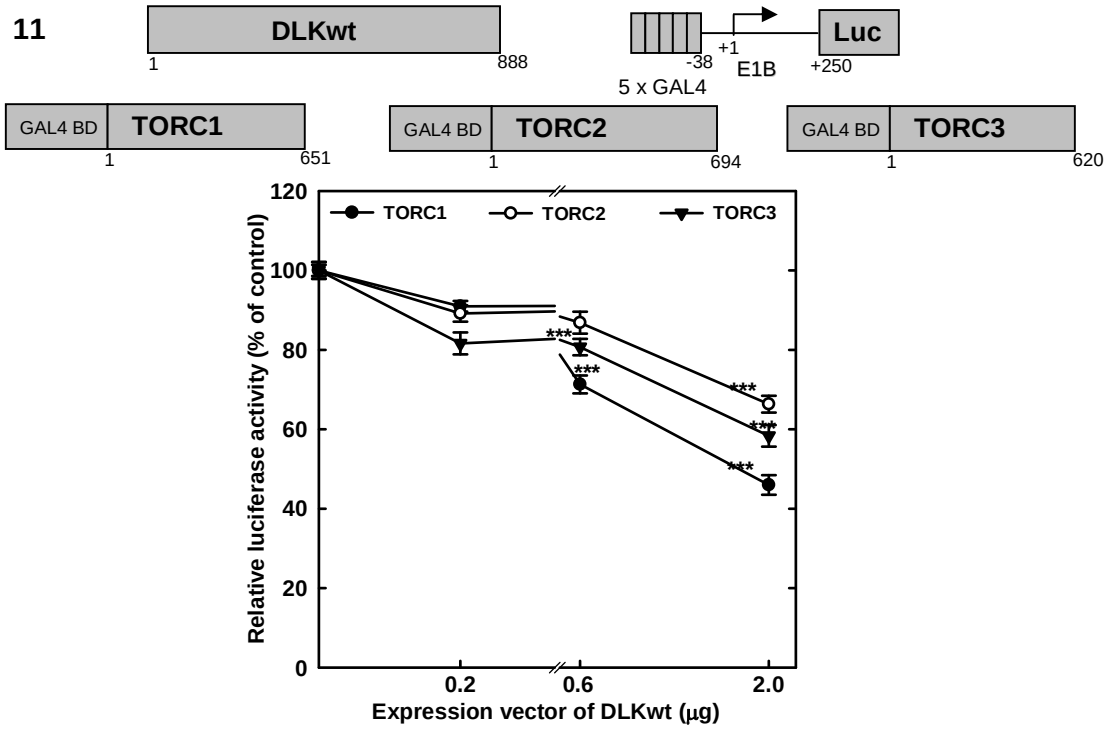

Figure 11: Increasing amount of overexpression vector for DLK enhances the inhibitory effect on TORCs
The effect of increasing amount (0; 0.2; 0.6 and 2 µg) of the expression vector for DLK on different TORC isoforms was investigated. The vector for Bluescript was used to keep the amount of transfected DNA constant among the experimental groups. 2µg of GAL4-TORC1, -TORC2 or -TORC3 was co-transfected with a total of 2µg of the expression vectors for DLK and Bluescript into HIT cells. Each TORC activity in the absence of DLK was considered as control (100%) for its own group. Luciferase activity is expressed relative to the activity of the control (Gal4-TORC only) in the absence of DLK. Relative luciferase activity values are means ± SEM of three independent experiments performed in duplicate. Statistical analysis was performed by two-way ANOVA followed by Student's *t*-test: $^{***}p \leq 0.005$.
The upper panel depicts expression vectors used in the experiments.
The lower panel is the graph of the results.

4.3. Mapping of TORC1 domains inhibited by DLK

TORC proteins activate transcription by interaction with the bZip domain of CREB. Structurally, the coiled-coil sequence of mouse TORC 1 located at aa 1-42 is (Conkright et al., 2003a) involved in this interaction. In addition, the C-termini of TORCs were shown to have transactivating potency (Iourgenko et al., 2003). In order to study which domain of TORC mediates the inhibitory action of DLK, a reporter gene assay using the GAL4 system was employed. HIT-T15 cells were transiently co-transfected (§3.8a) with the reporter gene pG5E1B, the expression vectors for GAL4 fusion proteins containing either TORC1 full length, or its deletions (C-terminus TORC1 aa44-651 (Δ44) or N-terminus TORC1 aa1-44) and expression vector for DLK wild-type or DLK K185A. 48 h after transfection cells were harvested and luciferase assays (§3.15) were performed.

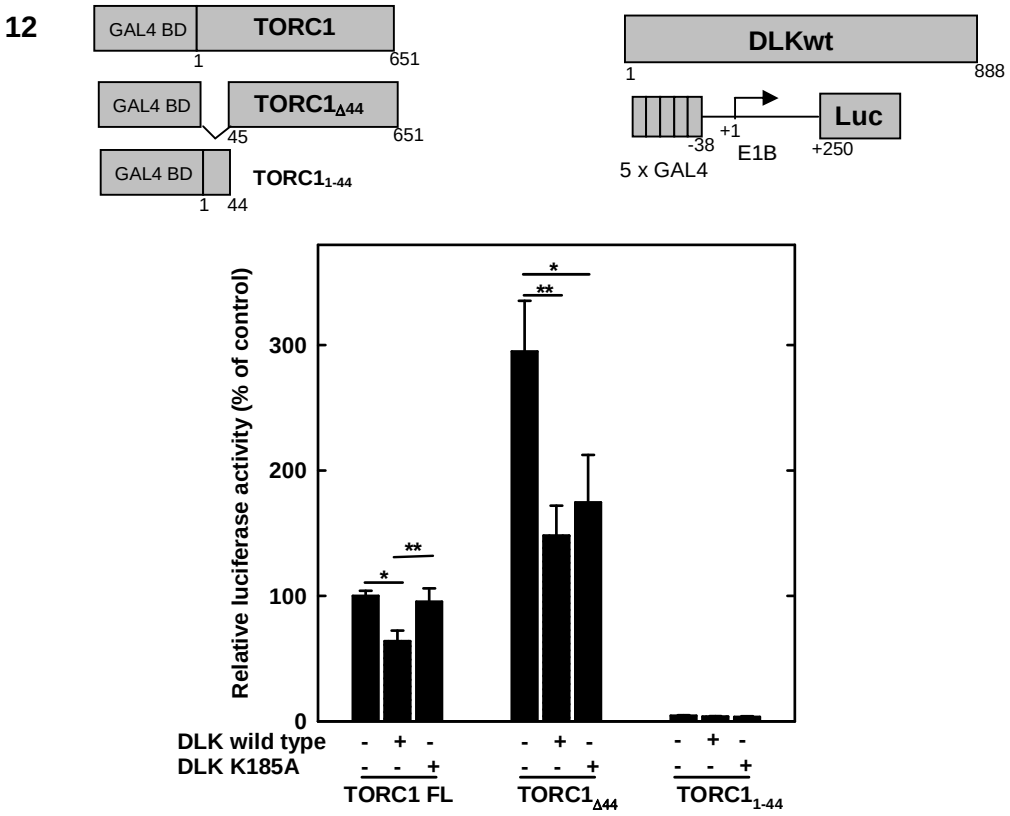

Figure 12: Effect of DLK on the transcriptional activity of TORC1 domains
Vector for Bluescript was used to keep the amount of transfected DNA constant among the experimental groups. 2µg of either GAL4-TORC1 full-length (FL), GAL4-TORC1$_{\Delta 44}$ or GAL4-TORC1$_{1\text{-}44}$ were co-transfected with 2µg of DLK wild-type or DLK K185A or Bluescript vectors into HIT cells. After 48 h, cells were harvested and luciferase activity was measured. The luciferase activity is expressed relative to the activity of TORC1 full length in the absence of DLK wild-type or DLK K185A. Relative luciferase activity values are means ± SEM of three independent experiments performed in duplicate, and are expressed in percent of control. Statistical analysis was performed by two-way ANOVA followed by Student's *t*-test: ** $p \leq 0.01$, * $p \leq 0.05$.
The upper panel depicts expression vectors used in the experiments.
The lower panel is the graph of results.

In **Fig. 12**, the deletion of N-terminal 44 amino acid of TORC1 increased transcriptional activity 3-fold. Its activity was inhibited by both DLK wild-type and DLK K185A, whereby both DLK mutant and wild-type reduced the transcriptional activity to the same extent. In the presence of DLK wild-type and its kinase dead mutant, $TORC1_{\Delta 44}$ transcriptional activity (294.9 ± 40.4%) were decreased nearly by half, with $p<0.014$ and $p<0.027$, respectively. The 44 N-terminal amino acid of TORC1 showed a decreased transcriptional activity which was inhibited neither by DLK wild-type nor by the kinase dead mutant of DLK (**Fig. 12**).

4.4. Effect of DLK on the transcriptional activity of TORC1 S167A and of TORC2 S171A

The above results (**Fig. 9**) suggested that the enzymatic activity of DLK is partly involved in the inhibition of TORC transcriptional activity. The phosphorylation of Ser-167 in TORC1 and of Ser-171 in TORC2 enhancing the interaction of TORC protein with the 14-3-3 protein and thus preventing the nuclear localization of TORC is considered as the key switching “on” and “off” the transactivating potency of TORC protein. Therefore, the effect of DLK on the transcriptional activity of TORC1 S167A and TORC2 S171A was investigated using the GAL4 system. HIT cells were transiently co-transfected (§3.8a) with the luciferase reporter gene pG5E1B, expression vectors for GAL4-TORC1 S167A or GAL4-TORC2 S171A fusion proteins, and DLK wild-type or DLK K185A as indicated. The transcriptional activity of the TORC mutants was measured by luciferase assay (§3.15) which was perfomed 48 hours after transfection. GAL4-TORC 1 or 2 wild-types were used as controls.

Both TORC1 S167A and TORC2 S171A exhibited 3- and 5-fold enhanced transcriptional activity when compared to their respective wild-types (**Fig. 13A, B**). In the experimental condition, the inhibitory effects on TORC1 and TORC 2 (wild-type) caused by DLK wild-type were different from the effects resulting from overexpression of DLK K185A. TORC1 S167A activity was increased to 315.3 ± 30.5% when compared to TORC1, whereas this activity was slightly changed to 293.8 ± 27.6% or 333.0 ± 39.6% by overexpression of DLK wild-type or DLK K185A, respectively. However, these changes were not significant. The transcriptional activity of TORC2 S171A was also enhanced to 541 ± 53.1% when compared to TORC2, whereas this activity was not inhibited in the presence of overexpressed DLK wild-type or insignificantly reduced to 509.6 ± 90.6% by overexpression of DLK K185A. The results indicated that overexpression of DLK wild-type or its kinase dead mutant resulted in an inhibition of TORC1- and TORC2-dependent gene

transcription, whereas the transcriptional activities of the TORC1 and 2 mutants were no longer reduced by DLK (**Fig. 13A, B**).

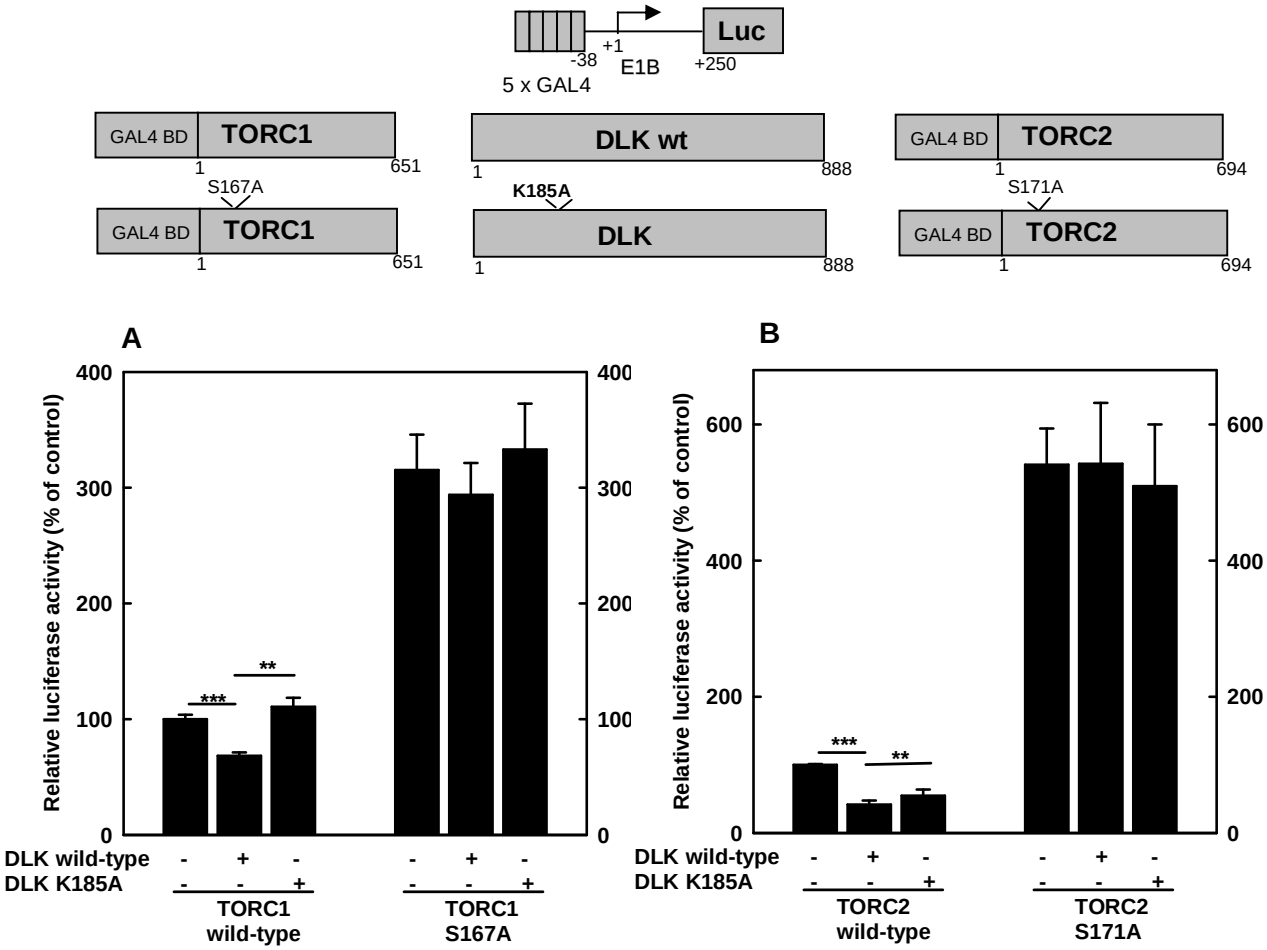

Figure 13: Effect of DLK on the transcriptional activity of TORC1S167A and TORC2 S171A.
A luciferase reporter fusion gene under the control of five DNA binding sequences for the yeast transcription factor GAL4 (plasmid G5E1B.Luc) was transiently transfected into HIT cells with an expression vector for a fusion protein consisting of DNA binding domain of GAL4 and TORC1 or TORC2 wild-type or mutants (TORC1 S167A or TORC2 S171A). The cells were co-transfected with expression vectors for DLKwt or DLK K185A as indicated and incubated for 48 hours before havesting and measuring luciferase activity. The luciferase activity in cells transfected with the reporter gene, the expression vectors for GAL4-TORC fusion protein and Bluescript was considered as control. Relative luciferase activity values are means ± SEM of three independent experiments performed in duplicate, and are expressed in percent of control. Statistical analysis was performed by two-way ANOVA followed by Student's *t*-test: $^{***}p \leq 0.005$, $^{**}p \leq 0.01$.
The most upper panel depicts expression vectors used in experiments

4.5. Effect of a dimerization-deficient DLK mutant on the transcriptional activity of the TORC isoforms

DLK P-P, in which the leucines 437 and 463 are changed into prolines, is a dimerization deficient mutant of DLK (Nihalani et al. 2000). Since homodimerization of DLK is required for its kinase activity, this mutant lacks enzymatic activity (Nihalani et al. 2000; Nihalani et al. 2003). It is possible that DLK may exert in part the inhibition on TORC through the zipper domain. The effect of DLK P-P on the transcriptional activity of TORC isoforms was

tested. To perform the investigation, HIT cells were transiently co-transfected with the reporter gene pG5E1B and vectors for GAL4-TORC1, -TORC2 or -TORC3 fusion proteins and DLK wild-type or DLK P-P, as indicated. The luciferase assay (§3.15) was performed 48 hours after transfection.

As shown in **Fig. 14**, DLK wild-type significantly reduced the transcriptional activities conferred by TORC1, TORC2 and TORC3 to 62.5 ± 4.2% ($p<0.001$), 90.4 ± 5.3% ($p<0.05$) and 66.6 ± 3.6% ($p<0.001$), respectively, whereas overexpression of the DLK P-P mutant did not decrease the transcriptional activities conferred by the three TORC isoforms.

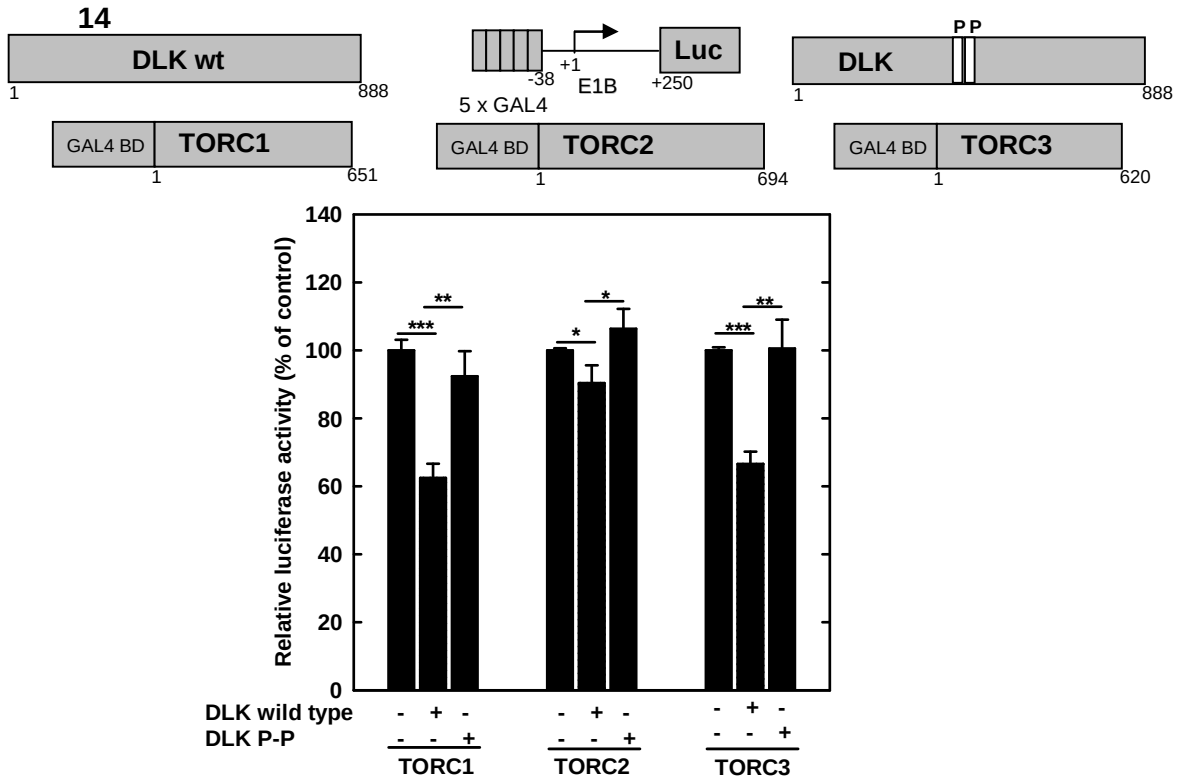

Figure 14: The dimerization-deficient DLK has no inhibitory effect on TORC
A luciferase reporter fusion gene under the control of five DNA binding sequences for yeast transcription factor GAL4 (plasmid G5E1B.Luc) was transiently co-transfected into HIT cells with an expression vector for a fusion protein consisting of DNA binding domain of GAL4 and TORC1, -TORC2 or -TORC3. The cells were co-transfected with expression vectors for DLK wild type or its dimerization-deficient mutant DLK P-P as indicated and incubated for 48 hours prior to harvesting and measuring luciferase activity. The luciferase activity in cells transfected with the reporter gene, the expression vectors for GAL4-TORC fusion protein and Bluescript was considered as control. Relative luciferase activity values are means ± SEM of three independent experiments performed in duplicate, and are expressed in percent of control. Statistical analysis was performed by two-way ANOVA followed by Student's *t*-test: $^{***}p \le 0.005$, $^{**}p \le 0.01$, $^{*}p \le 0.05$.

4.6. Overexpression of DLK wild-type and its mutants in HIT cells

In order to investigate whether the differences in the inhibitory effect of DLK wild-type and its mutants (the kinase dead or the dimerization deficient) on TORCs resulted from differences in the expression levels of DLK proteins, HIT cells were transiently transfected (§3.8b) with expression vector for DLK wild-type or its mutants. Cells were incubated for

48h before harvesting and lysis (§3.10). Cell lysates were analyzed by Western blot (§3.3d). DLK proteins were detected by using the antibody against the C-terminus of DLK. DLK wild-type and its mutants were differerently overexpressed in HIT cells (**Fig. 15**). When compared to DLK wild-type, the overexpression of DLK K185A resulted in 87 ± 4.3% ($p<0.021$) and the overexpression of DLK P-P resulted in 131.3 ± 13.2% of DLK content ($p<0.046$).

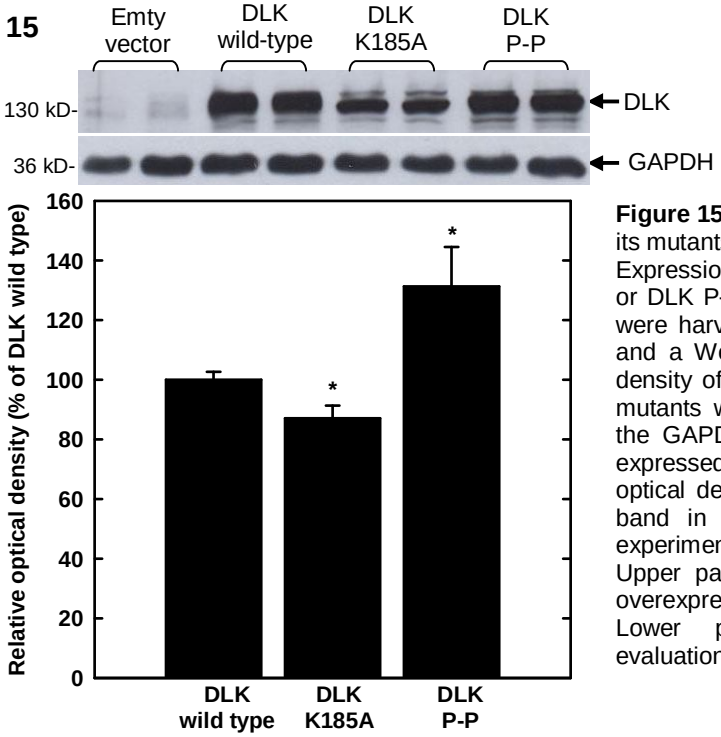

Figure 15: Expression levels of DLK wild-type and its mutants in HIT cells
Expression vectors for DLK wild-type, DLK K185A or DLK P-P were transfected into HIT cells. Cells were harvested after 48 hours. Cells were lysed and a Western blot was performed. The optical density of band representing DLK wild-type or its mutants was corrected for the optical density of the GAPDH representing band. The values are expressed relative to the mean value ± SEM of the optical density of the DLK wild-type representing band in each experiment in five independent experiments each done in duplicate.
Upper panel: The typical Western blot showing overexpressed DLKs and GAPDH.
Lower panel: graph showing quantitative evaluation of the expression levels of DLK proteins

4.7. Interaction between DLK and TORC as revealed by an in vitro assay

TORCs dependent transcription was reduced in part by the enzymatic activity of DLK. In addition, the kinase-dead DLK mutant showed also less inhibitory effect than the wild-type (Fig. 9). Therefore, it was investigated whether DLK interacts with TORC.

To investigate the interaction between DLK and TORC, an *in vitro* protein interaction assay (§3.6) was conducted. In principle, GST-TORC1$_{1-44}$ fusion proteins or His-tagged TORC1 full length and His-tagged TORC1$_{\Delta 44}$ proteins were bacterially expressed and purified using glutathione- or NTA-Ni-agarose beads (§3.4), respectively. The GST alone or NTA-Ni agarose beads were used as background control for GST-TORC$_{1-44}$ or His-tagged TORC fusion proteins. These on-beads immobilized proteins were incubated with [^{35}S] radio-labeled proteins (DLK wild-type, DLK K185A, DLK P-P, CREB wild-type or CREB R300A) (§3.5). If the radio-labelled proteins interact with the immobilized proteins, a complex will be formed on the agarose beads. Afterwards, the complex was separated from unbound proteins by several washing steps. The protein complex bound to agarose beads were eluted and subjected to SDS-PAGE for detection of the radio-labelled protein

(§3.6). Equal volume of input of [^{35}S] proteins was loaded on the same SDS-PAGE to calculate results.

Calculation:

Density of interacting [^{35}S] protein = [(density of band presenting [^{35}S] protein interacting with GST-or His- protein) – (density of band presenting the corresponding [^{35}S] protein interacting with GST or NTA-Ni agarose beads alone)]/density of band presenting the corresponding [^{35}S] protein input.

4.7.a. Purification of bacterially expressed proteins

His-tagged TORC1 full length and His-tagged TORC$_{\Delta 44}$ (a N-terminal deleted TORC1 mutant, lacking the interaction domain with the dimerized leucine zipper of CREB (Screaton et al. 2004)) were bacterially expressed and purified using NTA-Ni-agarose beads (§3.4 a, b). The GST protein or GST-TORC$_{1\text{-}44\text{-}}$ (C-terminal deleted TORC1 mutant consisting of the interaction domain with CREB) fusion protein were bacterially expressed and purified using glutathione agarose beads (§3.4 a, b).

The extracts from different steps of protein expression and purification were run on a SDS PAGE and stained with coomasive dye to detect the purified proteins. Consistent with the calculated molecular weight, His-tagged TORC 1 and His-tagged TORC1$_{\Delta 44}$ proteins migrated at 70 kD and 65 kD, respectively (the arrows in lanes 5 and 6, **Fig. 16**). GST-TORC$_{1\text{-}44}$ and GST proteins were the bands migrating at 31 kD and 26 kD (the arrows in lane 6 and 7, **Fig. 17**), respectively.

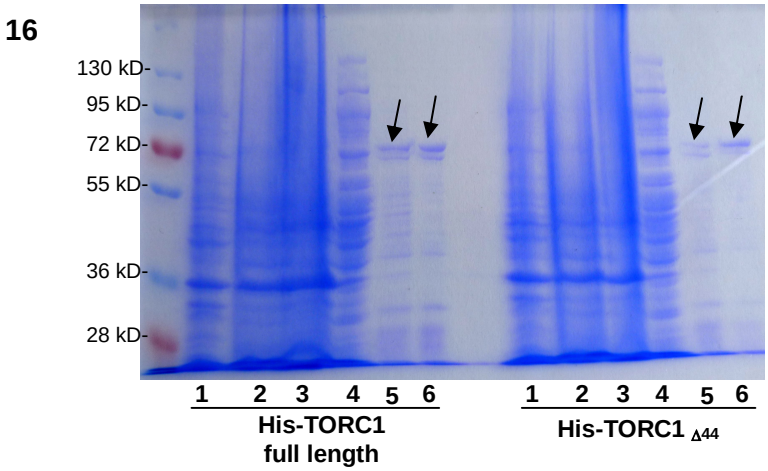

Figure 16: Purification of His tagged TORC1 full length and His-tagged TORC1$_{\Delta 44}$ proteins
The following protein extracts were run on the SDS-PAGE (8% acrylamide) and stained with coomassie dye. The bands at 70 kD and 65 kD indicated purified His-tagged TORC full length and His-tagged TORC$_{\Delta 44}$ (arrows).
1. Cell extract before induction with IPTG
2. Supernatant after induction with IPTG and cell disruption
3. Pellet after induction with IPTG and cell disruption
4. Supernatant after incubating with Ni-agarose beads
5. 5µl of proteins bound to Ni-agarose beads
6. 10µl of proteins bound to Ni-agarose beads

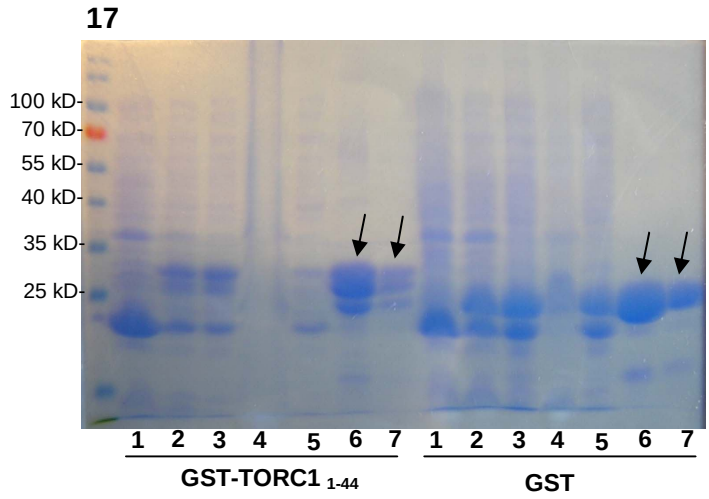

Figure 17: Purification of GST protein and GST-TORC1$_{1-44}$ fusion protein
The following protein extracts were subjected to SDS-PAGE (12% acrylamide) and stained with coomassie dye. The bands at 31 kD and 26 kD indicated purified GST- TORC1$_{1-44}$ and GST (arrows), respectively.
1. Cell extract before induction with IPTG
2. Cell extract after induction with IPTG
3. Supernatant after induction with IPTG and cell disruption
4. Pellet after induction with IPTG and cell disruption
5. Supernatant after incubating with Ni-agarose beads
6. 15 µl of proteins bound to Ni-agarose beads
7. 5 µl of proteins bound to Ni-agarose beads

To estimate the amounts of the purified protein used in *in vitro* protein interaction assay, a semi-quantitative analysis of proteins (3.3.a.II) was performed.

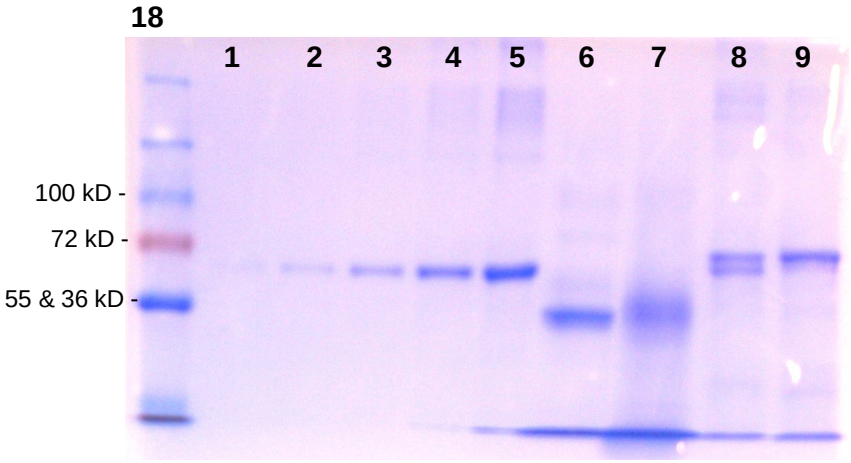

Figure 18: Semi-quantification of purified proteins
Different amounts and volume of BSA protein and purified proteins, respectively, as indicated were subjected to SDS-PAGE (8% acrylamide) and stained with coomassie dye. The marker bands at 55 and 36 kD overlapped. The bands at about 60 kD correspond to BSA (lane 1-5). GST protein and GST-TORC1$_{1-44}$ fusion protein migrated at 26 kD and 31 kD, respectively. His-tagged TORC1 full length and His-tagged TORC1$_{\Delta 44}$ proteins migrated at 70 kD, and 65 kD, respectively.
Lane 1: 0.1 mg BSA
Lane 2: 0.2 mg BSA
Lane 3: 0.5 mg BSA
Lane 4: 1 mg BSA
Lane 5: 2 mg BSA
Lane 6: 5 µl of GST protein bound to glutathione agarose beads
Lane 7: 5 µl of GST-TORC1$_{1-44}$ fusion protein bound to glutathione agarose beads
Lane 8: 15 µl of His-TORC1 full length fusion protein bound to Ni-agarose beads
Lane 9: 15 µl of His- TORC1$_{\Delta 44}$ fusion protein bound to Ni-agarose beads

In **Fig. 18**, equal volumes of GST and GST-TORC1$_{1-44}$ proteins and of His-tagged TORC1 full length and His-tagged TORC1$_{\Delta 44}$ proteins were loaded. The band representing GST-TORC1$_{1-44}$ was fuzzy due to the expression of GST protein in the same selected bacterial clone. In this 8% acrylamide gel, the low-weight proteins were not well separated. Therefore, the marker bands at 55 kD and 36 kD overlapped and both GST and GST-TORC1$_{1-44}$ migrated at the same size.

4.7.b. In vitro interaction of proteins

4.7.b.I. Interaction between TORC1 full length and DLK wild-type or DLK mutants.

Bacterially expressed His-tagged TORC1 full length protein bound to NTA-Ni agarose beads (§4.7.a, **Fig. 16**) was used in this experiment. The NTA-Ni agarose beads served as background control. DLK wild-type, its kinase-dead DLK K185A mutant and the dimerization-difficient DLK P-P mutant were labelled by in vitro transcription and translation using [^{35}S]-methionine (§3.5). Radio-labelled CREB wild-type and its mutant CREB R300A served as positive and negative controls, respectively. *In vitro* protein interaction assays were performed as described before (§3.6)

The upper panels of **Fig. 19A** and **B** represent typical gels showing the interaction between TORC1 full length and DLK wild-type or CREB wild-type. As seen in lane 7 and 8 (upper panel, **Fig. 19A**), the interaction between TORC1 and DLK wild-type or DLK K185A was stronger than the interaction between TORC1 and the dimerization-deficient DLK mutant (lane 9). In the control experiment (upper panel, **Fig. 19B**), CREB wild type (lane 5) interacted more with TORC1 full length than the CREB R300A (lane 6).

The lower panels of **Fig. 19A** and **B** are graphs showing the quantitative evaluation of the interaction assays. The kinase dead DLK mutant interacted a slightly better with TORC1 full length (121.3 $\pm$ 19.1%) when compared to DLK wild-type (lower panel, **Fig. 19A**). However, this difference was not significant. The interaction between TORC1 full length and the dimerization deficient DLK mutant was reduced to 62.5 $\pm$ 5.3% compared to that of the wild-type form ($p<0.04$) (lower panel, **Fig. 19A**). As positive control, under the same experimental condition, CREB R300A (unable to interact with TORC (Screaton et al., 2004) exhibited less interaction intensity with TORC1 full length (19.8 $\pm$ 1.5%, $p<0.01$) than CREB wild-type did (lower panel, **Fig. 19B**).

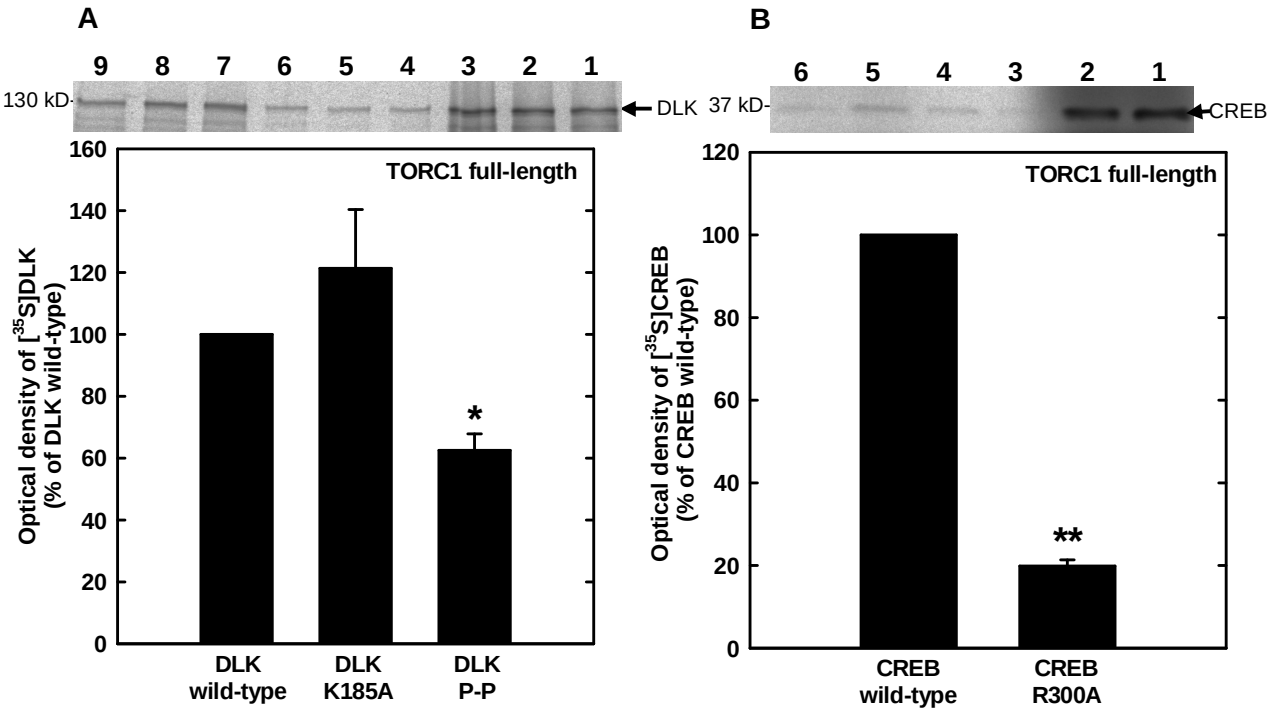

Figure 19: *In vitro* interaction between DLK/CREB and TORC1 full length

His-tagged TORC1 full length was expressed in *E.coli*, purified by affinity chromatography and immobilized on NTA-Ni agarose. NTA-Ni agarose alone was used as background. DLK wild-type and its mutants or CREB wild-type and CREB R300A were labelled with [^{35}S]methionine by *in vitro* transcription and translation. The amount of [^{35}S]DLK or [^{35}S]CREB proteins recovered from His-tagged protein was analyzed by SDS-PAGE followed by autoradiography and densitometric analysis of the bands corresponding to [^{35}S]DLK or [^{35}S]CREB. Typical gels are shown above the graphs.
The data are mean values ± SEM of three independent experiments and are expressed in percent of DLK wild-type (A) or CREB wild-type (B). Statistical analysis was performed by two-way ANOVA followed by two-sided paired Student's *t*-test: : $^{**}p \leq 0.01$, $^{*}p \leq 0.05$.

Figure 19A:
The upper panel
Lane 1, 2 and 3: 25% input of DLK wild-type, DLK K185A and DLK P-P, respectively.
Lane 4, 5 and 6: Interaction between NTA-Ni Agarose and DLK wild-type, DLK K185A and DLK P-P, respectively. These were used as corresponding backgrounds in calculation.
Lane 7, 8 and 9: Interaction between His-TORC1 full length and and DLK wild-type, DLK K185A and DLK P-P, respectively.
The lower panel
Graph of result showing interaction between DLK proteins and TORC1 full length

Figure 19B:
The upper panel
Lane 1 and 2: 25% input of CREB wild-type and CREB R300A, respectively.
Lane 3 and 4: Interaction between NTA-Ni Agarose and CREB wild-type and CREB R300A, respectively. These were used as corresponding backgrounds in calculation.
Lane 5 and 6: Interaction between His-TORC1 full length and CREB wild-type and CREB R300A, respectively.
The lower panel
Graph of result showing interaction between CREB proteins and TORC1 full length

4.7.b.II. Interaction between TORC1$_{1-44}$ and DLK wild-type or DLK mutants

The N-terminal coiled-coil domain of TORC was shown to interact with the dimerized leucine zipper domain of CREB (Conkright et al. 2003; Iourgenko et al. 2003; Screaton et al. 2004). In order to investigate whether DLK interacts with this region of TORC, the N-terminal 44 amino acid peptide of TORC1 in fusion with GST bound to glutathione agarose beads (§4.7.a, **Fig. 17**) was used in the *in vitro* protein interaction assay (§3.6). GST alone bound to glutathione agarose beads (**Fig. 17**) was used as background control. DLK and CREB proteins were radio-labelled and used as described above (4.7.b.I).

As shown in the typical gel (upper panel, **Fig. 20A**), the N-terminal domain of TORC1 interacted less with DLK P-P (lane 9) than with DLK wild-type (lane 7) or DLK K185A (lane 8). In **Fig. 20B** (upper panel), the N-terminus of TORC1 also interacted more with CREB wild-type (lane 5) than with CREB R300A (lane 6).

Analysis of the optical density of the pulled down [^{35}S] proteins shown in **Fig. 20A** indicates that DLK wild-type and DLK K185A interacted to the same extent with TORC1$_{1-44}$. DLK P-P interacted with the C-terminal-deleted TORC1 about 30% less than the wild-type form (**Fig. 20A**). However, no significant differences of interaction among those groups were observed. In the same experimental condition, CREB wild-type and R300A interacted with TORC1 $_{1-44}$ (lower panel, **Fig. 20B**).

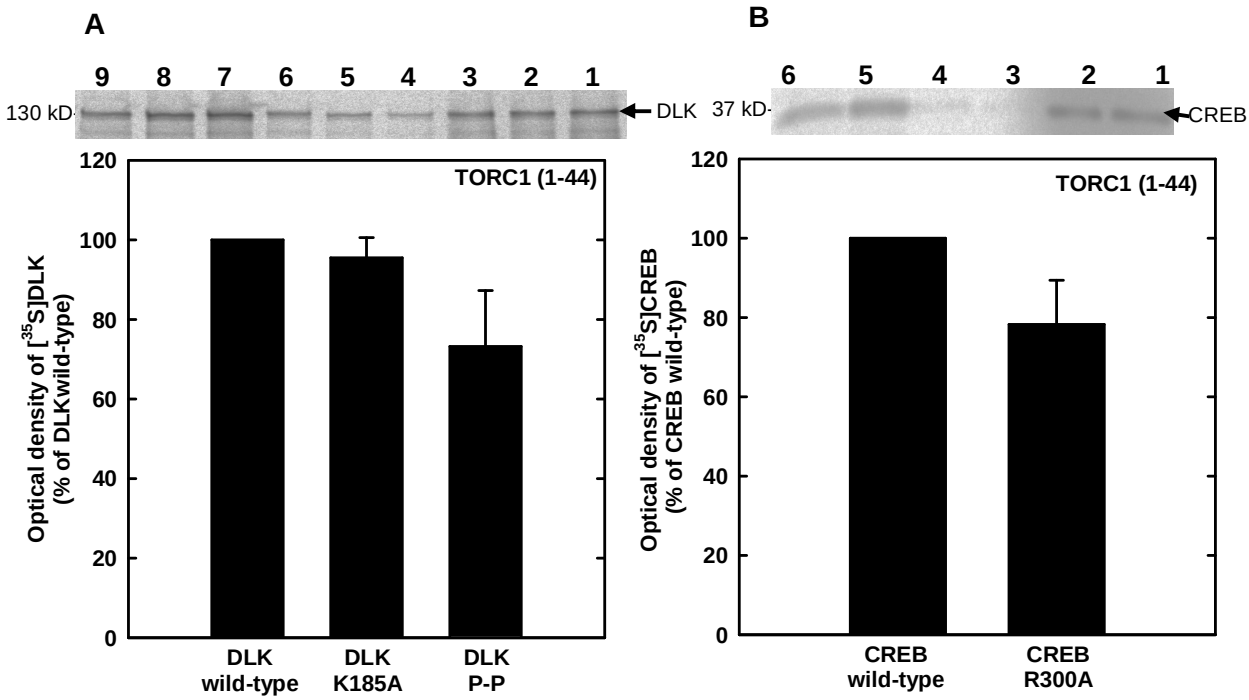

Figure 20: *In vitro* interaction between DLK/CREB and TORC1$_{1-44}$

GST-TORC1$_{1-44}$ fusion protein or GST alone was expressed in *E.coli*, purified by affinity chromatography and immobilized on glutathione agarose. GST alone was used as background. DLK wild-type, DLK mutants, CREB wild-type or CREB R300A were labelled with [^{35}S]methionine by *in vitro* transcription and translation. The amount of [^{35}S]DLK or [^{35}S]CREB proteins recovered from GST alone or GST fusion protein was analyzed by SDS-PAGE followed by autoradiography and densitometric analysis of the bands corresponding to [^{35}S]DLK or [^{35}S]CREB. Typical gels are shown above the graphs.
The data are mean values ± SEM of three independent experiments and are expressed in percent of DLK wild-type (A) or CREB wild-type (B). Statistical analysis was performed by two-way ANOVA followed by two-sided paired Student's *t*-test: $^{*}p \leq 0.05$.

Figure 20A:

The upper panel

Lane 1, 2 and 3: 25% input of DLK wild-type, DLK K185A and DLK P-P, respectively.
Lane 4, 5 and 6: Interaction between GST and DLK wild-type, DLK K185A and DLK P-P, respectively. These were used as corresponding backgrounds in calculation.
Lane 7, 8 and 9: Interaction between GST-TORC1$_{1-44}$ fusion protein and and DLK wild-type, DLK K185A and DLK P-P, respectively.

The lower panel

Quantitative evaluation of the interaction between DLK proteins and TORC1$_{1-44}$

Figure 20B:

The upper panel

Lane 1 and 2: 25% input of CREB wild-type and CREB R300A, respectively
Lane 3 and 4: Interaction between GST and CREB wild-type and CREB R300A, respectively. These were used as corresponding backgrounds in calculation.
Lane 5 and 6: Interaction between GST-TORC1 $_{1-44}$ and CREB wild-type and CREB R300A, respectively.

The lower panel

Quantitative evaluation of the interaction between CREB proteins and TORC1$_{1-44}$

4.7.b.III. Interaction between TORC1$_{\Delta 44}$ and DLK wild-type or DLK mutants

The His-tagged TORC1$_{\Delta 44}$ (§4.7.a, **Fig. 16**) was used to check if the C-terminus of TORC1 interacts with the radio-labelled DLK proteins. NTA-Ni agarose served as background control.

As seen in **Fig. 21**, the deletion of 44 N-terminal amino acids of TORC resulted in almost no interaction with DLK wild-type, DLK K185A or DLK P-P (**Fig. 21**)

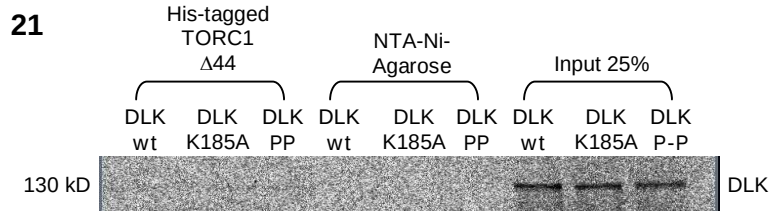

Figure 21: Interaction between the N-terminal deleted TORC1 and DLK wild-type, DLKK185A or DLKP-P.
His-tagged TORC1$_{\Delta 44}$ was expressed in *E.coli*, purified by affinity chromatography and immobilized on NTA-Ni agarose. NTA-Ni agarose alone was used as background. DLK wild-type and its mutants were labelled with [^{35}S]methionine by *in vitro* transcription and translation. The amount of [^{35}S]DLK proteins recovered from His-tagged protein was analyzed by SDS-PAGE followed by autoradiography and densitometric analysis of the bands corresponding to [^{35}S]DLK. Typical gel is shown.

4.7.b.IV. Interaction between DLK wild-type and different domains of TORC

In order to identify the region of TORC which interacts with DLK wild-type, a pull down assay was performed using bacterially expressed His-tagged TORC1 full length protein, His-tagged TORC1$_{\Delta 44}$ protein, GST-TORC1$_{1\text{-}44}$ and [^{35}S] labelled DLK wild-type.

All tested TORC1 proteins interacted with DLK wild-type, albeit to a different extent (**Fig. 22**). As demonstrated in the typical gel (the upper panel, **Fig. 22**), DLK wild-type interacted more with the N-terminal domain of TORC1 (lane 6) than the others. DLK wild-type interacted to a higher extent with TORC1 full length protein (lane 5) than with the C-terminus of TORC1 (lane 4).

The quantitative evaluation is shown in the graph (lower panel, **Fig. 22**). As compared to the interaction with TORC1 full length, the interaction between DLK wild-type and TORC1$_{\Delta 44}$ was reduced significantly to 64.2 $\pm$ 1.9% ($p<0.006$), whereas the interaction between DLK wild-type and TORC1$_{1\text{-}44}$ was about 6-fold ($p<0.03$) increased.

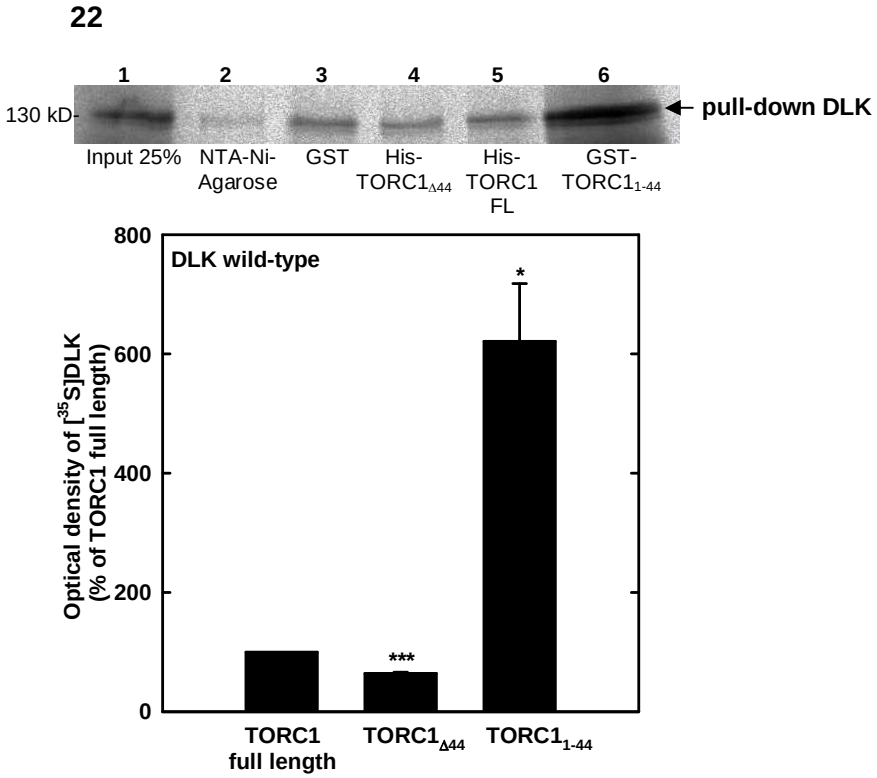

Figure 22: Interaction between TORC1 full length, TORC1Δ44, $TORC1_{1-44}$ and DLK wild-type.

GST-$TORC1_{1-44}$ fusion protein, GST alone, His-tagged TORC1 full length, His-tagged $TORC_{\Delta 44}$ were expressed in *E.coli*, purified by affinity chromatography and immobilized on appropriate agarose beads. GST alone and NTA-Ni agarose were used as background for GST-$TORC_{1-44}$ and His-tagged TORC proteins, respectively. DLK wild-type was labelled with [^{35}S]methionine by *in vitro* transcription and translation. The amount of [^{35}S]DLK recovered from GST alone, GST fusion protein or His-tagged proteins was analyzed by SDS-PAGE followed by autoradiography and densitometric analysis of the bands corresponding to [^{35}S]DLK. Typical gel is shown above the graph.
The data are mean values ± SEM of three independent experiments and are expressed in percent of TORC1 full-length. Statistical analysis was performed by two-way ANOVA followed by two-sided paired Student's *t*-test: $^{***}p \leq 0.005$, $^{*}p \leq 0.05$.

4.8. Interaction between DLK and TORC in HIT cells

The pull down assay showed that DLK interacted with TORC1. To investigate whether TORC1 interacts with DLK in a cellular context, a co-immunoprecipitation assay (§3.12) was performed. HIT cells were transiently co-transfected (§3.8a) with an expression vector for TORC1 full length and with flag epitope tagged expression vectors for DLK wild-type or its mutants. An equal overexpression of the proteins was tested by Western blot (§3.3d) using primary antibodies against DLK or TORC1 (**Fig. 23**). DLK or its mutants were immunoprecipitated using an antibody against the flag epitope, and co-immunoprecipitated TORC1 was detected by the antibody specifically against TORC1 (**Fig. 24**).

As demonstrated in **Fig. 23**, DLK wild-type, its mutants and TORC1 were overexpressed in HIT cells (lane 4, 6 and 8, **Fig. 23**). The expression levels of DLK proteins in the cells

co-transfected with TORC1 (lanes 4, 6 and 8, **Fig. 23**, upper panel) were less than in cells without TORC1 cotransfection (lanes 3, 5 and 7, **Fig. 23**, upper panel). Due to the reduced expression level of DLK wild-type or its mutants in the presence of overexpressed TORC1, co-immunoprecipitated TORC1 was corrected for the amount of the corresponding immunoprecipitated DLK.

23

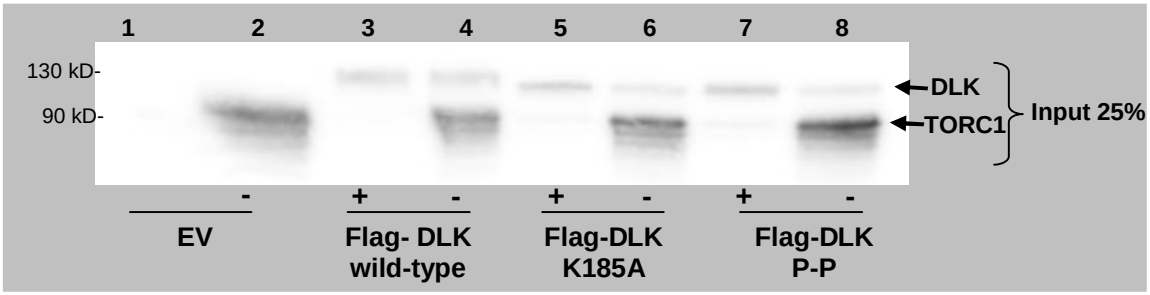

Figure 23: Overexpression of DLK wild-type, DLK K185A, DLK P-P and TORC1 in HIT cells
Expression vectors for flag-tagged DLK wild-type, DLK K185A or DLK P-P were co-transfected with the expression vector for TORC1 into HIT cells. Cells were harvested after 48 hours. Cells were lysed and the extracts were analyzed by western blot using antibodies against TORC1 and the C-terminal 223 aa of DLK.
The typical Western blot showing overexpression of TORC1 and DLK proteins: The bands at 130 kD represent DLK wild-type (lane 3, 4), DLK K185A (lane 5, 6) and DLK PP (lane 7, 8). The bands at 90 kD represent TORC1 (lanes 2, 4, 6 and 8)
EV: Empty vector pcDNA3

In the co-immunopreciptation assay, no TORC1 was detected in samples without overexpression of flag epitope tagged DLK (lanes 1 and 2, upper panel, **Fig. 24**)

In the presence of DLK wild-type or its mutants, overexpressed TORC1 co-immunoprecipitated with DLK wild-type and its mutants (lane 4, 6 and 8, upper panel, **Fig. 24**); however, as observed in the *in vitro* pull down assay, the interaction between TORC and the dimerization-deficient DLK mutant was somewhat less than its interaction with DLK wild-type (lane 8 and 4, upper panel and the graph, **Fig. 24**), which was about 77.2 ± 13.2% of DLK wild-type. This difference was not significant, however, the T-test with $p = 0.12$ implied the trend of a difference. The interactions of TORC with DLK wild-type or kinase dead DLK mutant were not significant different.

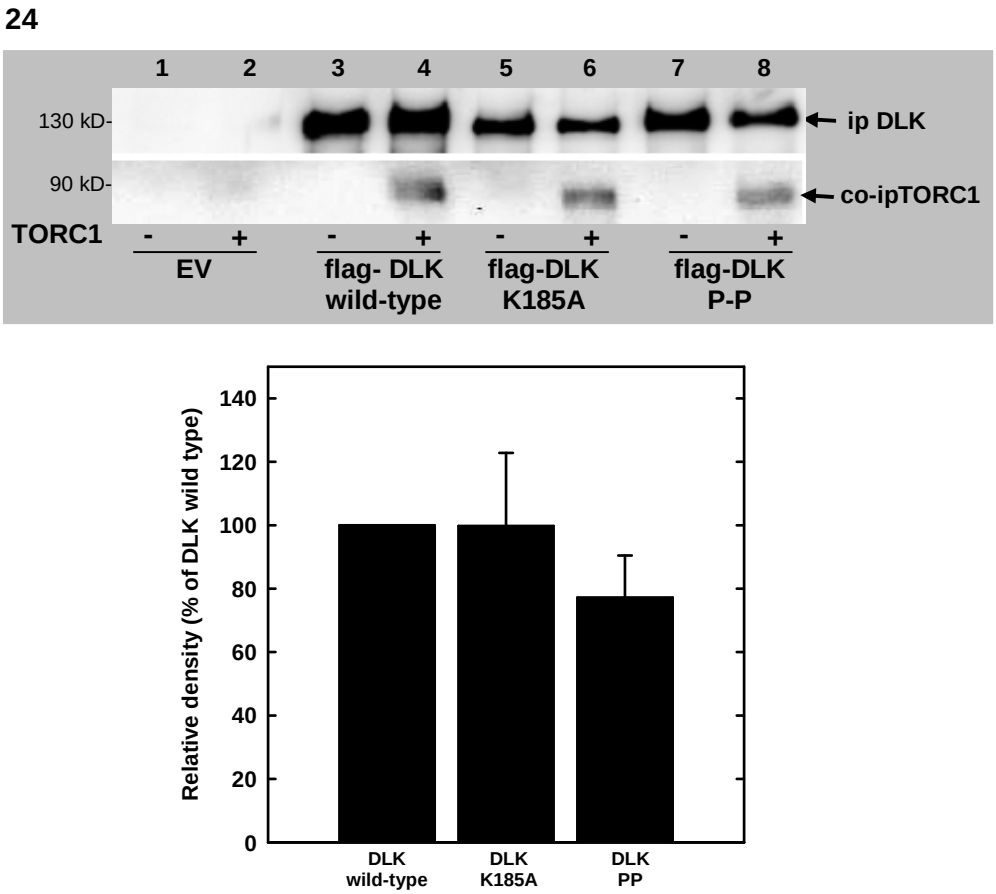

Figure 24: Interaction of TORC1 with DLK wild-type, DLK K185A and DLK P-P in HIT cells
Expression vectors for flag-epitope tagged DLK wild-type or its mutants were co-transfected with vector for TORC1 into HIT cells. Cells were harvested after 48 hours. Cells were lysed and flag epitope tagged DLK proteins were immunoprecipitated using anti-flag antibody and protein A agarose. TORC1 co-immunoprecipitated with DLK proteins was detected by Western blot using the antibodies against TORC1 and the C-terminal 223 aa of DLK.
Cells transfected with the empty vector pcDNA3 (EV) were used as negative control. The interaction between DLK wild-type and TORC1 was considered as 100%. All results are expressed as means ± SEM of five independent experiments.
Calculation: interaction level = (the density of band representing coimmunopreciptatated TORC) / (the density of band representing corresponding immunoprecipitated DLK)
The upper panel: Typical Western blot showing DLKs co-immunoprecipitated with TORC1
Immunoprecipitated DLKs migrated at 130 kD (lane 3-8)
Co-immunoprecipitated TORC1 was corresponding to the band migrating at 90 kD (lane 4, 6 and 8)
The lower panel: Quantitative evaluation of the co-immunoprecipitation assays.

4.9. Effect of DLK on the nuclear localization of TORC

TORC nuclear localization is required for CRE/CREB-directed gene transcription and its cellular localization is regulated by diverse signals (Bittinger et al. 2004; Screaton et al. 2004). The shuttling of TORC between nucleus and cytoplasm depends at least in part on its phosphorylation status. Therefore, the effect of DLK on the nuclear localization of TORC was investigated by immunocytochemistry (§3.11). The expression vector for flag epitope tagged DLK or its kinase-dead mutant were transiently transfected (§3.8b) into HIT cells. Cells were treated with 45 mM KCl for 30 min, as indicated. The overexpressed DLK protein and endogenous TORC protein were detected by the primary antibodies

against the flag epitope and against TORC, respectively, and the secondary anti-mouse protein TRITC labeled and anti-rabbit protein Alexa Fluor 488 labeled antibodies, respectively. Cell nuclei were stained with DAPI. The cells showing a nuclear localization of TORC in DLK-positive were counted manually using fluorescent microscopic analysis (§3.11).

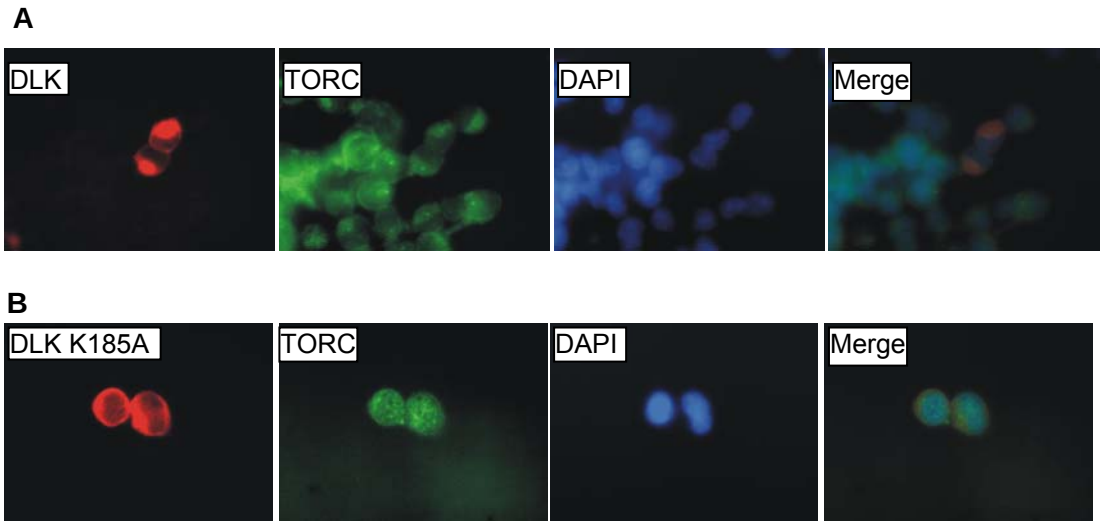

Figure 25: Typical pictures showing subcellular localization of TORC in the presence of overexpressed DLK wild-type (**A**) or overexpressed DLK K185A (**B**).
HIT cells were transiently transfected with expression vectors for flag-epitope tagged DLK wild-type or flag-epitope tagged DLK K185A. Cells were stained with anti-flag epitope antibody (mouse), anti-TORC antibody (rabbit) and with DAPI (stain nucleus with blue colour). The secondary antibodies were anti-mouse protein_TRITC (red colour) and anti-rabbit protein_Alexa Fluor 488 (green colour). In the pictures, flag-epitope tagged DLK proteins were stained with red colour, endogenous TORC proteins were stained with green colour, and the nuclei were blue.

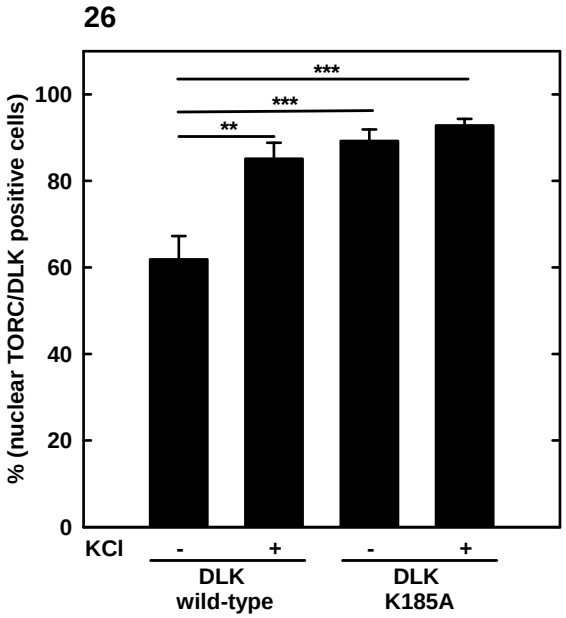

Figure 26: Effect of DLK on the nuclear localization of TORC
HIT cells were transiently transfected with expression vectors for flag-epitope tagged DLK wild-type or flag-epitope tagged DLK K185A. Cells were treated with 45 mM KCl for 30 min, as indicated. Cells were stained with anti-flag epitope antibody (mouse), anti-TORC antibody (rabbit) and with DAPI (stain nucleus with blue colour). The secondary antibodies were anti-mouse protein_TRITC (red colour) and anti-rabbit protein_Alexa Fluor 488 (green colour). In each single experiment about 30-80 DLK-positive cells were randomly selected and the number of cells presenting TORC in the nucleus was counted. The percentage of cells with nuclear TORC within the number of DLK-positive cells was calculated. All results are expressed as means ± SEM of three independent experiments, each done in duplicate. Statistical analysis was performed by two-way ANOVA followed by two-sided paired Student's *t*-test: $^{**}p \leq 0.01$, $^{***}p \leq 0.005$.

In the presence of DLK wild-type already 60% of cells exhibited nuclear localization of TORC (**Fig. 25A** and **Fig. 26**), which was further increased in the presence of DLK K185A (**Fig. 25B** and **Fig. 26**). In detail, endogenous TORC was observed in nuclei of about 61.9 ± 5.4% of DLK wild-type-positive cells (**Fig. 26**). Treatment of KCl increased significantly the nuclear localization of TORC within the DLK-positive cells (85.1 ± 3.7%, $p<0.006$, as compared to the basal condition of overexpressed DLK wild-type) (**Fig. 26**). Under basal or KCl treatment condition, up to 90% of DLK K185A-positive cells showed a nuclear localization of TORC, which was significant different from the percentage of DLK wild-type showed nuclear localization of TORC in the basal condition ($p<0.001$ or $p<0.002$, respectively) (**Fig. 26**).

4.10. Effect of DLK on the phosphorylation of TORC in an in vitro assay

The phosphorylation of TORC 1 and TORC2 at Ser-167 and Ser-171, respectively, is a decisive point in the process regulating TORC transactivating capacity (Screaton et al. 2004, Katoh et al. 2004, Bittinger et al. 2004). To study whether DLK phosphorylates TORC1 and TORC2 at these residues, an *in vitro* kinase assay (§3.13) was performed using the bacterially expressed His-tagged TORC proteins (§3.4) as subtrates and the flag epitope tagged DLK proteins which were overexpressed in HIT cells and purified by immunoprecipitation (§3.12a) as kinase.

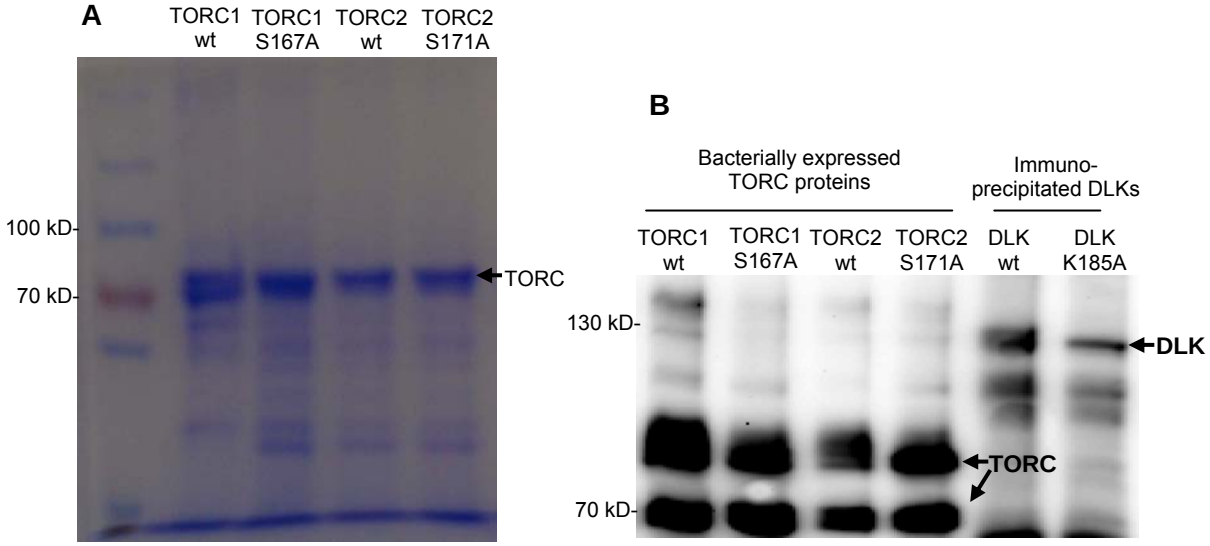

Figure 27A: TORC proteins were expressed and purified from E.coli. The proteins were subjected to SDS-PAGE (8% acrylamide) and stained with coomassie dye. The bands migrated between 70 kD and 74 kD (arrow) indicate the purified His-tagged TORC proteins (wt: wild-type).

Figure 27B: Western blot to check the bacterially expressed His-tagged TORC proteins and immunoprecipitated DLK proteins. The first four lanes from left to right show His-tagged TORC1 wild-type, TORC1 S167A, TORC2 wild-type and TORC2 S171A, respectively. The next two lanes show DLK wild-types and DLK K185A.
TORC proteins were expressed and purified from E.coli. DLK proteins were immunoprecipitated from HIT cells. Those proteins were applied to SDS-PAGE and followed by Western blot. TORCs and DLK were detected with anti-Pan TORC antibody and antibody against the C-terminal 223 aa of DLK, respectively. The double bands representing TORCs migrated between 70 kD and 74 kD, whereas DLK migrated at 130 kD.

As shown in **Fig. 27A** and **B**, all TORC proteins used were successfully expressed and purified from bacteria. The equal amount of TORC1 wild-type and TORC1 S167A or TORC2 wild-type and TORC2 S171A were used (**Fig. 27A**). TORC proteins were detected at the region between 70 kD and 74 kD by Western blot (**Fig. 27B**). The flag-epitope tagged DLK wild-type and DLK K185A were overexpressed and immunoprecipitated from HIT cells (**Fig. 27B**)

28

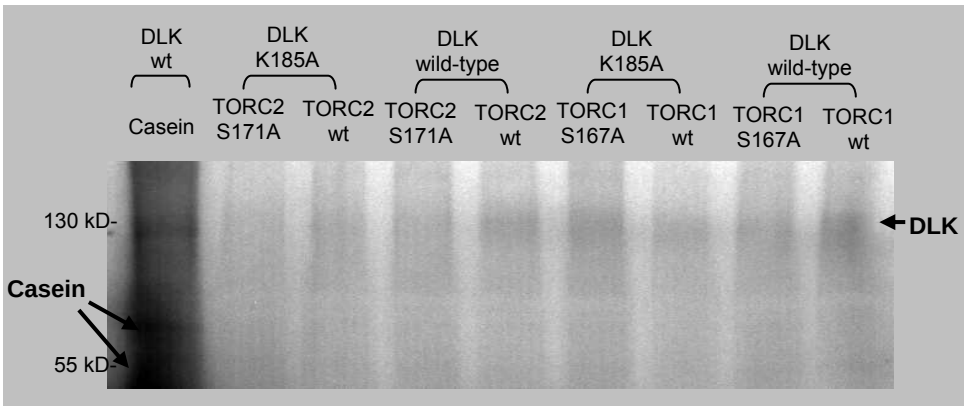

Figure 28: *In vitro* kinase assay
The immunoprecipitated DLKs were incubated with the bacterially expressed TORC proteins, as indicated, in kinase buffer supplemented with [^{32}P] labelled γ-ATP. After incubation for 3h at room temperature, the samples were subjected to SDS-PAGE and the intensity of phosphorylated proteins was evaluated using phosphor-imager scanner. The phosphorylation of the general substrate casein by DLK served as positive control.

The bands at 130 kD showed that DLK was autophosphorylated. Casein was phosphorylated by DLK wild-type (**Fig. 28**). However, no phosphorylation of TORC proteins was detected in this *in vitro* kinase assay.

4.11. Effect of DLK on the phosphorylation of TORC in HIT cells

The *in vitro* kinase assay provided no evidence that DLK directly phosphorylated TORC. To study whether DLK indirectly, i.e. via its downstream kinases, enhances the phosphorylation of TORC, the effect of DLK on the phosphorylation of TORC in HIT cells was investigated. To this aim, HIT cells were transiently co-transfected with expression vectors for DLK wild-type or DLK K185A and human TORC1 full length. 48 h after transfection, the cells were treated with CsA, or combination of KCl and Forskolin, as indicated. CsA enhances the phosphorylation of TORC, whereas KCl and forskolin treatment reduce the phosphorylation of TORC (Bittinger et al. 2004, Screaton et al. 2004, Katoh et al. 2004, Takemori and Okamoto, 2008). Cells were harvested, lysed (§3.3d) and a Western blot (§3.10) was performed. The phosphorylation of TORC1 was detected using an antibody specifically against on Ser-151 phosphorylated murine (m) TORC1 (equivalent to Ser-167 human (h) TORC1).

In these experiments, human TORC1 was used, whereas the antibody is against the Ser-151 phosphorylated TORC1 of mouse. Therefore, first, the specificity of the antibody against on Ser-151 phosphorylated mTORC1 was tested if it is able to detect on Ser-167 phosphorylated hTORC1. As shown in **Fig. 29**, this antibody was able to detect hTORC1 wild-type (lane 1) which was phosphorylated at Ser-167 and was unable to detect mTORC1 S151A (lane 2) in which the Ser-151 was changed to alanine.

29

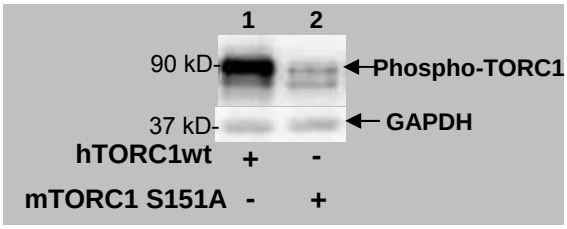

Figure 29: Western blot: Control of the antibody specifically against Ser-151 phospho-mTORC1 (equivalent to Ser-167 hTORC1
HIT cells were transiently transfected with expression vectors for human (h) TORC1 wild-type (wt) or mouse (m) TORC1 S151A. After 48 hours of incubation, cells were harvested and lysed in lysis buffer an a Western blot was perfomed using the antibody specifically against Ser-151 phospho-mTORC1 and an antibody against GAPDH.

In **Fig. 30** a typical Western blot showing the effect of DLK on the phosphorylation of TORC1 on Ser-167 is depicted.

30

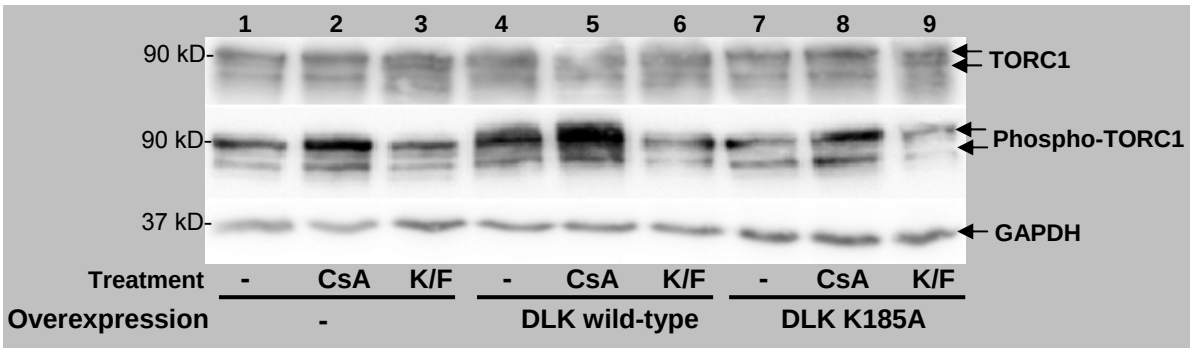

Figure 30: Typical Western blot: The effect of DLK on the phosphorylation of TORC on Ser-167
HIT cells were co-transfected with expression vectors for DLK wild-type or DLK K185A and human TORC1 wild-type. 48h after transfection, cells were treated with 5 µM CsA, or a combination of 45 mM KCl (K) and 10 µM forskolin (F) for 15 minutes. Cells were harvested and lysed in lysis buffer supplemented with phosphatase inhibitors. A Western blot was performed using antibodies specifically against GAPDH, Ser-167 phospho-TORC1 and TORC1.
No overexpression of DLK (lane 1-3): CsA (lane 2) enhanced, whereas KCl and forskolin (lane 3) reduced the phosphorylation of TORC1 on Ser-167, as compared to basal condition (lane 1).
Overexpression of DLK wild-type (lane 4-6): CsA (lane 5) enhanced, whereas KCl and forskolin (lane 6) reduced the phosphorylation of TORC1 on Ser-167, as compared to basal condition (lane 4).
Overexpression of DLK K185A (lane 7-9): CsA (lane 8) enhanced, whereas KCl and forskolin (lane 9) reduced the phosphorylation of TORC1 on Ser-167, as compared to basal condition (lane 7).
In basal condition (lanes 1, 4, 7): Overexpression of DLK wild-type (lane 4) enhanced the phosphorylation of TORC on Ser-167, as compared to the non-overexpression group (lane 1) or the overexpression of DLK K185A (lane 7).
Treatment of CsA (lanes 2, 5, 8): Overexpression of DLK wild-type (lane 5) enhanced the phosphorylation of TORC on Ser-167, as compared to the non-overexpression group (lane 2) or the overexpression of DLK K185A (lane 8).
The combined treatment of KCl and forskolin (lanes 3, 6, 9): no pronounced difference was observed among groups.

Independent of the overexpression of DLK wild-type or its mutant, CsA enhanced the phosphorylation of TORC1, whereas the combination of KCl and forskolin reduced it (see the legend, **Fig. 30**). Overexpression of DLK wild-type enhanced the phosphorylation of TORC1 on Ser-167 both in the basal condition (compare lane 4 with lane 1) and in the presence of CsA (compare lane 5 and lane 2) **(Fig. 30**). Overexpression of DLK K185A did not result in differences under both basal condition (compare lane 7 with lane 1) and CsA-treated condition (compare lane 8 and lane 2) (**Fig. 30**). Notably, in different experiments, in the presence of overexpressed DLK wild-type plus CsA, the band representing on Ser-167 phosphorylated TORC1 (lane 5, **Fig. 30**) migrated slower than the others.

Quantitative evaluation of five independent experiments and statistical analysis showed that under basal condition, DLK wild-type significantly enhanced the phosphorylation of TORC1 on Ser-167 to 191.1 ± 41.4% ($p<0.046$), whereas the kinase dead DLK mutant did not significantly increase the amount of on Ser-167 phosphorylated TORC1 (**Fig. 31**). Treatment with CsA increased the phosphorylation of TORC1 significantly from 187.5 ± 15.2% (in the absence of overexpressed DLK wild-type) to 267.1 ± 20.7% (in the presence of overexpressed DLK wild-type) ($p<0.017$, **Fig. 31**). However, treatment of KCl plus forskolin did not significantly change the level of on Ser-167 phosphoylated TORC1 (**Fig. 31**).

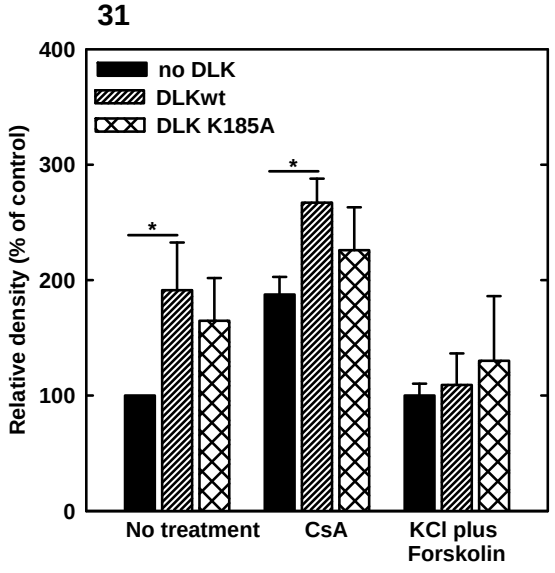

Figure 31: DLK wild-type induced the phosphorylation of TORC
HIT cells were co-transfected with expression vectors for DLK wild-type or DLK K185A and TORC1 wild-type. 48h after transfection, cells were treated with 5 µM CsA, or a combination of 45 mM KCl (K) and 10 µM forskolin (F) for 15 minutes. Cells were harvested and lysed in lysis buffer supplemented with phosphatase inhibitors. A Western blot was performed using antibodies specifically against GAPDH, Ser-167 phospho-TORC1 and TORC1, respectively.
To evaluate the phosphorylation of TORC, the density of the band representing phospho-TORC was normalized to the corresponding band representing TORC. The samples without transfection of DLK in basal condition were considered as control. All values are expressed as means ± SEM of five independent experiments. Statistical analysis was performed by two-way ANOVA followed by two-sided paired Student's *t*-test: $^{*}p \leq 0.05$.

In order to confirm that the shift of the band representing phospho-TORC in the sample with overexpression of DLK wild-type plus CsA treatment was due to the phosphorylation of TORC1 on additional sites (**see Fig. 30**), a Phos-tag SDS-PAGE was used. In Phos-tag SDS-PAGE, the acrylamide gel was supplemented with Phos-tag^{TM} AAL-107, a ligand of

acrylamide which is able to bind to the phospho groups of the proteins, thereby further retarding the migration of phosphorylated proteins (Kinoshita et al., 2008).

As shown in **Fig. 32**, the phosphorylated TORC1 was clearly detected as two shifted bands. CsA treatment in addition with the overexpression of DLK wild-type (lane 4, **Fig. 32**) resulted in the slower migration of the band representing on Ser-167 phosphorylated TORC1.

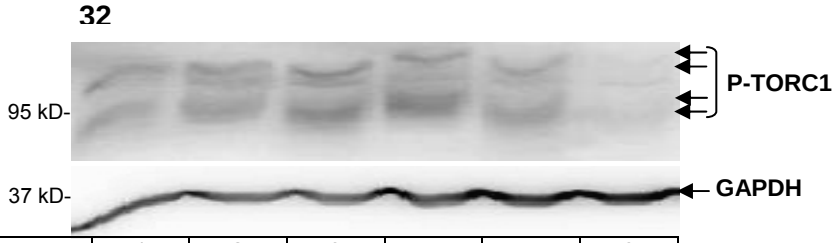

Lane	1	2	3	4	5	6
Overexpressed TORC1	wt	wt	wt	wt	wt	S151A
Overexpressed DLK	-	-	wt	wt	K185A	-
Treatment	-	CsA	-	CsA	-	-

Figure 32: Typical Western blot: The shift of of TORC1 protein phosphorylated on additional residues
HIT cells were transfected with expression vectors for DLK wild-type (wt), DLK K185A and hTORC1 wild-type (wt) or mTORC1S151A (equivalent to hTORC1 S167A). Cells were grown for 48h after transfection before harvest. Cells were treated, as indicated, with 5 µM CsA or a combination of 45 mM KCl (K) and 10 µM forskolin (F) for 15 min. Cells were lysed and the lysates were subjeted to phos-tag gel (8% acrylamide supplemented with 50 µM Phos-tag™ AAL-107). A Western blot was performed using antibody specically against on Ser-151 phosphorylated mTORC1 and an antibody against GAPDH.

JNK is the kinase downstream of DLK. To study whether JNK is involved in the phosphorylation of TORC, a Western blot analysis of phospho-TORC employing the antibody specifically against on Ser-151 phosphorylated mTORC1 (equivalent to Ser-167 phospho-hTORC1) was conducted. HIT cells were transfected with expression vectors for DLK wild-type and TORC1, as indicated. Cells were treated with a combination of KCl and forskolin, CsA or SP600125 (an inhibitor specific for JNK – Bennett et al., 2001) as indicated. 48 h after transfection, cells were harvested and lysed. The lysates were subjected to Phos-tag SDS-PAGE and a Western blot was perfomed.

A typical Western blot is shown in **Fig. 33**. Treatment with KCl plus forskolin (lane 2) reduced the amount of phosphorylated TORC1 (compared to non-treatment sample, lane 1). CsA increased the phosphorylation of TORC1 (lane 3) and this enhancement was more pronouced in the presence of overexpressed DLK (lane 6). The treatment of the JNK inhibitor SP600125 decreased pronoucedly the phosphorylation of TORC1 and prevented a slower migration of the phosphorylated TORC1 both in the absence or the presence of overexpressed DLK (lane 4 and 7, respectively, **Fig. 33**).

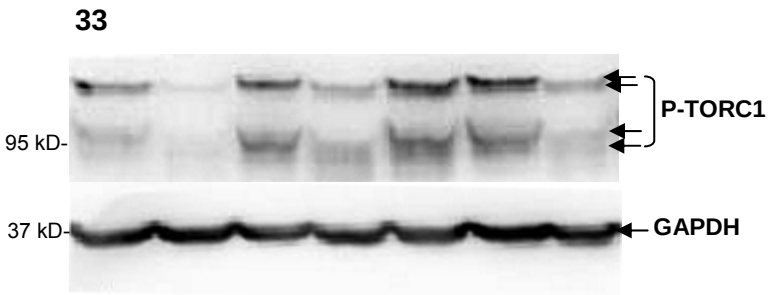

Lane	1	2	3	4	5	6	7
Overexpressed TORC1 wt	+	+	+	+	+	+	+
Overexpressed DLK wt	-	-	-	-	+	+	+
Treatment	-	K/F	CsA	SP	-	CsA	SP

Figure 33: Typical Western blot: Putative involvement of JNK in DLK-induced phosphorylation of TORC1
HIT cells were transfected with expression vectors for DLK wild-type and mouse TORC1. Cells were grown for 48 h after transfection before harvest. Cells were treated, as indicated, with 5 µM CsA or a combination of 45 mM KCl (K) and 10 µM forskolin (F) for 15 min or with 25 µM JNK inhibitor SP600125 (SP) for 12 h before harvest. Cells were lysed and the lysates were subjected to phos-tag gel (8% acrylamide supplemented with 50 µM Phos-tag^{TM} AAL-107). A Western blot was performed using an antibody specically against on Ser-151 phosphorylated mTORC1 (equivalent to Ser-167 phosphorylated hTORC1) and an antibody against GAPDH.

4.12. Effect of DLK on the recruitment of TORC to a CRE-containing promoter

The interaction with and the phosphorylation of TORC by DLK might result in decreased recruitment of TORC to a CRE-containing promoter. To investigate the effect of DLK on the recruitment of TORC to a CRE-containing promoter, a reporter gene assay (§3.15) was performed whereby a luciferase reporter gene controlled by the minimal promoter of the rat somatostatin gene (-65 SomCRE.Luc), containing a high affinity binding site for CREB (Oetjen et al. 1994), was transiently co-transfected into HIT cells with an expression vector for TORC1 (§3.8a). DLK wild-type or its mutants were overexpressed to observe their effect on TORC-induced CRE-dependent gene transcription. The cells were treated with a combination of KCl and forskolin, as indicated, to enforce the nuclear localization of TORC. By this way the nuclear translocation and an increased recruitment of TORC to the promoter can be demonstrated (Boer et al. 2007).

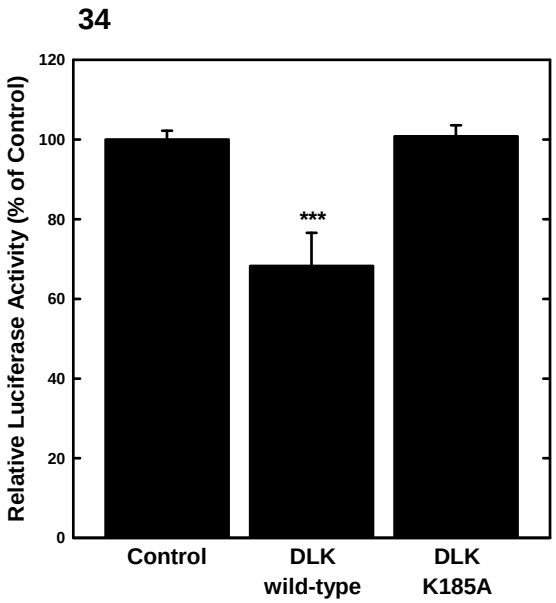

Figure 34: Effect of DLK on TORC dependent CRE-directed gene transcription under combined treatment of KCl and forskolin.
A luciferase reporter fusion gene under the control of the minimal promoter of the rat somatostatin gene (-65 SomCRE.Luc), containing a high affinity binding site for CREB, was transiently co-transfected with an expression vector for TORC1. The cells were co-transfected with expression vectors for DLKwt or its kinase dead mutant as indicated and incubated for 48 hours prior to harvesting and measuring luciferase activity. Treatment of cells with a combination of 45 mM KCl and 10 µM forskolin was applied 6 hours before harvesting. The luciferase activity in cells transfected with the reporter gene, the expression vector for TORC1 protein and Bluescript were considered as control. Relative luciferase activity values are means ± SEM of three independent experiments performed in duplicate, and are expressed in percent of control. Statistical analysis was performed by two-way ANOVA followed by Student's *t*-test: $^{***}p \leq 0.005$.

Of note, KCl plus forskolin treatment increased the TORC1 dependent CRE directed gene transcription to about 170-fold (data not shown). DLK wild-type, but not its kinase dead mutant, significantly inhibited this transcriptional activity in the presence of KCl plus forskolin treatment (**Fig. 34**).

To further elucidate the effect of DLK on TORC promoter recruitment a chromatin immunoprecipitation assay (§3.14) was employed. HIT cells were transfected (§3.8b) with a promoter containing four copies of the CRE of the rat somatostatin promoter and an expression vector for HA epitope tagged TORC1. In addition, the expression vector for DLK wild-type was co-transfected (§3.8b). DNA and proteins were cross-linked and immunoprecipitated with an antibody against the HA epitope. The amount of precipitated DNA was determined by qRT-PCR (Heinrich et al. 2009). Treatment of the cells with membrane depolarization and forskolin which enhance the amount of TORC protein recruited to CRE promoter was used as a positive control.

Fig. 35 shows the results of the ChIP assay. The combined stimulation with KCl and forskolin significantly increased the amount of precipitated DNA to 131.5 ± 1.7% ($p<0.0001$, **Fig. 35**). Overexpression of DLK wild-type significantly reduced the amount of precipitated DNA by 28% ($p<0.018$, **Fig. 35**).

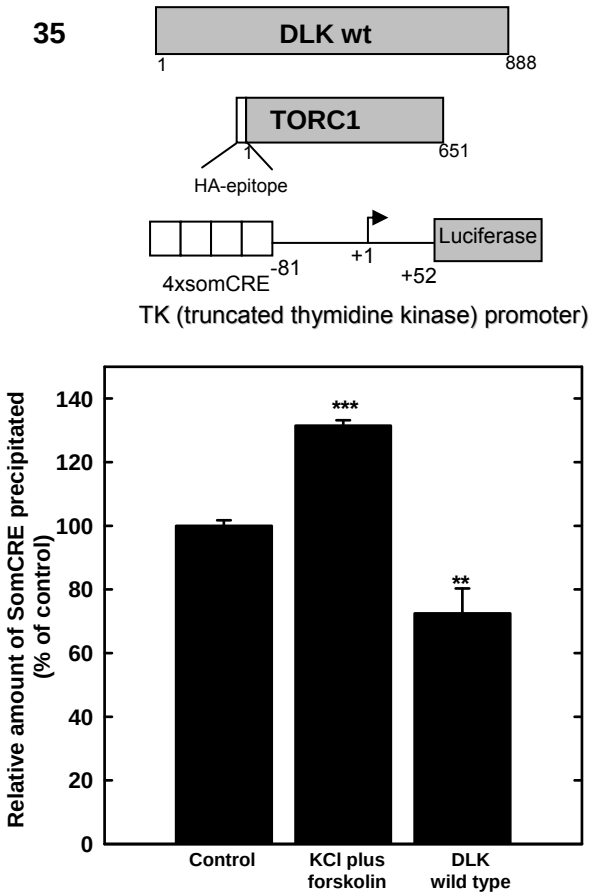

Figure 35: Effect of DLK on the recruitment of TORC to a CRE-containing promotor

HIT cells were transfected with a promoter containing four copies of the CRE of the rat somatostatin promoter and an expression vector for HA epitope tagged TORC1. In addition, the expression vector for DLK wild-type was co-transfected. The schemes of plasmids used in the experiment are depicted in the upper pannel. 48h after transfection, cells were treated with 45 mM KCl plus 10 µM forskolin for 30 min before performing the ChIP assay. DNA and proteins were cross-linked with 1% formaldehyde, the complexes were precipitated by an antibody against the HA epitope. The amount of precipitated DNA was determined by qRT-PCR. Cells transfected with vectors for TORC1, Bluescript and 4xsomCRE.Luc were used as control. The precipitated amount of DNA is expressed relative to the mean value of the control ± SEM. Values represent three independent experiments, each done in duplicate. Statistical analysis was performed by two-way ANOVA followed by Student's *t*-test: $^{***}p \leq 0.005$, $^{**}p \leq 0.01$.

5. DISCUSSION

In the present study the molecular mechanism by which the Dual Leucine Zipper-bearing Kinase (DLK) regulates the activity of Transducer of regulated CREB (TORC) in HIT cells was investigated. DLK was demonstrated to inhibit the transcriptional activity of the three isoforms of TORC under both the basal and stimulated condition. The inhibitory action of DLK on TORC can be explained first by indirect enhancement of the phosphorylation of TORC1 on Ser167; second, direct interaction between DLK and TORC1 may contribute to the reduction of TORC activity; finally, the ways by which DLK inhibits the transcriptional activity of TORC were further interpreted by the cytosolic accumulation of TORC and the reduction of TORC recruitment to a CRE-containing promoter.

5.1. DLK inhibits the transcriptional activity of TORC proteins

A huge number of cell signaling pathways converge on the transcription factor CREB which enables the cell to adapt to various environmental changes or demands of the organism. Many components of the transcriptional machinery, like CBP, $TAF_{II}130$/ $TAF_{II}D$, TORC, interact with CREB and activate the gene transcription (Mayr and Montminy, 2001; Shaywitz and Greenberg, 1999; Nakajima et al., 1997). Among these, CREB's coactivators CBP and TORC which are regulated by diverse signals are most examined. By distinct regulations on the action of CBP and TORC, CREB-directed gene transcription is sophistically modulated (Screaton et al. 2004; Zhou et al. 2004; Oetjen et al. 2005; Jansson et al. 2008; He et al. 2009). Especially, the transcriptional activity of TORC is modulated in a more complicated way, including the processes such as the phosphorylation of TORC, the shuttling of TORC between the nucleus and the cytoplasm, and the interaction between TORC and the CBP/CREB complex (Katoh et al. 2004, Takemori and Okamoto 2008, Screaton et al. 2004, Ravnskjaer et al. 2007, Xu et al. 2007). The regulation of TORC action by phosphorylation or translocation is, therefore, crucial for CREB-dependent gene transcription. The present study shows for the first time that TORC is a target of the inhibitory action of DLK.

By using the reporter gene assay combined with the Gal4 system, whereby TORC is artificially recruited to the promoter, the effect of DLK on all three isoforms of TORC was investigated in the HIT-T15 cell line under basal condition. Over expression of DLK inhibited the transcriptional activity of all three TORC isoforms to various extents, whereby the inhibition of TORC1 transcriptional activity was most pronounced (**Fig. 9A-C**).

Treatment of HIT cells with KCl and Forskolin enhanced pronouncedly the transactivational activity of TORC1 and TORC2 (**Fig. 10A**), which is consistent with

previous studies (Bittinger et al., 2004; Screaton et al., 2004, Katoh et al., 2004; Takemori and Okamoto, 2008). Under these conditions, the transcriptional activity of TORC3 was slightly increased (**Fig. 10A**). Therefore, other KCl or forskolin-dependent signaling cascades might result in a further activation of the transcriptional activities of TORC1 and TORC2 in HIT cells – not or less so of TORC3. The stimulated transcriptional activities of three TORC isoforms were inhibited to the same extent as the basal activities by DLK (**Fig. 10B-D**).

By increasing the amount of the expression vector for DLK, the inhibition of TORC was shown to be dependent on the amount of DLK expression vector. Among the three TORC isoforms, TORC1 is inhibited most pronouncedly by DLK (**Fig. 11**). It is not clear at the moment why DLK inhibited different TORC isoforms at distinct levels.

The result of the mapping experiments to identify a DLK-responsive domain within TORC was not clear for the short 44 aa N-terminus of TORC1 due to its low transcriptional activity. The C-terminus lacking in the first 44 aa of TORC1 but containing the transactivation domain (Conkright et al., 2003, Siu et al., 2009) was inhibited by DLK (**Fig. 12**). It is noteworthy that phosphorylation of TORC1 on the C-terminal 220 aa containing transaction domain by MEKK1 promotes TORC's nuclear translocation and recruitment to CRE-containing promoter in HEK293 cells (Siu et al., 2009). By this way, MEKK1 activates TORC, which is in contrast to the inhibitory effect of DLK on TORC. MEKK1 and DLK might act on TORC through different pathways and differently in distinct cell lines, even though they are considered belonging to the big family of MAPKKK.

5.2. DLK enhances the phosphorylation of TORC on the regulatory sites

A comparison between the effect of DLK wild-type and its kinase dead mutant showed that the later one exhibited less inhibition on TORC than the wild-type form (**Fig. 9A-C**). However, the kinase dead DLK mutant was less overexpressed than DLK wild-type in HIT cells (**Fig. 15**). These results can be interpreted by two possibilities: first, the lower amount of DLK K185A protein results in less inhibitory effect as compared to DLK wild-type; second, even though DLK K185A is less overexpressed than the wild-type form, however, an equal amount of DLK wild-type or DLK K185A protein are involved in all the biochemical reactions leading to the reduction of TORC transcriptional activity. The second possibility implies that DLK-induced TORC inhibition depended at least in part on the enzymatic activity of DLK.

The experiments, in which TORC transcriptional activity was stimulated by KCl and forskolin confirmed the findings in basal condition. In both conditions, DLK exerted a

reduction of the transactivating capacity of TORC depending on its an enzymatic activity (**Fig. 10B-D**). As a kinase, it is possible that DLK directly phosphorylates TORC or DLK may induce other kinases to participate in this process, which might reduce the nuclear localization of TORC.

It has been shown that the phosphorylation of TORC 1 and TORC2 on Ser-167 and Ser-171, respectively, is a pivotal step in the TORC regulating signalling pathways (Screaton et al., 2004; Katoh et al., 2004, Bittinger et al., 2004). By assuming that the enzymatic activity of DLK may contribute to the inhibition of TORC through the phosphorylation on these residues, the reporter gene assay using the GAL4 system and TORC1 and TORC2, carrying the mutations of Ser-167 and Ser-171 to alanine, respectively, was performed. Mutation of TORC1 and 2 at Ser-167 and Ser-171 to alanine increased their transcriptional activity 3 and 5 folds (**Fig. 13A**, **B**), respectively. This might be explained that, the lack of the serine residues results in the constitutive nuclear localisation and thus activation of TORC1 and TORC2. These results are consistent with the findings before which demonstrated that the phosphorylation of TORC1 and TORC2 at Ser-167 and Ser-171, respectively, switches off their transcriptional activity (Screaton et al., 2004; Katoh et al., 2004 & 2006). On the other hand, it is assumed that the DNA binding domain of GAL4 efficiently translocates fusion proteins to the nucleus (Silver et al., 1984). The enhanced transcriptional activity conferred by the TORC1 S167A and TORC2 S171A mutants (**Fig. 13A**, **B**), respectively, suggests that the phosphorylation of these residues has additional inhibitory effects i.e. a reduced interaction with components of TFIID (Conkright et al. 2003). Under the same experimental condition, DLK was shown to decrease the activity of TORC1 and TORC2 wild-type but exhibited no effect on both TORC1 S167A and TORC2 S171A mutants (**Fig. 13A**, **B**). This indicates that DLK-induced inhibition of TORC transcriptional activity depended at least in part on the phosphorylation on Ser-167 or Ser-171 residues of TORC1 or TORC2, respectively.

In line with the hypothesis assuming DLK may contribute to the phosphorylation of TORC, the *in vitro* kinase assay was performed using recombinant bacterially expressed TORC1 wild-type, TORC1 S167A, TORC2 wild-type and TORC2 S171A as substrates. In this experimental condition DLK was shown to phosphorylate casein and to be auto-phosphorylated (**Fig. 28**), as observed before by Mata et al. (1996). This evidence indicates that the enzymatic activity of immunoprecipitated DLK was intact. However, it directly phosphorylated neither the recombinant TORC1 nor TORC2 (**Fig. 28**).

There might be a possibility that in the cellular environment DLK downstream kinases are involved in the phosphorylation of TORC to some extent. Indeed, in HIT cells overexpressing DLK the analysis of the phosphorylation level of TORC by Western blot

showed that DLK induces the phosphorylation of TORC1 on Ser-167 (**Fig. 30** and **Fig. 31**). Especially, treatment of cells with CsA in the presence of overexpressed DLK resulted in a phosphorylation of TORC1 on Ser-167 and on other as yet unidentified residues, as suggested by the band shift of phosphorylated TORC1 on the Western blot using SDS-PAGE (**Fig. 30**).

A Western blot using a SDS-PAGE supplemented with Phos-tag^{TM} AAL-107 resulting in an improved separation of the phosphoprotein isotypes (Kinoshita et al., 2008) revealed that the overexpression of DLK wild-type cooperated with CsA treatment to induce a hyperphosphorylation of TORC1, which was observed clearly by the retardation of the band representing phosphorylated TORC1 (**Fig. 32**). CsA was shown to enhance the kinase activity of DLK (Plaumann et al., 2008) and thereby possibly increasing the phosphorylation of TORC on other sites. Besides Ser-167 or Ser-171 on TORC1 or TORC2, Jansson et al. (2008) identified Ser-275 of TORC2 as another regulatory phosphorylation site. Low level glucose-induced activation of MARK2 results in phosphorylation of TORC specifically on Ser-275 and on Ser-171, leading to TORC2 interaction with 14-3-3 proteins and attenuation of CREB-dependent gene transcription in beta-cells (Jansson et al. 2008). In the same way, Ser-261 of TORC1 has possibly the same function: when phosphorylated on Ser-261, TORC1 might be sequestered in the cytosol and thereby attenuating the transcriptional activation. Possibly DLK enhanced phosphorylation of TORC1 on both Ser-167 and Ser-261.

The regulation of CREB-dependent gene transcription is critical for islet cell proliferation and survival (Jhala et al., 2003; Hussain et al., 2006; Inada et al., 2004). Phosphorylation of TORC2 on Ser-171 and Ser-275 block this process by attenuating the transcriptional activity of CREB (Jansson et al. 2008). In addition, the MARK2$^{-/-}$ -mice displayed an increased metabolic rate and insulin hypersensitivity (Hurov et al., 2007). By acting in the same way as MARK2, activation of DLK in pancreatic islets might inhibit the proliferation and survival of beta-cells.

Although DLK enhanced the phosphorylation of TORC in HIT cells, neither TORC1 nor TORC2 are direct substrates of DLK, since both coactivators were not phosphorylated in the *in vitro* kinase assay (**Fig. 28**). This indicates that DLK downstream-kinases like JNK or p38 confer DLK-induced TORC phosphorylation (Fan et al. 1996; Gallo and Johnson 2002). In line with this deduction, treatment of cells with SP600125, a JNK-specific inhibitor (Bennett et al., 2001), resulted in a reduction of phosphorylation of mouse TORC1 on Ser-151 (equivalent to Ser-167 of human TORC1) in both the presence and absence of overexpressed DLK, as compared with the basal condition (**Fig. 33**). These findings indicate that DLK presumable through activation of its down-stream kinase JNK

results in the phosphorylation of TORC. Since JNK is able to translocate to the nucleus (Chang and Karin 2001) this phosphorylation can either occur in the cytoplasm, thereby preventing TORC nuclear translocation or in the nucleus, thereby advancing TORC's nuclear exclusion.

In hepatocytes, phosphorylation of TORC2 on Ser-171 is a key point in the regulation of gluconeogenesis (Koo et al., 2005; Dentin et al., 2007, 2008; Jansson et al., 2008). SIK's activity is inhibited by cAMP-responsive PKA, which is activated by glucagon in condition of low circulating glucose (Screaton et al., 2004; Katoh et al., 2006). In response to the fasting condition, the SIK-induced Ser-171 phosphorylation of TORC2 is inhibited through glucagon and thereby leading to the transcriptional activation of gluconeogenic genes such as PEPCK and G6Pase. Hyperglucagonemia leading to fasting hyperglycaemia due to elevated gluconeogenesis is often present in individuals with type 2 diabetes. In contrast, SIK is activated by insulin-induced AKT activation which results in the phosphorylation of TORC2 and abolishment of gluconeogenic gene transcription (Dentin et al., 2007). However, low energy conditions, or low ATP level, also activate AMPK which bring about the phosphorylation of TORC2 on Ser-171 and block the transcription of gluconeogenic genes (Koo et al., 2005). AMPK plays a role as negative regulator of gluconeogensis in hepatocytes. Of note, DLK transcripts were detected in liver of the adult mouse (Blouin *et al*. 1996). It is not known at the moment if DLK, acting similar to AMPK, enhances the phosphorylation of TORC proteins on inhibitory sites and thereby inhibits gluconeogenesis in hepatocytes.

5.3. DLK may inhibit TORC through direct interaction

Besides the kinase activity, the ability of DLK to homodimerize via its leucine zipper domain was also demonstrated to contribute to the inhibitiory action on TORC. Under the same conditions, DLK wild-type but not DLK P-P, a dimerization deficient mutant of DLK (Nihalani et al. 2000), reduced the transactivating ability of TORC (**Fig. 14**), although DLK P-P was overexpressed to a higher extent than DLK wild-type in HIT cells (**Fig. 15**). This observation indicated that the dimerization ability of DLK is one of the essential characteristics contributing in DLK-induced reduction of TORC transcriptional activity. Because the homodimerization of DLK is required for its kinase activity (Nihalani et al. 2000; Nihalani et al. 2003), the dimerization deficient mutant has no longer an enzymatic function. This result is, therefore, consistent with the above finding about the role of enzymatic activity of DLK on inhibition of TORC. Furthermore, it seems that when DLK wild-type or its mutants were overexpressed in HIT cells, the differences in the overexpression level of DLK proteins were not the reason causing different levels of

inhibition. In these cases, the amounts of overexpressed DLK proteins were possibly enough to mediate the inhibitory reactions. By reasoning like this, the difference in inhibition of TORC caused by DLK wild-type and DLK K185A, as mentioned above, was due to the enzymatic activity of DLK, not to the difference levels of overexpression.

In addition to phosphorylating TORC, the present work has demonstrated that DLK directly interacts with TORC. As shown by *in vitro* pull down assays, this interaction depended on DLK's ability to homodimerize, since the DLK P-P mutant bound to a lesser extent to the immobilized His-TORC fusion proteins (**Fig. 19A** and **Fig. 20A**). In addition, in the coimmunoprecipitation assays, overexpressed TORC1 was coimmunoprecipitated to a slightly lesser extent by DLK P-P, than by DLK wild-type or its kinase dead mutant (**Fig. 24**). However, homodimerisation is a prerequisite for the enzymatic activity of DLK as well (Nihalani et al. 2000). The finding that both DLK wild-type and its kinase-dead mutant bound to the same extent to immobilized His-TORC fusion proteins (**Fig. 19A** and **Fig. 20A**) indicates that indeed the formation of a leucine zipper structure is required for the TORC-DLK interaction. The coiled-coil structure formed by the N-terminal domains of tetramerized TORCs seems to be required for the interaction with the leucine zipper of DLK since GST-TORC$_{1\text{-}44}$ fusion protein interacted with DLK wild-type to a larger extent than the binding between DLK wild-type and His-TORC full length or His-TORC$_{\Delta 44}$ (**Fig. 22**). Thus, besides the leucine zipper of CREB TORC interacts with other proteins able to form this structure like the transcription factor AP-1 (Canettieri et al. 2009b). Given that TORC and DLK are able to translocate to the nucleus (Bittinger et al. 2004; Screaton et al. 2004, unpublished results of the group) it is unclear in which cellular compartment this interaction occurs.

By acting as a coactivator of CREB TORC proteins have been shown to mainly regulate metabolic control in various tissues (Wang et al., 2010; Canettieri et al. 2005; Koo et al. 2005; Wu et al. 2006; Altarejos et al. 2008), to promote β-cell survival (Jansson et al. 2008) and to be involved in hippocampal long-term synaptic plasticity (Kovacs et al. 2007). Mucoepidermoid carcinomas are associated with a chromosomal translocation, t(11;19) which results in the formation of the oncoprotein CRTC1-MAML2. This oncoprotein consists of the N-terminal 42 aa of TORC1 fused to the C-terminal 981 aa of the Notch coactivator MAML2 (Tonon et al. 2003). The oncogenic capacity of this fusion protein is due to its ability to interact via its TORC1 fraction with CREB and with AP-1, both of them promoting cell proliferation (Coxon et al. 2005; Wu et al. 2005; Siu and Jin 2007; Canettieri et al. 2009a; Canettieri et al. 2009b). Given that DLK interacts with the N-terminal domain of TORC and reduces the recruitment of TORC to CREB, an accumulation of DLK might prevent the cell proliferation.

5.4. DLK inhibits the nuclear translocation of TORC and recruitment of TORC to a CRE-containing promoter

In normal condition, TORC is located to some extent in the nucleus. Enhancement of phosphorylated TORC is generally assumed to result in the cytoplasmic retention or the nuclear exclusion of TORC (Bittinger et al. 2004; Screaton et al. 2004; Canettieri et al. 2005; Koo et al. 2005; Katoh et al. 2006; Jansson et al. 2008; Takemori and Okamoto 2008).

Indeed, in the present study, the immunocytochemistry analysis showed that DLK depending on its enzymatic activity prevented the nuclear localization of TORC in basal condition (**Fig. 25A, B** and **Fig. 26**). Treatment of cells with KCl enhanced the amount of TORC in nucleus regardless of overexpression of DLK (**Fig. 26**). KCl treatment increased the activation of calcineurin thereby dephosphorylating TORCs and leading to TORC nuclear localization (Bittinger et al., 2004; Screaton et al., 2004). Moreover, intracellular calcium might enhance dephosphorylation of DLK via calcineurin activation-related pathway (Mata et al. 1996), which reduces the enzymatic activity of DLK, decreases the phosphorylation of TORC and thereby elevating the nuclear localization of TORC.

The chromatin-immunoprecipitation (ChIP) assay in the present study showed that overexpression of DLK wild-type reduced the amount of CRE-containing promoter precipitated by TORC (**Fig. 35**). As shown in the *in vitro* interaction assay and the immunocytochemistry experiments, DLK interacted with TORC and reduced the nuclear localization of TORC, respectively. By this way, overexpression of DLK wild-type resulted in a decreased recruitment of TORC to the CRE-promoter. The dimerized DLK might interact with TORC via its N-terminus in the nucleus, thereby preventing the recruitment of TORC to the promoter. In the same line with this finding, DLK wild-type was also observed to reduce the TORC dependent CRE-directed gene transcription in the reporter gene assay (**Fig. 34**). Taken together, DLK was demonstrated to inhibit the recruitment of TORC to a CRE-containing promoter and thereby reducing the transactivating potency of TORC on CRE-directed gene transcription.

A recent report showed the activation of TORC1 by the mitogen activated kinase kinase kinase MEKK1 (Siu et al. 2008). Like DLK MEKK1 can activate the down-stream kinases JNK and p38 (Chang and Karin 2001; Gallo and Johnson 2002), but MEKK1 was demonstrated to directly phosphorylate a region encompassing the aa 431 to 650 of TORC1, to enhance TORC nuclear localization and thus CRE-dependent IL-8 gene transcription (Siu et al. 2008). MEKK1 is a potent activator of the AP-1 transcription factor complex (Chang and Karin 2001), and TORC1 was shown to promote cell proliferation and transformation via AP-1 (Canettieri et al. 2009b). Like AP-1 CREB confers cell

proliferation (Mayr and Montminy 2001) and might contribute to the pathogenesis of cancer (Siu and Jin 2007; Canettieri et al. 2009a). It is tempting to speculate that TORC activating signals will promote cell proliferation through the interaction with DNA-bound CREB and AP-1. Conversely, signals inhibiting TORC might prevent cell proliferation and even result in apoptosis. In line with this, overexpression of DLK did not enhance c-Jun transcriptional activity whereas overexpression of MEKK1 enhanced it 9-fold (unpublished observation, G. Ficz and E. Oetjen) although both kinases activate the c-Jun kinase JNK (Chang and Karin 2001). Furthermore, overexpression of DLK induced apoptosis in neuronal cells and in a β-cell line (Xu et al. 2001; Plaumann et al. 2008) and the adenoviral delivery of dominant-negative DLK mutants had antiapoptotic and trophic effects on dopamine neurons of the substantia nigra in mice (Chen et al. 2008). These findings suggest that the activation of DLK leading to the inhibition of TORC and thereby to the inhibition of CREB- and AP-1- dependent gene transcription has anti-proliferative effects.

The balance of beta-cell replication and apoptosis is critical for beta-cell mass and function. Disruption of this balance results in reduced beta-cell mass and reduced insulin secretion, contributing to the pathogenesis of type 2 diabetes (Butler et al., 2003). Therefore, the DLK-induced inhibition of TORC is a newly identified pathway which may govern the apoptosis and proliferation of beta-cells, and thereby represent possibly a new target for the treatment of diabetes.

Taken together, the present study shows that TORC is a target of the inhibitory action of DLK in beta-cells. DLK acts on TORC at distinct levels: (1) it enhanced the phosphorylation of TORC and (2) interacted with TORC and (3) prevented the nuclear translocation of TORC, the recruitment of TORC to CRE-containing promoter and ultimately the stimulus-induced CREB transcriptional activity. This action of DLK might contribute to its inhibitory effect on CREB dependent gene transcription. **Fig. 36** describes a putative mechanism by which TORC is inhibited by DLK.

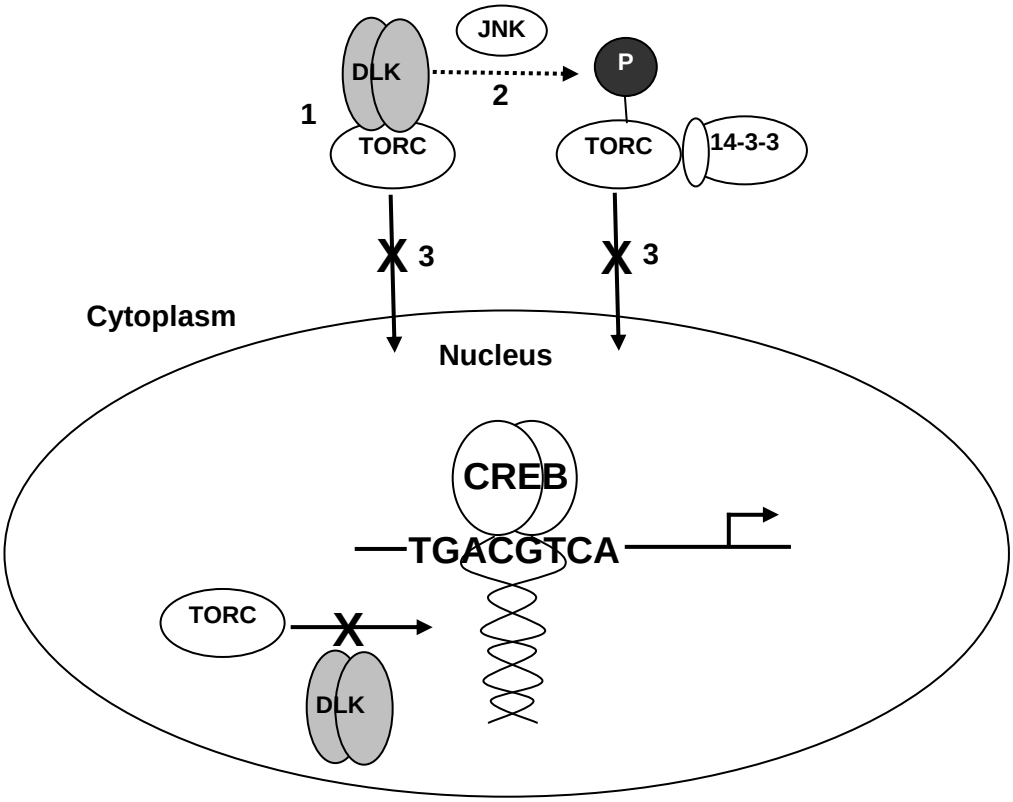

Figure 36: DLK inhibits transcriptional activity of TORC at distinct levels: (1) indirect enhancement of phosphorylation and (2) direct interaction and (3) prevention of the nuclear translocation of TORC, the recruitment of TORC to CRE-containing promoter and ultimately the stimulus-induced CREB transcriptional activity. The inhibitory action may take place in the nucleus or in the cytoplasm.
In the cytoplasm, DLK interacts with TORC and plays a role as a docking protein. DLK also induces the phosphorylation of TORC presumably through JNK, thereby increasing the cytoplasmic localization of TORC through interaction with 14-3-3 proteins. These activities result in reduced CREB-dependent gene transcription.
In the nucleus, on one hand DLK enhances the phosphorylation of TORC possibly through JNK, which reduces the number of TORC molecules in the nucleus due to the cytoplasmic retranslocation. On the other hand DLK interacts with TORC, thereby reducing number of TORC recruited to CRE-promotor and attenuating CREB-dependent gene transcription.

6. SUMARY AND CONCLUSION

The ubiquitously expressed transcription factor CREB is involved in numerous cell signalling pathways including metabolic process, cell cycle or survival, cell growth and immune regulation. Recently, the three isoforms of Transducer of Regulated CREB (TORC) have been identified as additional CREB co-activators. TORC2 phosphorylated on Ser-171, or TORC1 phosphorylated on Ser-167, is retained in the cytosol by binding to the 14-3-3 proteins. Upon dephosphorylation of TORC on these residues, TORC translocates to the nucleus, interacts with the dimerized leucine zipper of CREB and confers transcriptional activity to CREB-dependent genes. A previous study showed that the dual leucine zipper kinase DLK inhibits membrane depolarization-induced CREB transcriptional activity in a beta-cell line. The recruitment of TORC is required for CREB transcriptional activity. Therefore, TORC might be a target of DLK action. In the present study the effect of DLK on the regulation of TORC activity was investigated.

To this aim the effect of DLK on the transcriptional activity of TORC in the beta-cell line HIT-T15 was examined using luciferase reporter gene assays. The interaction between DLK and TORC was tested by *in vitro* protein interaction assays and by co-immunoprecipitation assays. Whether DLK is able to result in phosphorylation of TORC was elucidated by Western blot and *in vitro* kinase assays. Finally, the effect of DLK on the nuclear translocation of TORC and the recruitment of TORC to a CRE-containing promoter were investigated by immunocytochemistry and by chromatin-immunoprecipitation assay in cooperation with luciferase reporter gene assays.

DLK inhibited the transcriptional activities of all three TORC isoforms. This inhibitory action was dependent on the ability of DLK to homodimerize via its leucine zipper domain as well as on its enzymatic activity. Neither TORC1 nor TORC2 were direct substrates of DLK, since both coactivators were not phosphorylated in the *in vitro* kinase assay. However, the Western blot analysis showed that DLK induced the phosphorylation of TORC1 on Ser-167 and presumably on other as yet unidentified residues, as suggested by the retarded migration of TORC1. Interestingly, treatment of HIT cells with SP600125, a JNK inhibitor, reduced pronouncedly the Ser-167 phosphorylation of TORC1 regardless of the presence or absence of overexpressed DLK. Taken into account that DLK is able to phosphorylate and thus to activate JNK, these findings indicate, that DLK presumable through activation of its down-stream kinase JNK results in the phosphorylation of TORC.
Besides induction of TORC phosphorylation, DLK directly interacts with TORC as shown by *in vitro* pull down assays and co-immunoprecipitation assays. This interaction

depended on DLK's ability to homodimerize, since the DLK-PP mutant bound to a lesser extent to the immobilized His-TORC fusion protein. The finding that both DLK wild-type and its kinase-dead mutant bound to the same extent to immobilized His-TORC fusion protein indicates that the formation of a leucine zipper structure is required for the TORC-DLK interaction. The coiled-coil structure formed by the N-terminal domains of tetramerized TORCs seems to be required for the interaction with the leucine zipper of DLK.

In addition, DLK depending on its enzymatic activity reduced the nuclear translocation of TORC and TORC-dependent CRE-directed gene transcription as shown by immunocytochemistry and reporter gene assay, respectively. Moreover, the chromatin-immunoprecipitation assay demonstrated that DLK prevented the recruitment of TORC to a CRE-containing promoter.

Taken together, the present study shows that TORC is a target of the inhibitory action of DLK in beta-cells. The DLK-induced inhibition of TORC is a newly identified pathway, which may through regulation of CREB-dependent gene transcription govern the apoptosis and the proliferation of beta-cells, and thereby represent possibly a new target for the treatment of diabetes.

Zusammenfassung mit Schlußfolgerung

Der ubiquitär exprimierte Transkriptionsfaktor CREB ist an zahlreichen zellulären Signaltransduktionswegen einschließlich der Regulation des Stoffwechsels, des Zellzyklus und –überlebens, des Zellwachstums und der Immunregulation beteiligt. Drei Isoformen des Transducer of Regulated CREB (TORC) wurden kürzlich als weitere Kofaktoren von CREB identifiziert. Die Phosphorylierung von TORC2 am Ser-171 bzw. von TORC1 am Ser-167 führt zu einer Interaktion mit 14-3-3 Proteinen, wodurch TORC im Zytosol verbleibt. Die Dephosphorylierung dieser Aminosäuren resultiert in der nukleären Lokalisation von TORC, wo es mit dem homodimesierten Leuzin-Zipper von CREB interagiert und so die CREB-abhängige Gentranskription vermittelt. Eine frühere Untersuchung zeigte, daß die Dual Leucine Zipper Kinase DLK die durch Membrandepolarisation stimulierte CREB-abhängige Gentranskription in Beta-Zellen hemmte. Da die Rekrutierung von TORC notwendig für die volle transkriptionelle Aktivität von CREB ist, könnte TORC ein Ziel von DLK sein. In der vorliegenden Untersuchung wurde die Regulation von TORC durch die DLK untersucht.

Hierzu wurde die Wirkung von DLK auf die transkriptionelle Aktivität von TORC in Beta-Zellen mittels Luciferasereportergenassays untersucht. Eine Interaktion zwischen DLK und TORC wurde durch *in vitro* Protein-Proteininteraktionsassays und Koimmunpräzipitation analysiert. Für die Untersuchungen zur Phosphorylierung von TORC durch DLK wurden Western Blot Analysen und *in vitro* Kinaseassays eingesetzt. Die Wirkung von DLK auf die nukleäre Translokation von TORC und die Rekrutierung an CRE enthaltende Promotoren wurde mittels immunzytochemischen Untersuchungen, Chromatinimmunpräzipitation und Luciferasereportergenassays untersucht.

DLK hemmte die transkriptionelle Aktivität aller drei TORC Isoformen. Diese hemmende Wirkung war abhängig von der Fähigkeit DLK's zu homodimerisieren und von ihrer Kinaseaktivität. Der *in vitro* Kinase Assay zeigte, daß weder TORC1 noch TORC2 direkte Substrate der Kinase waren. Jedoch zeigte sich im Immunoblot, daß die Überexpression von DLK zu einer verstärkte Phosphorylierung von TORC1 am Ser-167 und an anderen nicht identifizierten Aminosäuren führte. Zusätzliche Behandlung der HIT Zellen mit einem Hemmstoff von JNK, einer der DLK untergeordneten Kinase, reduzierte die Phosphorylierung von TORC1 am Ser-167 und hob die langsamere Migration weiterer phospho-TORC1 Banden auf. Diese Daten lassen vermuten, daß DLK wahrscheinlich durch Aktvierung von JNK die Phosphorylierung von TORC induziert.

Neben einer Phosphorylierung konnte mittels *in vitro* Protein-Protein Interaktionsassays und Koimmunpräzipitationen gezeigt werden, daß DLK mit TORC interagiert. Diese Interaktion war abhängig von der Fähigkeit DLK's zu homodimerisieren, da die DLK-PP

Mutante in einem deutlich geringeren Ausmaß als DLK Wildtyp an das immobilisierte His-TORC Fusionsprotein band. Da DLK Wildtyp und seine Kinase-tote Mutante in demselben Ausmaß mit immobilisierten His-TORC Fusionsprotein interagierten, kann geschlossen werden, daß die Ausbildung eines Leuzin-Zippers notwendig für die DLK TORC Interaktion ist. Ebenfalls scheint die coiled-coil Stuktur, die durch die N-terminalen Domänen des TORC Tetramers gebildet wird, für die Interaktion mit dem Leuzin-Zipper von DLK erforderlich zu sein.

In Abhängigkeit von seiner enzymatischen Aktivität verminderte DLK die nukleäre Lokalisation von TORC und die TORC-abhängige, CRE-dirigierte Gentranskription. Die Chromatinimmunpräzipitation zeigte, daß DLK die Rekrutierung von TORC an einen CRE enthaltenden Promotor verminderte.

Zusammengefaßt zeigt die vorliegende Untersuchung, daß TORC ein Ziel der hemmenden Wirkung von DLK in Beta-Zellen ist. Die DLK induzierte Hemmung von TORC stellt einen neuen Signalweg dar, der durch Modifikation der CREB-abhängigen Gentranskription zur Regulation von Apoptose und Proliferation in Beta-Zellen beiträgt. Die Hemmung von DLK in Beta-Zellen könnte somit ein Ziel für die Therapie des Diabetes mellitus darstellen.

7. REFERENCES

Altarejos JY et al. (2008) The Creb1 coactivator Crtc1 is required for energy balance and fertility. Nat Med 14:1112-1117

Bennett, B.L., Sasaki, D.T., Murray, B.W., O'Leary, E.C., Sakata, S.T., Xu, W., Leisten, J.C., Motiwala, A., Pierce, S., Satoh, Y., Bhagwat, S.S., Manning, A.M. and Anderson, D.W. (2001) SP600125, an anthrapyrazolone inhibitor of Jun N-terminal kinase, Proc Natl Acad Sci U S A, *24, 13681-13686.*

Bittinger MA et al. (2004) Activation of cAMP response element-mediated gene expression by regulated nuclear transport of TORC proteins. Curr Biol 14:2156-2161

Bloom, A.J., Miller, B.R., Sanes, J.R., DiAntonio, A. (2007) The requirement for Phr1 in CNS axon tract formation reveals the corticostriatal boundary as a choice point for cortical axons. Genes Dev, 21(20), 2593-2606.

Blouin, R., Beaudoin, J., Bergeron, P., Nadeau, A., Grondin, G. (1996) Cell-specific expression of the ZPK gene in adult mouse tissues.DNA Cell Biol. 15(8):631-42

Boer, U., Eglins, J., Krause, D., Schnell, S., Schofl, C. and Knepel, W. (2007) Enhancement by lithium of cAMP-induced CRE/CREB-directed gene transcription conferred by TORC on the CREB basic leucine zipper domain. Biochem J, 408, 69-77.

Bonni, A., Brunet, A., West, A.E., Datta, S.R., Takasu, M.A., Greenberg, M.E. (1999) Cell survival promoted by the Ras-MAPK signaling pathway by transcription-dependent and independent mechanisms. Science, 286, 1358-1362.

Bradford, M.M. (1976) A rapid and sensitive method for the quantitation of microgram quantities of protein utilizing the principle of protein-dye binding. Anal Biochem, 72, 248-254.

Butler, A.E., Janson, J., Bonner-Weir, S., Ritzel, R., Rizza, R.A., Butler, P.C. (2003) Beta-cell deficit and increased beta-cell apoptosis in humans with type 2 diabetes. Diabetes, 52(1),102-10.

Canettieri G, Coni S, Antonucci L, Di Magno L, Gulino A (2009a) TORCs/CRTCs: more than mere coincidence. Cell Cycle 8:963-964

Canettieri, G., Coni, S., Guardia, M.D., Nocerino, V.,Antonucci, L., Magno, L.D., Screaton, R., Screpanti, I., Giannini, G. , and Gulino, A.(2009b) The coactivator CRTC1 promotes cell proliferation and transformation via AP-1. Proc Natl Acad Sci U S A 106:1445-1450

Canettieri, G., Koo, S. H., Berdeaux, R., Heredia, J., Hedrick, S., Zhang, X., and Montminy, M. (2005). Dual role of the coactivator TORC2 in modulating hepatic glucose output and insulin signaling. Cell Metab *2*, 331–338.

Chang L, Karin M (2001) Mammalian MAP kinase signalling cascades. Nature 410:37-40

Chen, X., Rzhetskaya, M., Kareva, T., Bland, R., During, M.J., Tank, A.W., Kholodilov, N., Burke, R.E. (2008) Antiapoptotic and trophic effects of dominant-negative forms of dual leucine zipper kinase in dopamine neurons of the substantia nigra in vivo. J Neurosci, 28(3), 672-680.

Collins, C.A., Wairkar, Y.P., Johnson, S.L., DiAntonio, A. (2006) Highwire restrains synaptic growth by attenuating a MAP kinase signal. Neuron, 51(1), 57-69.

Conkright, M.D., Canettieri, G., Screaton, R., Guzman, E., Miraglia, L., Hogenesch, J.B. and Montminy, M. (2003a) TORCs: transducers of regulated CREB activity. Mol Cell, 12, 413-423.

Conkright, M.D., Guzman, E., Flechner, L., Su, A.I., Hogenesch, J.B. and Montminy, M. (2003b) Genome-wide analysis of CREB target genes reveals a core promoter requirement for cAMP responsiveness. Mol Cell, 11, 1101-1108.

Couture, J.P., Daviau, A., Fradette, J., Blouin, R. (2009) The mixed-lineage kinase DLK is a key regulator of 3T3-L1 adipocyte differentiation. PLoS One, 4(3):e4743

Coxon A et al. (2005) Mect1-Maml2 fusion oncogene linked to the aberrant activation of cyclic AMP/CREB regulated genes. Cancer Res 65:7137-7144

Cuenda, A., Dorow, D.S. (1998) Differential activation of stress-activated protein kinase kinases SKK4/MKK7 and SKK1/MKK4 by the mixed-lineage kinase-2 and mitogen-activated protein kinase kinase (MKK) kinase-1. Biochem J, 333 (Pt 1), 11-15.

D'Amico, M., Hulit, J., Amanatullah, D.F., Zafonte, B.T., Albanese, C., Bouzahzah, B., Fu, M., Augenlicht, L.H., Donehower, L.A., Takemaru, K., Moon, R.T., Davis, R., Lisanti, M.P., Shtutman, M., Zhurinsky, J., Ben-Ze'ev, A., Troussard, A.A., Dedhar, S., Pestell, R.G. (2000) The integrin-linked kinase regulates the cyclin D1 gene through glycogen synthase kinase 3β and cAMP-responsive element-binding protein-dependent pathways. J Biol Chem, 275, 32649-32657.

de Wet, J.R., Wood, K.V., DeLuca, M., Helinski, D.R. and Subramani, S. (1987) Firefly luciferase gene: structure and expression in mammalian cells. Mol Cell Biol, 7, 725-737.

Daviau, A., Proulx, R., Robitaille, K., Di Fruscio, M., Tanguay, R.M., Landry, J., Patterson, C., Durocher, Y., Blouin, R. (2006) Down-regulation of the mixed-lineage dual leucine zipper-bearing kinase by heat shock protein 70 and its co-chaperone CHIP. J Biol Chem, 281(42), 31467-31477.

Daviau, A., Di Fruscio, M., Blouin, R. (2009) The mixed-lineage kinase DLK undergoes Src-dependent tyrosine phosphorylation and activation in cells exposed to vanadate or platelet-derived growth factor (PDGF). Cell Signal, 21(4), 577-587.

Dentin, R., Hedrick, S., Xie, J., Yates, J., 3rd and Montminy, M. (2008) Hepatic glucose sensing via the CREB coactivator CRTC2. Science, 319, 1402-1405.

Dentin, R., Liu, Y., Koo, S.H., Hedrick, S., Vargas, T., Heredia, J., Yates, J., 3rd and Montminy, M. (2007) Insulin modulates gluconeogenesis by inhibition of the coactivator TORC2. Nature, 449, 366-369.

Desdouets, C., Matesic, G., Molina, C.A., Foulkes, N.S., Sassone-Corsi, P., Brechot, C. and Sobczak-Thepot, J. (1995) Cell cycle regulation of cyclin A gene expression by the cyclic AMP-responsive transcription factors CREB and CREB. Mol Cell Biol, 15, 3301-3309.

Dorow, D.S., Devereux, L., Dietzsch, E. and De Kretser, T. (1993) Identification of a new family of human epithelial protein kinases containing two leucine/isoleucine-zipper domains. Eur J Biochem, 213, 701–710

Douziech, M., Laberge, G., Grondin, G., Daigle, N., Blouin, R. (1999) Localization of the mixed-lineage kinase DLK/MUK/ZPK to the Golgi apparatus in NIH 3T3 cells.J Histochem Cytochem, 47(10):1287-1296.

Eggers A, Siemann G, Blume R, Knepel W (1998) Gene-specific transcriptional activity of the insulin cAMP-responsive element is conferred by NF-Y in combination with cAMP response element binding protein. J Biol Chem, 273,18499-18509.

Fan, G., Merritt, S.E., Kortenjann, M., Shaw, P.E., Holzman, L.B. (1996) Dual leucine zipper-bearing kinase (DLK) activates p46SAPK and p38mapk but not ERK2. J Biol Chem, 271, 24788-24793

Fukuyama, K., Yoshida, M., Yamashita, A., Deyama, T., Baba, M., Suzuki, A., Mohri, H., Ikezawa, Z., Nakajima, H., Hirai, S., Ohno, S. (2000) MAPK upstream kinase (MUK)-

binding inhibitory protein, a negative regulator of MUK/dual leucine zipper-bearing kinase/leucine zipper protein kinase. J Biol Chem, 275(28), 21247-21254.

Gallo, K.A., Mark, M.R., Scadden, D.T., Wang, Z., Gu, Q., Godowski, P.J. (1994) Identification and characterization of SPRK, a novel src-homology 3 domain-containing proline-rich kinase with serine/threonine kinase activity. J Biol Chem, 269,15092-15100.

Gallo, K.A., Johnson, G.L. (2002) Mixed-lineage kinase control of JNK and p38 MAPK pathways. Nat Rev Mol Cell Biol, 3, 663-672.

Garrington T.P. & Johnson G.L. (1999) Organization and regulation of mitogen-activated protein kinase signaling pathways. Curr. Opi. Cell. Biol, 11, 211-218.

Germain, L., Fradette, J., Robitaille, H., Guignard, R., Grondin, G., Nadeau, A., Blouin, R. (2000) The mixed lineage kinase leucine-zipper protein kinase exhibits a differentiation-associated localization in normal human skin and induces keratinocyte differentiation upon overexpression. J Invest Dermatol, 115(5), 860-867 .

Gonzalez, G.A. & Montminy.M.R. (1989) Cyclic AMP stimulates somatostatin gene transcription by phosphorylation of CREB at serine 133. Cell, 59, 675-680.

Hammarlund, M., Nix, P., Hauth, L., Jorgensen, E.M., Bastiani, M. (2009) Axon regeneration requires a conserved MAP kinase pathway. Science, 323(5915), 802-806. He L et al. (2009) Metformin and insulin suppress hepatic gluconeogenesis through phosphorylation of CREB binding protein. Cell 137:635-646

Heinrich A, Boer U, Tzvetkov M, Oetjen E, Knepel W (2009) Stimulation by lithium of the interaction between the transcription factor CREB and its co-activator TORC. Biosci Rep 29:77-87.

Herzig, S., Hedrick, S., Morantte, I., Koo, S.H., Galimi, F. and Montminy, M. (2003) CREB controls hepatic lipid metabolism through nuclear hormone receptor PPAR-gamma. Nature, 426, 190-193.

Herzig, S., Long, F., Jhala, U.S., Hedrick, S., Quinn, R., Bauer, A., Rudolph, D., Schutz, G., Yoon, C., Puigserver, P., Spiegelman, B., and Montminy, M. (2001) CREB regulates hepatic gluconeogenesis through the coactivator PGC-1. Nature 413:179-183

Hirai, S., Izawa, M., Osada, S., Spyrou, G., Ohno, S. (1996) Activation of the JNK pathway by distantly related protein kinases, MEKK and MUK. Oncogene, 12(3), 641-650.

Hirai, S., Katoh ,M., Terada, M., Kyriakis, J.M., Zon, L.I., Rana, A., Avruch, J., Ohno, S. (1997) MST/MLK2, a member of the mixed lineage kinase family, directly phosphorylates and activates SEK1, an activator of c-Jun N-terminal kinase/stress-activated protein kinase. J Biol Chem, 272(24), 15167-15173.

Hirai, S., Noda, K., Moriguchi, T., Nishida, E., Yamashita, A., Deyama, T., Fukuyama, K., Ohno, S. (1998) Differential activation of two JNK activators, MKK7 and SEK1, by MKN28-derived nonreceptor serine/threonine kinase/mixed lineage kinase 2. J Biol Chem, 273(13), 7406-7412.

Hirai, S., Kawaguchi, A., Hirasawa, R., Baba, M., Ohnishi, T., Ohno, S. (2002) MAPK-upstream protein kinase (MUK) regulates the radial migration of immature neurons in telencephalon of mouse embryo. Development, 129(19), 4483-4495.
Hirai, S., Kawaguchi, A., Suenaga, J., Ono, M., Cui, D.F., Ohno, S. (2005) Expression of MUK/DLK/ZPK, an activator of the JNK pathway, in the nervous systems of the developing mouse embryo. Gene Expr Patterns, 5(4):517-523.

Hirai, S., Cui, D., Miyata, T., Ogawa, M., Kiyonari, H., Suda, Y., Aizawa, S., Banba, Y., Ohno, S. (2006) The c-Jun N-Terminal Kinase Activator Dual Leucine Zipper Kinase Regulates Axon Growth and Neuronal Migration in the Developing Cerebral Cortex. TheJournal of Neuroscience, 26(46):11992-12002.

Hishiki, T., Ohshima, T., Ego, T., and Shimotohno, K. (2007). BCL3 acts as a negative regulator of transcription from the human T-cell leukemia virus type 1 long terminal repeat through interactions with TORC3. J. Biol. Chem *282*, 28335–28343

Holzman LB, Merritt SE, Fan G (1994) Identification, molecular cloning, and characterization of dual leucine zipper bearing kinase. A novel serine/threonine protein kinase that defines a second subfamily of mixed lineage kinases. J Biol Chem 269:30808-30817.

Horiuchi, D., Collins, C.A., Bhat, P., Barkus, R.V., Diantonio, A., Saxton, W.M. (2007) Control of a kinesin-cargo linkage mechanism by JNK pathway kinases. Curr Biol, 17(15), 1313-1317.

Inoescu, A. M., Schwarz, E.M., Vinson, C., Puzas, J.E., Rosie, R., Reynolds, P.R., O'Keefe, R.J. (2001) PTHrP modulates chrondrocyte differentiation through AP-1 and CREB signaling. J Biol Chem, 276, 11639-11647.

Iourgenko, V., Zhang, W., Mickanin, C., Daly, I., Jiang, C., Hexham, J.M., Orth, A.P., Miraglia, L., Meltzer, J., Garza, D., Chirn, G.W., McWhinnie, E., Cohen, D., Skelton, J.,

Terry, R., Yu, Y., Bodian, D., Buxton, F.P., Zhu, J., Song, C. and Labow, M.A. (2003) Identification of a family of cAMP response element-binding protein coactivators by genome-scale functional analysis in mammalian cells. Proc Natl Acad Sci U S A, 100, 12147-12152.

Jansson D, Ng AC, Fu A, Depatie C, Al Azzabi M, Screaton RA (2008) Glucose controls CREB activity in islet cells via regulated phosphorylation of TORC2. Proc Natl Acad Sci U S A 105:10161-10166.

Jhala, U.S., Canettieri, G., Screaton, R.A., Kulkarni, R.N., Krajewski, S., Reed, J., Walker, J., Lin, X., White, M., and Montminy, M. (2003) cAMP promotes pancreatic cell survival via CREB-mediated induction of IRS2. Genes Development 17:1575–1580

Katoh, Y., Takemori, H., Lin, X.Z., Tamura, M., Muraoka, M., Satoh, T., Tsuchiya, Y., Min, L., Doi, J., Miyauchi, A., Witters, L.A., Nakamura, H. and Okamoto, M. (2006) Silencing the constitutive active transcription factor CREB by the LKB1-SIK signaling cascade. Febs J, 273, 2730-2748.

Katoh, Y., Takemori, H., Min, L., Muraoka, M., Doi, J., Horike, N. and Okamoto, M. (2004) Salt- inducible kinase-1 represses cAMP response element-binding protein activity both in the nucleus and in the cytoplasm. Eur J Biochem, 271, 4307-4319.

Kim, S. J., Nian, C., Widenmaier, S., and McIntosh, C. H. (2008). Glucose-dependent insulinotropic polypeptide-mediated up-regulation of β-cell antiapoptotic *Bcl-2* gene expression is coordinated by cyclic AMP (cAMP) response element binding protein (CREB) and cAMP-responsive CREB coactivator 2. Mol. Cell. Biol *28*, 1644–1656

Kinoshita, E., Kikuta, E.K., Matsubara, M., Yamada, S., Nakamura, H., Shiro, Y., Aoki, Y., Okita, K., and Koike, T. (2008) Separation of phosphoprotein isotypes having the same number of phosphate groups using phosphate-affinity SDS-PAGE. Proteomics, 8, 2994-3003.

Koga, H., Ohshima, T., and Shimotohno, K. (2004). Enhanced activation of tax-dependent transcription of human T-cell leukemia virus type I (HTLV-I) long terminal repeat by TORC3. J. Biol. Chem *279*, 52978–52983.

Koo, S.H., Flechner, L., Qi, L., Zhang, X., Screaton, R.A., Jeffries, S., Hedrick, S., Xu, W., Boussouar, F., Brindle, P., Takemori, H. and Montminy, M. (2005) The CREB coactivator TORC2 is a key regulator of fasting glucose metabolism. Nature, 437, 1109-1111.

Kovacs, K.A., Steullet, P., Steinmann, M., Do, K.Q., Magistretti, P.J., Halfon, O. and

Cardinaux, J.R. (2007) TORC1 is a calcium- and cAMP-sensitive coincidence detector involved in hippocampal long-term synaptic plasticity. Proc Natl Acad Sci U S A, 104, 4700-4705.

Krauss, G. (2003) Biochemistry of signal transduction and regulation, 3rd completedly revised edition, ©2003 WILEY-VCH Verlag GmbH & Co. KGaA, Weinheim, Druckhaus Darmstadt GmbH, Darmstadt, Germany.

Kruger, M., Schwaninger, M., Blume, R., Oetjen, E. and Knepel, W. (1997) Inhibition of CREB- and cAMP response element-mediated gene transcription by the immunosuppressive drugs cyclosporin A and FK506 in T cells. Naunyn Schmiedebergs Arch Pharmacol, 356, 433-440.

Kuraishy, A. I., French, S. W., Sherman, M., Herling, M., Jones, D., Wall, R., and Teitell, M. A. (2007). TORC2 regulates germinal center repression of the TCL1 oncoprotein to promote B cell development and inhibit transformation. Proc. Natl. Acad. Sci. USA *104*, 10175–10180.

Kyriakus, J.M., Avruch, J. (1996) Protein kinase cascades activated by stress and inflammatory cytokines. Bioassays, 18, 567-577.

Kyriakus, J.M. and Avruch, J. (2001) Mammalian mitogen-activated protein kinase signal transduction pathways activated by stress and inflammation. Physiol Rev, 81, 807-869.

Laemmli, U.K. (1970) Cleavage of structural proteins during the assembly of the head of bacteriophage T4. Nature, 227, 680-685.

Lee, L.G., Connell, C.R. and Bloch, W. (1993) Allelic discrimination by nick-translation PCR with fluorogenic probes. Nucleic Acids Res, 21, 3761-3766.

Lee, R.J., Albanese, C., Stenger, R.J., Watanabe, G., Inghirami, G., Haines III, G.K., Webster, M., Muller, W.J., Brugge, J.S., Davis, R.J. and Pestell, R.G. (1999) pp60(v-src) induction of cyclin D1 requires collaborative interactions between the extracellular signal-regulated kinase, p38, and Jun kinase pathways. A role for cAMP response element-binding protein and activating transcription factor-2 in pp60(v-src) signaling in breast cancer cells. J Biol Chem, 274, 7341-7350.

Lewcock, J.W., Genoud, N., Lettieri, K., Pfaff, S.L. (2007) The ubiquitin ligase Phr1 regulates axon outgrowth through modulation of microtubule dynamics. Neuron, 56(4):604-620.

Lillie, J.W. and Green, M.R. (1989) Transcription activation by the adenovirus E1a protein.

Nature, 338, 39-44.

Liu, F. and Green, M.R. (1990) A specific member of the ATF transcription factor family can mediate transcription activation by the adenovirus E1a protein. *Cell*, 61, 1217-1224.

Liu, Y., Dentin, R., Chen, D., Hedrick, S., Ravnskjaer, K., Schenk, S., Milne, J., Meyers, D.J., Cole, P., Yates, J., 3rd, Olefsky, J., Guarente, L. and Montminy, M. (2008) A fasting inducible switch modulates gluconeogenesis via activator/coactivator exchange. Nature, 456, 269-273.

Lodish, H., Berk, A., Kaiser, C. A., and Matsudaira, P. (2004) Molecular Cell Biology, 5th E dition, Palgrave Macmillan, Houndmills, Basingstoke, Hampshire, England.

Long, F., Schipani, E., Asahara, H., Kronenberg, H. And Montminy, M. (2001) The CREB family of activators is required for endochrondral bone development. Development, 128, 541-550.

Mata, M., Merritt, S.E., Fan, G., Yu, G.G., Holzman, L.B. (1996) Characterization of dual leucine zipper-bearing kinase, a mixed lineage kinase present in synaptic terminals whose phosphorylation state is regulated by membrane depolarization via calcineurin. J Biol Chem, 271, 16888-16896.

Mayr, B. and Montminy, M. (2001) Transcriptional regulation by the phosphorylation-dependent factor CREB. Nat Rev Mol Cell Biol, 2, 599-609.

Merritt, S.E., Mata, M., Nihalani, D., Zhu, C., Hu, X., Holzman, L.B. (1999) The mixed lineage kinase DLK utilizes MKK7 and not MKK4 as substrate. J Biol Chem, 274(15), 10195-10202.

Miller, B.R., Press, C., Daniels, R.W., Sasaki, Y., Milbrandt, J., DiAntonio, A. (2009) A dual leucine kinase-dependent axon self-destruction program promotes Wallerian degeneration.Nat Neurosci, 12(4), 387-389.

Montminy, M., Sevarino, K.A., Wagner, J.A., Mandel, G., and Goodman, R.H. (1986) Identification of a cyclic AMP – responsive element within the rat somatostatin gene. Proc Natl Acad Sci USA, 83, 6682-6686.

Nakajima, T., Uchida, C., Anderson, S.F., Parvin, J.D. and Montminy, M. (1997) Analysis of a cAMP-responsive activator reveals a two- component mechanism for transcriptional induction via signal-dependent factors. Genes Dev, 11, 738-747.

Nakata, K., Abrams, B., Grill, B., Goncharov, A., Huang, X., Chisholm, A.D., Jin, Y. (2005) Regulation of a DLK-1 and p38 MAP kinase pathway by the ubiquitin ligase RPM-1 is

required for presynaptic development. Cell, 120(3), 407-420.

Nihalani, D., Merritt, S., Holzman, L.B. (2000) Identification of structural and functional domains in mixed lineage kinase dual leucine zipper-bearing kinase required for complex formation and stress-activated protein kinase activation. J Biol Chem, 275 (10), 7273-7279.

Nihalani, D., Meyer, D., Pajni, S., and Holzman, L.B. (2001*)* Mixed lineage kinase-dependent JNK activation is governed by interactions of scaffold protein JIP with MAPK module components. EMBO J, 20, 3447-3458.

Nihalani, D., Wong, H.N., Holzman, L.B. (2003) Recruitment of JNK to JIP1 and JNK-dependent JIP1 phosphorylation regulates JNK module dynamics and activation. J Biol Chem, 278, 28694-28702.

Nordeen, S.K. (1988) Luciferase reporter gene vectors for analysis of promoters and enhancers. Biotechniques, 6, 454-458.

Oetjen, E., Diedrich, T., Eggers, A., Eckert, B. and Knepel, W. (1994) Distinct properties of the cAMP-responsive element of the rat insulin I gene. J Biol Chem, 269, 27036-27044.

Oetjen E, Baun D, Beimesche S, Krause D, Cierny I, Blume R, Dickel C, Wehner S, Knepel W (2003a) Inhibition of the human insulin gene transcription by the immunosuppressive drugs cyclosporine A and tacrolimus in primary, mature islet of transgenic mice. Mol Pharmacol 63:1289-1295.

Oetjen E, Grapentin D, Blume R, Seeger M, Krause D, Eggers A, Knepel W (2003b) Regulation of human insulin gene transcription by the immunosuppressive drugs cyclosporine A and tacrolimus at concentrations that inhibit calcineurin activity and involving the transcription factor CREB. Naunyn-Schmiedeberg's Arch Pharmacol 367:227-236.

Oetjen, E., Thoms, K.M., Laufer, Y., Pape, D., Blume, R., Li, P. and Knepel, W. (2005) The immunosuppressive drugs cyclosporin A and tacrolimus inhibit membrane depolarization-induced CREB transcriptional activity at the coactivator level. Br J Pharmacol, 144, 982-993.

Oetjen E, Lechleiter A, Blume R, Nihalani D, Holzman L, Knepel W (2006) Inhibition of membrane depolarization-induced transcriptional activity of cyclic AMP response element binding protein (CREB) by the dual-leucine-zipper-bearing kinase in a pancreatic islet beta cell line. Diabetologia 49:332-342.

Pearson, G., Robinson, F., Gibson, T.B., Xu, B., Karandikar, M., Berman, K. and Cobb, M.H. (2001) Mitogen-activated protein (MAP) kinase pathways: Regulation and physiological functions. Endocr Rev, 22 (2), 153-183.

Plaumann, S., Blume, R., Borchers, S., Steinfelder, H.J., Knepel, W. and Oetjen, E. (2008) Activation of the dual-leucine-zipper-bearing kinase and induction of beta-cell apoptosis by the immunosuppressive drug cyclosporin A. Mol Pharmacol, 73, 652-659.

Pollard, T.D. and Earnshaw, W.C. (2002) Cell biology, W.B. Saunders Company.

Powers, A.C., Tedeschi, F., Wright, K.E., ChanQ, S.J. and Habenerli, J.F. (1989) Somatostatin gene expression in pancreatic islet cells is directed by cell-specific DNA control elements and dna-binding proteins. J. Biol. Chem., 264, 10048-10056.

Rana, A., Gallo, K., Godowski, P., Hirai, S., Ohno, S., Zon, L., Kyriakis, J.M., Avruch, J. (1996) The mixed lineage kinase SPRK phosphorylates and activates the stress-activated protein kinase activator, SEK-1. J Biol Chem, 271(32), 19025-19028. Ravnskjaer, K., Kester, H., Liu, Y., Zhang, X., Lee, D., Yates, J.R., 3rd and Montminy, M. (2007) Cooperative interactions between CBP and TORC2 confer selectivity to CREB target gene expression. Embo J, 26, 2880-2889.

Reddy, U.R., Pleasure, D. (1994) Cloning of a novel putative protein kinase having a leucine zipper domain from human brain. Biochem Biophys Res Commun. 202(1):613-20; 205(2):1494-1495.

Reddy, U.R., Nycum, L., Slavc, I., Biegel, J.A. (1995) Localization of the human zipper protein kinase gene (ZPK) to chromosome 12q13 by fluorescence in situ hybridization and somatic cell hybrid analysis.Genomics, 25(2):597-598.

Riccio, A., Ahn, S., Davenport, C.M., Blendy, J.A. and Ginty, D.D. (1999) Mediation by a CREB family transcription factor of NGF-dependent survival of sympathetic neurons. Science, 286, 2358-2361.

Robitaille, H., Proulx, R., Robitaille, K., Blouin, R., Germain, L. (2005) The mitogen-activated protein kinase kinase kinase dual leucine zipper-bearing kinase (DLK) acts as a key regulator of keratinocyte terminal differentiation. J Biol Chem, 280(13), 12732-41.

Robitaille, K., Daviau, A., Lachance, G., Couture, J.P., Blouin, R. (2008) Calphostin C-induced apoptosis is mediated by a tissue transglutaminase-dependent mechanism involving the DLK/JNK signaling pathway. Cell Death Differ, 15, 1522–1531.

Rudolph, D., Tafuri, A., Gass, P., Hämmerling, G.J., Arnold, B., and Schütz, G. (1998) Impaired fetal T cell development and perinatal lethality in mice lacking the cAMP response element binding protein. Proc. Natl Acad. Sci. USA, 95, 4481-4486.

Sadowski, I. and Ptashne, M. (1989) A vector for expressing GAL4(1-147) fusions in mammalian cells. Nucleic Acids Res, 17, 7539.

Sakuma, H., Ikeda, A., Oka, S., Kozutsumi, Y., Zanetta, J.P., Kawasaki, T. (1997) Molecular cloning and functional expression of a cDNA encoding a new member of mixed lineage protein kinase from human brain. J Biol Chem, 272(45), 28622-28629. Sambrook, J., Fritsch, E. F. and Maniatis, T. (1989) Molecular cloning. A laboratory manual, 2nd Edition, Cold Spring Harbor Laboratory Press, Cold Spring Harbor, USA.

Sanger, F., Nicklen, S. and Coulson, A.R. (1977) DNA sequencing with chain-terminating inhibitors. Proc Natl Acad Sci U S A, 74, 5463-5467.

Santerre, R.F., Cook, R.A., Crisel, R.M., Sharp, J.D., Schmidt, R.J., Williams, D.C. and Wilson, C.P. (1981) Insulin synthesis in a clonal cell line of simian virus 40-transformed hamster pancreatic beta cells. Proc Natl Acad Sci U S A, 78, 4339-4343.

Schlabach, M.R., Luo, J., Solimini, N.L., Hu, G., Xu, Q., Li, M.Z., Zhao, Z., Smogorzewska, A., Sowa, M.E., Ang, X.L., Westbrook, T.F., Liang, A.C., Chang, K., Hackett, J.A., Harper, J.W., Hannon, G.J., Elledge, S.J. (2008) Cancer proliferation gene discovery through functional genomics. Science, 319(5863), 620-624.

Schwaninger, M., Blume, R., Kruger, M., Lux, G., Oetjen, E. and Knepel, W. (1995) Involvement of the Ca(2+)-dependent phosphatase calcineurin in gene transcription that is stimulated by cAMP through cAMP response elements. J Biol Chem, 270, 8860-8866.

Schwaninger, M., Blume, R., Oetjen, E., Lux, G. and Knepel, W. (1993a) Inhibition of cAMP- responsive element-mediated gene transcription by cyclosporin A and FK506 after membrane depolarization. J Biol Chem, 268, 23111-23115.

Schwaninger, M., Lux, G., Blume, R., Oetjen, E., Hidaka, H. and Knepel, W. (1993b) Membrane depolarization and calcium influx induce glucagon gene transcription in pancreatic islet cells through the cyclic AMP-responsive element. J Biol Chem, 268, 5168-5177.

Screaton, R.A., Conkright, M.D., Katoh, Y., Best, J.L., Canettieri, G., Jeffries, S., Guzman, E., Niessen, S., Yates, J.R., 3rd, Takemori, H., Okamoto, M. and Montminy, M. (2004) The CREB coactivator TORC2 functions as a calcium- and cAMP-sensitive coincidence

detector. Cell, 119, 61-74.

Shaw, R.J., Lamia, K.A.,Vasquez, D.,Koo S.H., Bardeesy,N., Depinho,R.A., Montminy,M. & Cantley,L.C.(2005) The kinase LKB1 mediates glucose homeostasis in liver and therapeutic effects of metformin. Science 310,1642-1646.

Shaywitz, A.J. and Greenberg, M.E. (1999) CREB: a stimulus-induced transcription factor activated by a diverse array of extracellular signals. Annu Rev Biochem, 68, 821-861.

Silver, P.A.; Keegan, L.P.; Ptashne, M.(1984) Amino Terminus of the Yeast GAL4 Gene Product is Sufficient for Nuclear Localization. Proc. Nadl. Acad. Sci. USA, 81, 5951-5955.

Siu YT, Ching YP, Jin DY (2008) Activation of TORC1 transcriptional coactivator through MEKK1-induced phosphorylation. Mol Biol Cell 19:4750-4761.

Siu, Y. T., Chin, K. T., Siu, K. L., Choy, E.Y.W., Jeang, K. T., and Jin, D. Y. (2006). TORC1 and TORC2 coactivators are required for tax activation of the human T-cell leukemia virus type 1 long terminal repeats. J. Virol *80*, 7052–7059

Siu Y.T., Jin, D.Y. (2007) CREB--a real culprit in oncogenesis. Febs J 274:3224-3232

Struthers, R. S., Vale, W. W., Arias, C., Sawchenko, P. E. and Montminy, M. R. (1991) Somatotroph hypoplasia and dwarfism in transgenic mice expressing a non-phosphorylateable CREB mutant. Nature, 350, 622-624

Sun, P., Ensien, H., Myung, P. & Maurer, R. (1994). Differential activation of CREB by Ca2+/calmodulin-dependent protein kinase type II and IV involves phosphorylation of a site that negatively regulates activity. Genes Dev. 8, 2527-2539

Takemori, H. and Okamoto, M. (2008) Regulation of CREB-mediated gene expression by salt inducible kinase. J Steroid Biochem Mol Biol, 108, 287-291.

Takemori, H., Kajimura, J., and Okamoto, M. (2007a). TORC-SIK cascade regulates CREB activity through the basic leucine zipper domain. FEBS J *274*, 3202–3209.

Takemori, H., Kanematsu, M., Kajimura, J., Hatano, O., Katoh, Y., Lin, X. Z., Min, L., Yamazaki, T., Doi, J., and Okamoto, M. (2007b). Dephosphorylation of TORC initiates expression of the StAR gene. Mol. Cell. Endocrinol *265–266*, 196–204.

Tan Y., Rouse J, Zhang A, Cariati S, Cohen P, Comb MJ. (1996) FGF and stress regulate CREB and ATF-1 via a pathway involving p38 MAP kinase and MAPKAP kinase-2. EMBO J. 15, 4629-4642.

Tanaka, S., Hanafusa, H. (1998) Guanine-nucleotide exchange protein C3G activates JNK1 by a ras-independent mechanism. J Biol Chem, 273, 1281-1284.

Tardito, D., Perez, J., Tiraboschi, E., Musazzi, L., Racagni, G., Popoli, M. (2006) Signaling pathways regulating gene expression, neuroplasticity, and neurotrophic mechanisms in the action of antidepressants: a critical overview. Pharmacol Rev, 58, 115-134.

Tibbles, L.A., Ing, Y.L., Kiefer, F., Chan, J., Iscove, N., Woodgett, J.R., Lassam, N.J. (1996) MLK-3 activates the SAPK/JNK and p38/RK pathways via SEK1 and MKK3/6. EMBO J, 15(24), 7026-7035.

Tsien, R.Y. (1998) The green fluorescent protein. Annu Rev Biochem, 67, 509-544.

Wang, Y., Inoue, H., Ravnskjaer, K., Viste, K., Miller, N., Liu, Y., Hedrick, S., Vera, L. and Montminy, M. (2010) Targeted disruption of the CREB coactivator CRTC2 increases insulin sensitivity. Proc Natl Acad Sci U S A, 107:3087-3092

Watanabe, T,, Yanagisawa, M,, Matsubara, N., Obinata, M., Matsui, Y. (1997) Assignment of the murine protein kinase gene DLK to chromosome 15 in the vicinity of the bt/Koa locus by genetic linkage analysis.Genomics, 40(2):375-376.

Webster, N., Jin, J.R., Green, S., Hollis, M. and Chambon, P. (1988) The yeast UASG is a transcriptional enhancer in human HeLa cells in the presence of the GAL4 trans-activator. Cell, 52, 169-178.

Widmann, C., Gibson, S., Jarpe, M.B., Johnson, G.L. (1999) Mitogen-activated protein kinase: conservation of a three-kinase module from yeast to human. Physiol Rev, 79(1),143-80.

Wu, C., Daniels, R.W., DiAntonio, A.D. (2007) Fsn collaborates with Highwire to down-regulate the Wallenda/DLK kinase and restrain synaptic terminal growth. Neural Dev, 2, 16.

Wu, L., Liu, J., Gao, P., Nakamura, M., Cao, Y., Shen, H., and Griffin, J.D. (2005) Transforming activity of MECT1-MAML2 fusion oncoprotein is mediated by constitutive CREB activation. Embo J 24:2391-2402

Wu Z et al. (2006) Transducer of regulated CREB-binding proteins (TORCs) induce PGC-1alpha transcription and mitochondrial biogenesis in muscle cells. Proc Natl Acad Sci U S A 103:14379-14384

Xu, W., Kasper, L.H., Lerach, S., Jeevan, T. and Brindle, P.K. (2007) Individual CREB-

target genes dictate usage of distinct cAMP-responsive coactivation mechanisms. Embo J, 26, 2890-2903.

Xu Z, Maroney AC, Dobrzanski P, Kukekov NV, Greene LA (2001) The MLK family mediates c-Jun N-terminal kinase activation in neuronal apoptosis. Mol Cell Biol 21:4713-4724

Xu, Z., Kukekov, N.V., Greene, L.A. (2005) Regulation of apoptotic c-Jun N-terminal kinase signaling by a stabilization-based feed-forward loop. Mol Cell Biol, 25(22), 9949-9959.

Zhou, Y., Wu, H., Li, S., Chen, Q., Cheng, X.W., Zheng, J., Takemori, H. and Xiong, Z.Q. (2006) Requirement of TORC1 for late-phase long-term potentiation in the hippocampus. PLoS ONE, 1, e16.

Acknowledgements

I would like to express my deep thanks to PD. Dr. Elke Oetjen for giving me the opportunity to work on this interesting project concerning the molecular regulation of TORC by DLK. Her help, supervison and advice in all stages of my PhD work were invaluable.

I am grateful to my thesis committee Professor Ralf Heinrich and Professor Frauke Melchior for helpful advice, scientific support and contribution to the progress of my PhD thesis.

I thank Professor Willhart Knepel for giving me a position to work in the Department of Molecular Pharmacology, Göttingen University.

I also thank Professor Wolfram- Hubertus Zimmermann for his support and advice during my latest phases of my work.

I am thankful to Dr. Mladen Tzvetkov for supporting me in the work related to real-time PCR.

I am grateful to Dr. Tran Cong Tuoc, Dr. Nguyen Van Phuc for contributing some support and advice to my work.

I greatly appreciate technical assistance from Doris Krause, Roland Blume, Corinna Dickel, Irmgard Chierny and Iris Quentin.

To all members of the Department of Molecular Pharmacology, especially to the former members Annette, Ulrike, Catarina, Manuel, Svenja, Anne, Marcel, Andrei, Cordula, as well as the current members Marie, Rohallah, Poh Loong, Simin, Meiling and others: Many thanks to all of you for the friendship, your sharing and help in many issues.

To all my friends: Thank you so much for your support, sharing troubles and joys during my working time in Germany.

Above all, my deep gratitude is sent to my family for encouragement, understanding, believing in my work and life.

POSTER ABSTRACTS

Poster 1:

Presented at the 52th Annual Meeting: Deutsche Gesellschaft für Endokrinologie, organized in Gießen, Germany, from 4-7th March, 2009.

Inhibition of the CREB co-activator TORC by the mitogen-activated kinase DLK in pancreatic beta cells

P. Do Thanh and E. Oetjen

Department of Pharmacology, University of Göttingen, 37099 Göttingen, Germany

Objectives: The ubiquitously expressed transcription factor CREB was shown to play a pivotal role in the maintenance of beta cell function and mass. Recently, the three isoforms of Transducer of Regulated CREB (TORC) were identified as additional CREB co-activators. Upon dephosphorylation of S171 in TORC2, or S167 in TORC1, TORC translocates to the nucleus, interacts with the dimerized leucine zipper of CREB and confers transcriptional activity to CREB-dependent genes. Our previous studies showed that the dual leucine zipper bearing kinase DLK inhibits membrane depolarization-induced CREB transcriptional activity in beta cells. In the present study the effect of DLK on TORC was investigated.

Methods: Luciferase reporter gene assays using the beta cell line HIT and an *in vitro* protein interaction assay were employed.

Results: Using the GAL4-system, overexpression of DLK inhibited TORC1/2-directed transcription by 80 and 40%, respectively. This reduction was less pronounced using the DLK kinase dead mutant (DLK-K185A), whereas a DLK mutant unable to homodimerize (DLK-PP) showed no inhibitory effect on TORC activity. In addition, mutation of S167 or Ser171 in TORC1 and 2, respectively, prevented the inhibitory effect of DLK on TORC transcriptional activity. The *in vitro* protein interaction assays revealed that bacterially expressed His-tagged full length TORC1 and GST-tagged TORC1(1-44 amino acids) interacted with [^{35}S]-labelled DLK and DLK-K185A to the same extent. Deletion of the first 44 amino acids prevented the interaction. In addition, the interaction between DLK-PP and TORC1 was reduced by 40%.

Conclusion: Our data suggest that DLK might inhibit the CREB coactivator TORC in beta cells by two mechanisms: 1. the DLK kinase activity might result in the phosphorylation of S167 in TORC1, thus preventing its nuclear translocation; 2. the DLK leucine zipper structure might interact with TORC, thereby retaining it in the cytosol.

Poster 2:

Presented at the 50th Spring Meeting of the Deutsche Gesellschaft für Experimentelle und Klinische Pharmakologie und Toxikologie, organized in Mainz, Germany, from 10-12th March, 2009.

The mitogen-activated protein kinase DLK inhibits the CREB co-activator TORC

Phu Do Thanh and Elke Oetjen

Abteilung Pharmakologie, Universität Göttingen, D-37075 Göttingen

Recently, three isoforms of Transducer of Regulated CREB (TORC) were identified as additional CREB co-activators. Whereas the co-activator CBP interacts with on Ser-119 phosphorylated CREB, TORC1 and TORC2 after dephosphorylation of Ser-167 and Ser-171, respectively, translocate into the nucleus and interact with the dimerized leucine zipper of CREB. TORC translocation is inhibited by the immunosuppressive drugs cyclosporin and tacrolimus. Our previous studies showed that both drugs activate the dual leucine zipper bearing kinase DLK. In the present study the effect of DLK on TORC was investigated.

A luciferase reporter gene under control of 5 copies of the GAL4 binding-site was transiently cotransfected with expression vector for GAL4-TORC fusion proteins into the beta cell line HIT. Over expression of DLK inhibited TORC1 and TORC2 transcriptional activity by 80 and 40%, respectively. This reduction was less pronounced using the DLK kinase dead mutant (DLK-K185A), whereas a DLK mutant unable to homodimerize (DLK-PP) showed no inhibitory effect on TORC activity. The mutation of Ser-167 or Ser-171 in TORC1 and 2, respectively, to Ala prevented the inhibitory effect of DLK on TORC transcriptional activity. The interaction between TORC and DLK was investigated by an *in vitro* pull down assay. Bacterially expressed His-tagged full length TORC1 or GST-tagged TORC1(1-44 amino acids) interacted with [^{35}S]-labeled DLK and with DLK-K185A to the same extent. Deletion of the first 44 amino acids of TORC1 prevented this interaction. In addition, the interaction between DLK-PP and TORC1 was reduced by 40%. Our data show that DLK inhibits TORC activity, presumably by phosphorylation of Ser-167 or Ser-171 in TORC1 and TORC2, respectively, thus preventing the nuclear translocation of TORC. In addition, DLK interacts with TORC1. This interaction depends on the N-terminal amino acids of TORC1 and the ability of DLK to dimerize. Thus, DLK might inhibit TORC through an interaction with and by the phosphorylation of TORC, thereby preventing the nuclear translocation of TORC and ultimately the stimulus-induced CREB transcriptional activity.

Curriculum Vitae

Personal information

Name:	Do Thanh Phu
Date of birth:	May 6th, 1975
Place of birth:	Hoa Binh, Vietnam
Current address:	Gutenberg str.12 37075 Göttingen
Phone:	+49-551-9956419
E-mail:	ntkdophu@yahoo.com

Education

since October 2006	PhD Program - GAUSS Georg-August-University Göttingen Centre of Pharmacology and Toxicology Department of Molecular Pharmacology PhD project: Molecular mechanisms of Inhibition of the CREB co-activator TORC by the mitogen-activated kinase DLK in pancreatic beta cells
1992 - 1996:	Bachelor program Studied Biology in the Natural Sciences University, HoChiMinh City.
2001-2003:	Master program Studied Biochemistry in the Natural Sciences University, HoChiMinh City.